Recycled Polymer Composites for Structural Applications

by

Annie-May Hugo

A thesis submitted for the degree of

Doctor of Philosophy

In the Composite Systems Innovations Centre

Department of Mechanical Engineering

July 2015

Abstract

This thesis documents the development and testing of recycled, immiscible polymer blends for structural applications. The project was a Knowledge Transfer Partnership co-funded by Innovate UK and a Plastic Lumber manufacturer, who had a development contract with Network Rail. Network Rail contributed towards a permanent fatigue testing facility for full-size sleepers.

Recycled plastic lumber converts lower grade, recyclate waste streams into products for decking, fencing, etc.. The aim was to create formulations capable of carrying significant in-service, dynamic loads over a wide spectrum of outdoor temperatures and conditions with 50 years minimum service life for railway sleepers.

Mixed polyethylene/polypropylene recyclates were tested in iterative laboratory trials reinforced with polystyrene, mineral fillers and glass fibre. Flexural properties and impact resistance amongst other tests aided formulation design for production trials. A synergistic reinforcing effect was found between glass fibre and mica within an immiscible recycled polymer blend.

Polymer blends and fibre reinforced grades were manufactured by intrusion moulding into profiles up to 2800x250x130 mm. Profiles of four trial and two production grades were tested in flexure, compression and thermal expansion. Large statistical sample sizes were required due to waste stream batch-to-batch variability. Strength and modulus were found to change with manufacturing technique, profile size, profile orientation, test type, and test parameters. Strengths were good, though lower than predicted due to premature failure. The fracture process was found to initiate at inclusions, ductile crack growth continued to a critical size followed by brittle facture. Glass fibre significantly improved strength, modulus, maximum operating temperature and thermal expansion.

In 2012, two major product approvals were attained after extensive qualification testing that included fatigue testing equivalent to 20 years in service. British Board of Agrément accredited a crib earth retaining wall system. Network Rail approved for track trial sleepers made from the glass fibre reinforced grade.

Acknowledgements

During the 5 year development phase, the project complexity required expertise and services from the university, the company, Network Rail, suppliers, compounders, fabricators, external test houses, and customers. Thank you all for your hard work, skills, wealth of knowledge, and support.

Technology Strategy Board (now Innovate UK) funded my KTP, which enabled the project. I particularly remember the late Mike Willis, my KTP Advisor.

Network Rail provided the Development Contract with i-plas that created the project. In particular I would like to thank Peter Squire and Charlton Hawley.

At University of Sheffield, I benefited from helpful staff, expertise and test facilities in 5 different departments. In particular, my gratitude goes to Professor Alma Hodzic, my supervisor, for 7.5 enjoyable years working together. Your dedication and commitment to your work is exceptional. I would like to thank: Emeritus Professor Frank Jones for stepping into the breach; Dr Simon Hayes, Dr Peter Bailey and Dr Austin Lafferty for their advice and encouragement; Michael Jackson for his cheerfulness, attention to detail, and patience during my whirlwind visits; Mike Rennison for his help and tolerance of my numerous, very large samples.

It is a great shame that the team at i-plas is no longer together. The investors withdrew funding in September 2012, causing the company to close. Everyone I worked with was supportive and helped in anyway possible, from the shop floor to the management team. In particular I would like to thank Howard Waghorn and Phil Bruce. I bow to your positive attitude, ability to just get things done, and wealth of knowledge on recycled plastics.

Finally to thank my husband, son, parents and friends. Tom and Alison for their support and friendship forged so long ago during our Materials degree. I wrote my thesis in Suzhou, China. Thank you to my new friends for their support.

Abbreviations and Nomenclature

AMIPP	Advanced Materials via Immiscible Polymer Processing (AMIPP) Advanced Polymer Centre at Rutgers University
ASTM	American Society for Testing and Materials
$CaCO_3$	Calcium Carbonate
CTE	Co-efficient of thermal expansion
DSC	Differential Scanning Calorimeter
DBTT	Ductile to Brittle Transition
EPDM	Ethylene Propylene Diene terpolymer rubber
EPR	Ethylene Propylene rubber
EVA	Ethylene Vinyl Acetate copolymer
EU	European Union
HIPS	High Impact Polystyrene
HDT	Heat Deformation Temperature (ASTM D648 and ISO 75-1) [1, 2]
ISO	International Standards Organisation
LDPE	Low Density Polyethylene
LLDPE	Linear Low Density Polyethylene
HDPE	High Density Polyethylene
MDPE	Medium Density Polyethylene
MFI	Melt Flow Index
MRF	Materials Recovery Facility
PCR	Post consumer resin
PE	Polyethylene
PET	Polyester
PMMA	Poly methyl methacrylate
PP	Polypropylene
PRF	Plastics Recycling Facility
PS	Polystyrene
PVC	Poly Vinyl Chloride polymer
RECOUP	Recycling of Used Plastics Limited
RoHS	Restriction of Hazardous Substances Directive [3]

RT	Room Temperature
SBS	Styrene Butadiene Styrene elastomer
SEBS	Styrene Ethylene Butadiene Styrene elastomer
SEM	Scanning Electron Microscope
T_c	Crystallisation Temperature
T_g	Glass Transition Temperature
T_m	Crystalline melting Point
UK	United Kingdom of Great Britain
UTS	Ultimate tensile strength
UV	Ultraviolet radiation e.g. sunlight
WEEE	Waste Electronic and Electrical Equipment Regulations, European Community Directive 2012/19/EU [4]
WRAP	Waste & Resources Action Programme

Table of Contents

Overview

This PhD thesis documents the development, characterization and large scale testing of composite formulations made from recycled plastic waste streams.

The purpose of the testing was to select compounds capable of carrying significant in-service dynamic loads over a wide spectrum of temperatures and harsh environments. To achieve this ambitious goal, the formulations were iteratively developed by mixing numerous combinations of the available and selected recycled polymers, in order to keep available resources within a broad recycling range. The optimised blends were then scaled up to the level of standard materials tests, further standard component tests and finally the full railway sleeper system tests.

This section outlines the aims and objectives, and describes the structure of the thesis.

Aims, Objectives and Research Constraints

The aim of the research was to develop a composite suitable for structural applications that used recycled plastics. The project started as a 2.5 year Knowledge Transfer Partnership co-funded by Innovate UK (previously Technology Strategy Board) and I-plas, a plastic lumber manufacturer. I-plas continued to fund the project for a further 2 years following the completion of the KTP. At the start of the project, Network Rail signed a development contract with I-plas to produce a specification for recycled plastic railway sleepers and a product suitable for track trial. Hence, Network Rail was closely involved in the project to the extent that it contributed funds to establish the fatigue testing equipment in the Department of Mechanical Engineering, to evaluate in-service conditions for full sized sleepers.

I-plas recycled plastic waste, and manufactured plastic lumber profiles. The existing product was used for benches, fences, boardwalks, and similar

applications. The company wished to introduce a new, high value product range for selected structural applications such as railway sleepers and crib walling. In order to do this it needed the expertise and test facilities of the University of Sheffield.

Network Rail stipulated that the product must be a drop-in replacement for softwood sleepers with exactly the same dimensions and would use standard equipment to install identical "rail furniture" (baseplates, chairscrews, rail pads, etc.). Network Rail specified certain railway specific tests. They also required a range of material tests that had to be developed during the project. After a lifetime of 50 years in track the product had to be recyclable.

The Company constrained the research by the following practical criteria:
–   all materials must be recycled and available in sufficient quantities within the UK waste stream
–   additives must not be used unless essential
–   manufacturing must use the existing process equipment within the business
–   the final formulation must be economically viable
–   the formulation must not infringe current intellectual property.

Structural applications require extensive qualification testing to ensure all aspects of performance are satisfactory. A wide variety of properties required consideration:-
–   mechanical performance
–   weathering stability
–   resistance to burial in soil and other substrates
–   long-term performance
–   resistance to chemical attack
–   non-pollution of the environment
–   flammability.

The nature of the raw materials and the final product structure required that full size profiles were tested wherever possible. To achieve this standard equipment and test methods had to be adapted in order to test the unusually large sizes.

Thesis Structure

There are 7 chapters in this thesis.

Chapter 1 provides information that explains the recycled plastics market and plastic lumber market. The chapter details the changes in the plastics recycling industry, the plastic lumber manufacturing process and plastic lumber products. During the period of research the recycled plastic market was in a cycle of significant growth and technological change. This changed the market and the sources of material that were both available and economically viable.

Chapter 2 studies polymers, polymer blends and reinforcement through a review of previous research and existing technology. The purpose of the review was to aide design of a set of formulations for testing.

Chapter 3 describes laboratory mechanical testing on a range of blends reinforced using polymers, mineral fillers and fibres. Over the course of the project, five trials were completed looking at different aspects of the formulation. The testing was used to select compounds for production trials and large scale testing.

Chapter 4 reports the testing of full-sized profiles in three point bend, four point bend and compression. A wide range of profile sizes were tested made from the trial compounds and standard production grades. The effect of test conditions, cross-section size, batch-to-batch variation and failure modes were investigated.

Chapter 5 draws the research to a conclusion. The material and product performance of the polymer blend and fibre reinforced blends are compared then put into context with their performance in selected railway system testing.

Chapter 6 discusses proposals for technology enhancement and improving understanding of the performance. Some recommendations are to obtain greater understanding of the compound properties to enabling adoption for structural applications. Other recommendations are for further optimisation of the formulation to improve morphology, mechanical properties, and lifetime.

Chapter 7 summarises the conclusions and further work.

1   Introduction to Recycled Plastics Industry

This chapter gives background information on the recycled plastics industry to put the research into context and to explain some of the decisions made. It details the changes in the plastics recycling industry over the course of the project, the plastic lumber manufacturing process and the range of plastic lumber products. During the period of research the recycled plastics market was in a cycle of significant growth and technological change. This changed the sources of materials that were both available and economically viable.

1.1   The Market for Recycled Plastics

The United Kingdom currently uses over 5 million tonnes of plastic a year, of which only 24% is recovered or recycled [5]. The UK government and the European Union have a range of strategies and legislation in place to improve this situation. The Waste Framework Directive has a hierarchy of options for managing waste, which is shown in Table 1.1.

Over the time period of the project both the legislative and global economic conditions significantly affected the market for recycled raw materials available to the project.

Economic demand saw the prices of base polymers increased dramatically from the start of the project. The price of recycled plastic tracks to that of virgin polymers, which generally tracks the crude oil price index. Between 2008 and 2011 the price of crude oil increased from $40 a barrel to $120; the LDPE virgin polymer price increased from 800 to 1300 $/tonne and LDPE regrind price rose from 500 to 890 $/tonne [6, 7].

Table 1.1 Hierachy of Waste Reduction [3–5, 8–11]

Strategy	Implementation examples
Prevention	Eco-design legislation aims to reduce the amount of materials used in products, and make them easier to recycle at the end-of-life.
Re-use	PAS 141 is a process management specification for the reuse of electrical and electronic equipment. Eco-design legislation also considers servicing, repair and supply of spare parts.
Recycling	Producer responsibility legislation makes manufacturers responsible for financing the treatment, recycling and reprocessing of products when they reach end-of-life, for example: – Packaging and Packaging Waste Directive – End of Life Vehicles Directive – Waste Electrical and Electronic Equipment Directive (WEEE).
Other recovery	Incineration, gasification, pyrolysis, and similar facilities to generate energy from waste.
Disposal	Reducing the amount of landfill by increasing of landfill charges and weight based recycling targets for Local Authorities.

An economic downturn saw volumes of recycled plastics diminish from the sponsor company's main traditional source of post industrial waste from plastics converters and manufacturing companies. Manufacturing companies put significant emphasis on minimising their production waste in order to reduce manufacturing costs and comply with new national and European wide legislation. The sector now is estimated to equate to 250,000 - 300,000 tonnes annually [5]. Most of this material is now made up of off-specification mouldings or thermoforming grades of material, which is not suitable for the company's production process.

Legislative requirements increased the amount and variety of material sent for recycling e.g. packaging, agricultural films and electrical equipment. While competition to recycle the material also increased, the number of accredited reprocessors/exporters increased from 52 to 66 between 2006 and 2011 [12]. The company saw a noticeable effect on both cost and availability for raw materials when competing with global exporters during this period. The export market for plastic waste grew strongly and from 2008 to 2011 the amount of exported recycled plastics rose from 650,000 to over 850,000 tonnes [13]. The exporters drove up the market by offering higher prices for unprocessed, and graded materials. This was now more affordable to them, due to the global increase in virgin polymer costs, their lower energy and labour costs for material reprocessing and, lower shipping costs from West to East. It is estimated that 50-70% of all plastic packaging waste was exported in 2012 [8].

Manufacturing companies increased their acceptance of recycled material as:
– Virgin polymer prices increased and the pressure to control product cost rose,
– Recyclate quality, consistency and volumes improved due to investment and technological developments,
– Legislation permitted the use of recycled materials allowing cost savings to be leveraged e.g. food grade recyclates, and
– Environmental credentials became seen to be important.

In summary, the changes in the market increased raw material prices, increased demand for high quality waste streams and altered the waste streams available to the project.

1.2   The Waste Stream

Material available for recycling (recyclates) can come from a variety of sources. Table 1.2 breaks down the typical waste sources for processors or exporters.

Table 1.2 Typical sources of plastic for recycling.

Waste Source	Example
Manufacturing waste	Contaminated process scrap and purgings Rejected parts - incorrect colour, faulty printing, incorrect contents Excess product/end of lines
Post industrial waste	End of life products - wheelie bins, sharps containers, barrels and bulk containers, astroturf, exhibition carpet, coat hangers
Industrial /Commercial packaging	Plant pots, bottle and bread crates, agricultural film, stretch-wrap films and returnable transit packaging such as pallets, crates and drums.
Post-consumer packaging	Plastic bottles Rigid/flexible plastic – pots, tubs, trays Films
Post-consumer waste	Fridges, televisions, electronics, electrical goods, carpet, cars, etc.

Manufacturing, industrial and commercial waste are easier to recycle than post-consumer waste. This is because they tend to be sent for recycling in batches of the same product. Also the suppliers can be educated to segregate their waste; the advantage for them is that they get paid a higher price.   The recyclate is segregated by source and viscosity (melt flow index - MFI) according to the original manufacturing process.   Injection moulded products have high melt flow and high value. Extrusion and blow moulding are low melt flow and lower value. Thermoformed and sheet materials have very low melt flow and low value.

Post-consumer waste has many different products mixed together, which can be a significant challenge for recyclers separating the high grade recyclates from the low grade recyclates and residuals. Post-consumer waste such as waste electrical and electronic equipment (WEEE) has different parts made from a range of plastics, metals and other materials joined together by screws and adhesives. The products are often very dirty as well. They first need to be disassembled or shredded, before they can be segregated and washed. The range of post-consumer packaging is very diverse and complex. Table 1.3 gives examples of the packaging that is collected with their material type.

Table 1.3 Examples of packaging sent for recycling with their material type [14].

Packaging Type	Typical Polymers
Bottles	PET HDPE
Margarine and ice cream tubs Fruit pots, flexible spread jars	PP
Meat and microwaveable trays Pasta sauce pots, sandwich filler tubs	PP PET
Fruit/Vegetable punnets and trays	PET PP PS
Household cleaning Items	HDPE PP
Yoghurt, cream and diary pots	PP PS
Bakery goods trays	PET PS
Films	PE PP

Plastic bottles are a desirable, high grade, waste stream. They have high value, because they are composed of a single polymer, available in large quantities, and are easily sorted and washed.

Pots, tubs and trays (Rigid/flexible plastic packaging) are a low grade recyclate and a real challenge to the recycling industry. They are often contaminated with food. They are often coloured with carbon black, which prevents near infrared sorting. They consist of many different types of plastic and commonly have films attached. Thin plastic films are difficult to handle, because they are lightweight, cannot be cut and, are often multi-layer laminates of different polymers and tie layers to give superior barrier properties. Films are generally considered as a contaminator of other waste streams.

Post consumer packaging is a good example of how the waste stream has changed. It is estimated that 2.5 million tonnes of packaging is used annually, and represents a significant proportion of the plastic used in the UK [12]. 1.2 million tonnes of this packaging is from households of which 37% is recycled [8].

Local authority waste collection is a key source of recyclates. Figure 1.1 shows the increase in plastic packaging collected from 1994 to 2012 [8]. Some key facts local authority recycling in 2012 are:
–   bottles account for over 70% of the packaging collected,
–   58% of plastic bottles, 19% of pots, tubs and trays and 37% of rigid plastic packaging used in the UK are recycled through local authority schemes,
–   the quantities collected are increasing due to incentives both local and European wide:
     –   In 2007, 10,856 tonnes of pots tubs and trays were collected,
     –   In 2012, 124,347 tonnes of pots tubs and trays were collected,
–   the cost of waste going to landfill is £85 a tonne,
–   mixed bottle recyclates could be sold for £110.45 a tonne, and
–   pots, tubs and tray recyclates sold for up to £20 a tonne
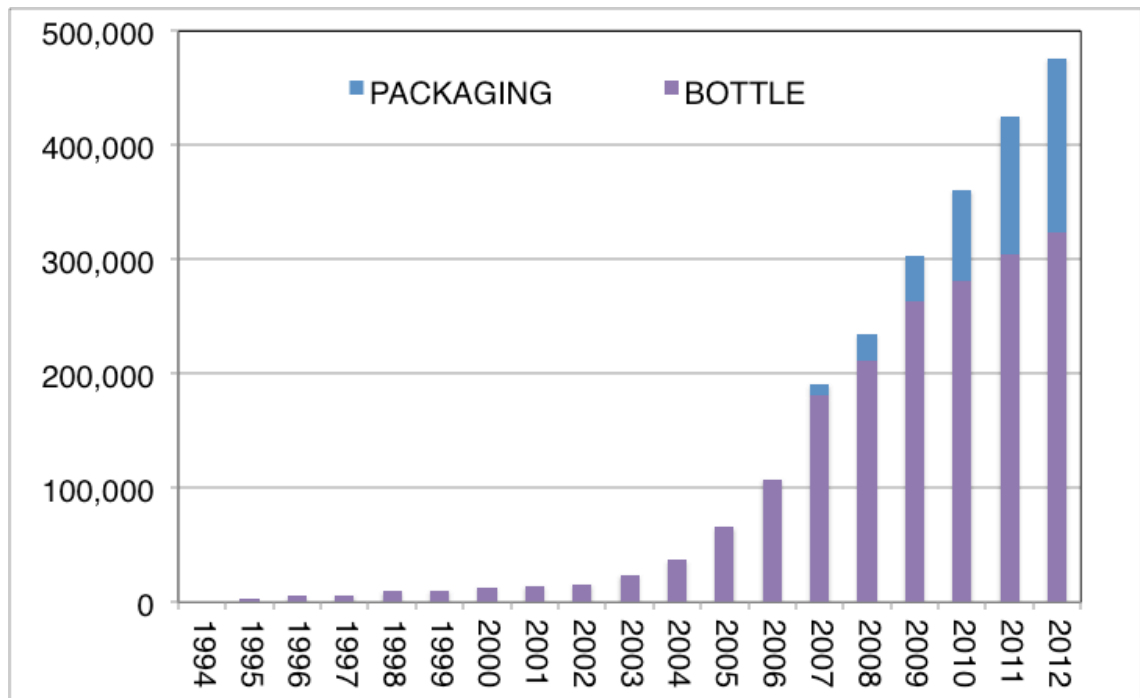
Figure 1.1 Tonnes of plastic packaging collected each year by UK Local Authorities [8].

The EU packaging recycling target is 22.5% and the UK government is increasing its own 32% target by 5% a year in 2014 to 57% in 2017 [15].

In summary, the sources of materials used in the formulations changed over the course of the project. For example, packaging waste streams were not widely available at the start of the project, however, by the end of the project they were an important source of material.

1.3   Recycling Processors

Recycling is only an economical option, if the market can afford the cost of processing raw recyclates into products that can be re-used within a specific manufacturing process. Higher quality, pure materials can be used for injection moulded and thin wall products where specifications justify a higher price point. The use of food grade recyclates for reuse in food packaging [8] is an example of a high quality recyclate usage.

The waste plastic recyclates are sorted by both Materials Recovery Facilities (MRF) and Plastics Recycling Facilities (PRF). Materials Recovery Facilities take co-mingled waste, separate it through both manual and automated systems, and sell on the different recyclable bales (paper, card, metal, plastic, etc.). Some plants increase the bale value by using automated optical sorting facilities to separate the types of plastic containers. Typical plastic waste streams are film, PET bottle bales, HDPE bottle bales, PP bales, and mixed rigid plastic bales [14]. Contamination of these waste streams decreases the value of the bales e.g. additional films, multilayer plastics, PVC and engineering plastics.

Plastics Recycling Facilities (PRF) take manually sorted kerbside collections and the sorted bales from MRFs. PRF plants tend to be set up for particular incoming waste streams of certain proportions. They are complex facilities with high capital costs as the process makes significant use of automated separators. Significant extra investment is required to change the process, for example, the necessity to reprocess an increasing amount of pots, tubs and trays would require additional separator lines. PRFs generally separate out PET, HDPE, PP and PS and then separate them further into coloured and unpigmented streams. The streams are then converted into 10-20mm flakes. Figure 1.2 shows a typical flow chart for a PRF plant with reprocessing equipment.

To be commercially viable a PRF needs the capacity to handle 80-100,000 tonnes per annum [14]. The yield per tonne is economically very important. For example, the yield is commonly only 40% for unprocessed bales of rigid plastic household containers. This means for every 2.5 tonnes processed there is: 1 tonne of high value recyclate and 1.5 tonnes of low value material or waste. This waste can include labels, contents residues, film and other non-target plastic types. If the film content of a bale was increased to 10%, the yield could drop by 30% because the entire product would be rejected or good material might be pulled out along with the film when it is removed.
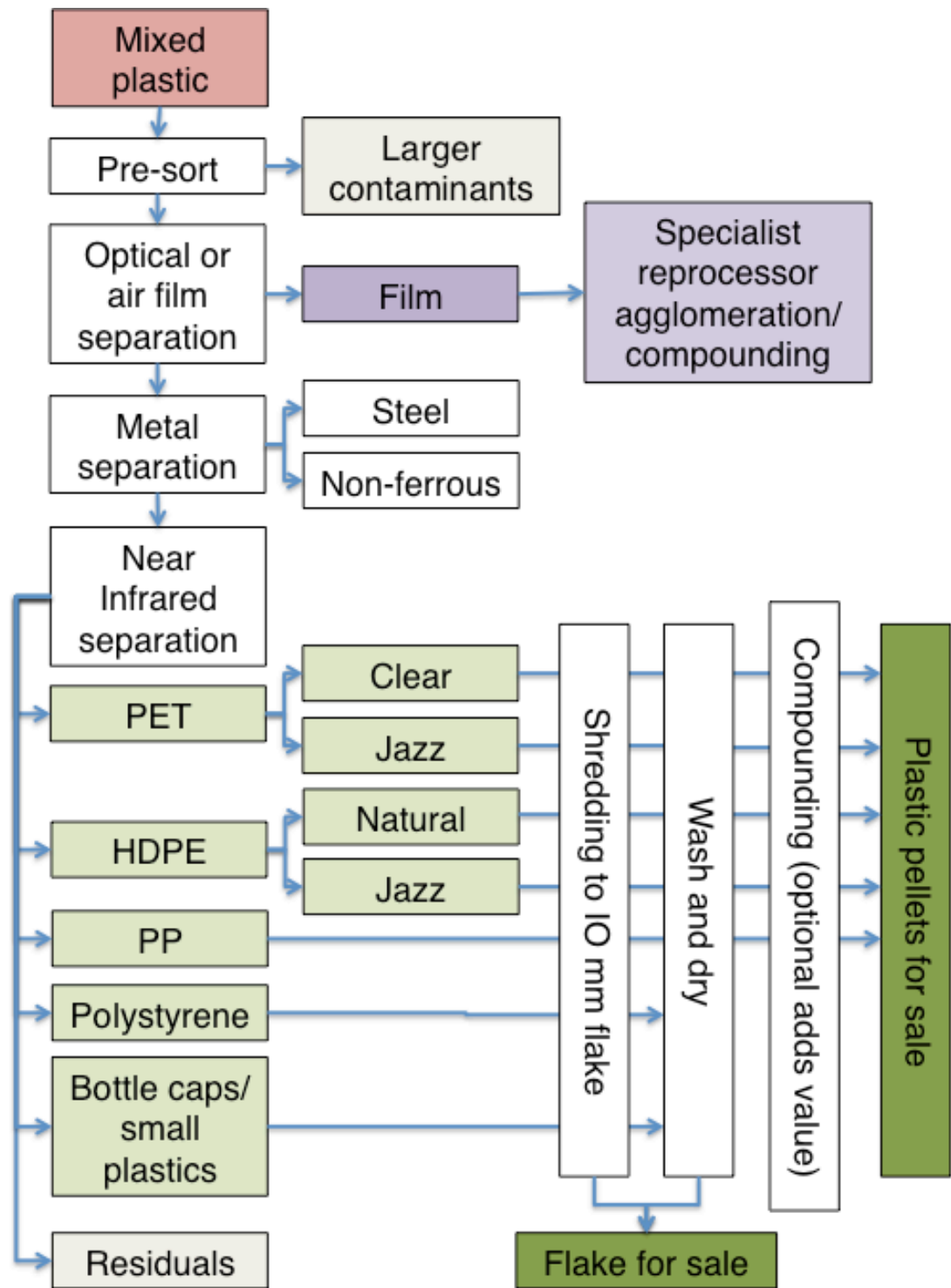
Figure 1.2 Typical recycling and reprocessing plant flowchart [14].

Some of these PRF companies have invested in additional downstream reprocessing equipment to make a high-grade recyclate pellet. Good quality pellet, with material specifications, can be worth up to 70-80% of the virgin material price. Table 1.4 gives representative prices for the different streams [14].

Table 1.4 Representative 2011 prices for types and formats of recyclates [14]. Jazz means mixed colours.

Material	Format	Price £/tonne
PET	Baled bottles (coloured)	11-130
	Baled Bottles (clear)	328-361
	Jazz flake (non-food grade)	600-800
	Food-grade flake	750-950
	Food-grade pellet	900-1100
HDPE	Baled bottles (natural)	330-358
	Jazz flake	300-500
	Black pellet (non-food grade)	750-850
	Food-grade natural pellet	900-1000
PP	Baled containers	100-200
PS	Baled containers (mixed)	0-50
Films	Films (LDPE and others)	0-255
Other	Residual metal	155-185

| Baled bottles | Flake and bottle top | Pellet | Agglomerate film |
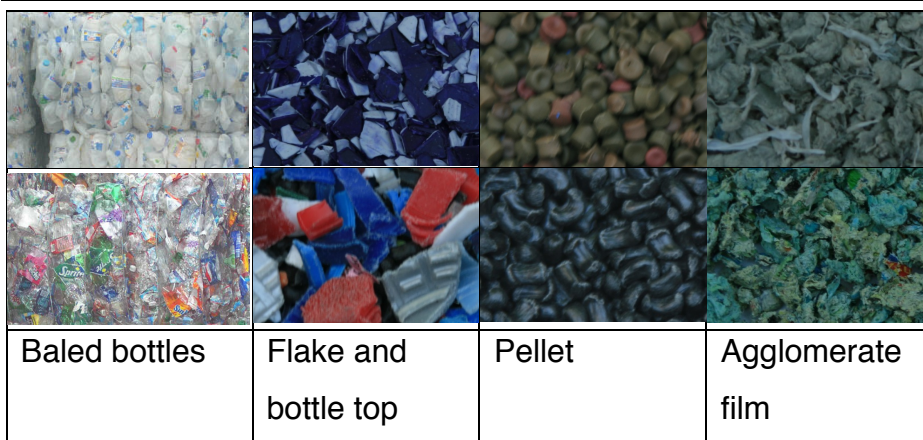
The recycling industry has improved their sorting and cleaning techniques to manage the different waste streams in order to obtain improved purity recyclate

streams in significant quantities and minimize the residual fraction. This high consistency of sorted recyclates and guaranteed volumes were important to the project as certain products had to go through a rigorous qualification process and formulation consistency was important.

Clear and natural plastics have a higher value, because they can be easily coloured. Jazz (mixed colours) produces a grey colour. Colour masterbatch changes the colour, though it does not fully hide the underlying tint. Even with recycled materials, customers demand batch-to-batch colour consistency.

For the project, PET from post consumer packaging was both expensive and too much in demand for other uses such as high value food grade packaging, fleece and strapping. Jazz HDPE flake, PP, PS and films were more economically viable materials, especially since they also possessed lower processing (melting) temperatures.

1.4   Plastic Lumber Manufacturing Technique

There are a variety of different methods for making plastic lumber – modified injection moulding, extrusion and intrusion moulding. The equipment tends to be bespoke and processes kept as a trade secret.

The sponsor company had significant experience with intrusion moulding. Over the course of the project, production was quadrupled with additional production machines and ancillary equipment, which increased the commitment to intrusion moulding. It was stipulated that all formulations had to be suitable for running on the existing process equipment. The process is shown in Figure 1.3.

| Shred to 40mm | Granulate to 20mm | Mix flake |

| Feed to extruder | Extrude into moulds | Remove profile |
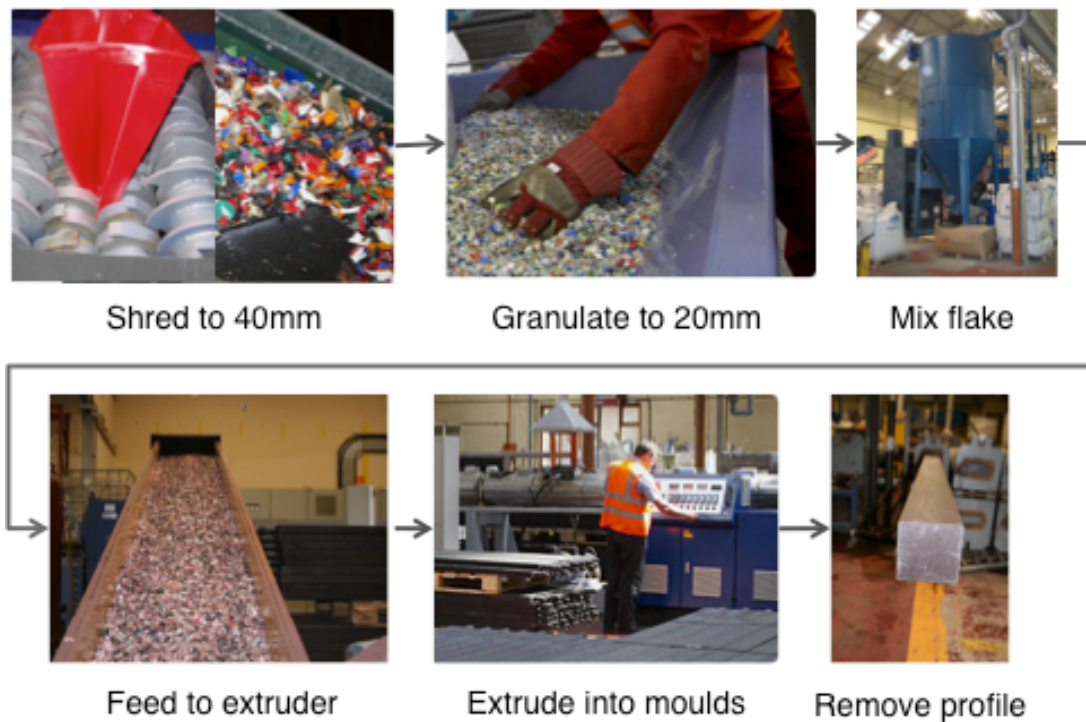
Figure 1.3 The production process to make plastic lumber by intrusion moulding.

In intrusion moulding, the molten plastic is fed directly from the extruder via a manifold system into the moulds. Moulds can be closed or coffin type depending on the desired shape. The mouldings are ejected once sufficiently cooled. Compared to injection moulding, far larger mouldings can be made because it is not limited by the shot size, platen size and holding pressure. The feed points are large making it tolerant of mixed plastics with contaminants such as sand, glass, wood and paper providing there is a minimum polymer fraction of 40% [16]. The long flow path means that the process is not suitable for very stiff materials. Cycle times are long because the cross-sections are large and take a long time to cool. Intrusion moulding is very adaptable to a wide variety of profile sizes and shapes. The company could produce profiles 3 m in length and, cross-sections ranging from 50x25 mm to 250x130 mm, plus specialist shapes.

The company reprocessed post-industrial waste from a variety of sources. It was supplemented with purchased jazz flake. The post-industrial waste was shredded to 40 mm flake, then granulated to 20 mm. The formulation was made by tumble blending tonnes of different types of polymer flake with additives in the form of masterbatch pellet. The formulation was melted and

blended in a single screw extruder then extruded into moulds. Cooling time depended on the mould cross-sectional area. The company produced several different formulations that balanced stiffness and impact strength for different applications.
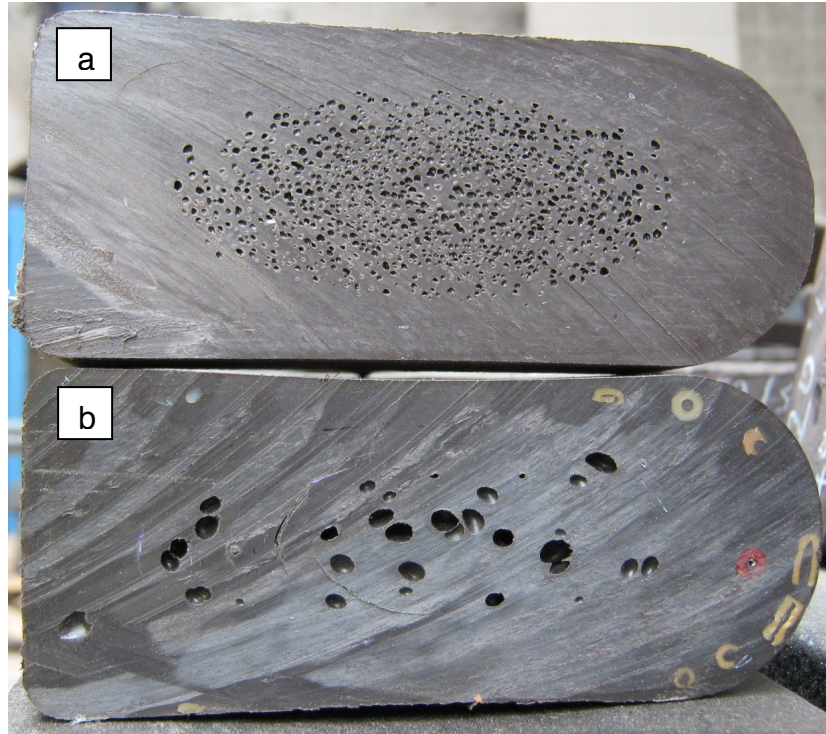
Figure 1.4 The effect of blowing agent on the cross-section of a profile: (a) with the blowing agent, (b) without the blowing agent.

Blowing agent was included in the formulation to give an even cross-section with flat outer surfaces. In the mould, the profile cools and hardens rapidly at the mould surface. As it cools further, the surface is solid and cannot shrink inwards, hence the polymer molecules are pulled towards the profile surface generating internal voids. The blowing agent breaks down to form gases that counteract surface shrinkage and forms a uniform "honeycomb" in the centre. The centre is where the profile remains exposed to the highest internal processing temperature for a relatively long period of time, see Figure 1.4.

The process machinery was mainly designed for polyethylene and polypropylene. ABS could have been processed, however, the major source was WEEE waste, which was contaminated with flame retardants, and hence ABS was not used.

1.5 Plastic Lumber

Recycled plastic lumber was first developed in the 1990s in America. It is produced by a wide range of companies across the world with major markets in America, Germany, UK and Australia. Technologies range from 100% polyethylene products to the use of proprietary reinforced blends.

Plastic lumber is more expensive than wood, heavier and mechanically less stiff. Markets are very competitive. Plastic lumber is not purchased because of its green credentials alone. It is selected over wood because it has performance advantages for certain applications:

– It is low maintenance – it maintains its appearance without the need to paint or use preservative. This is important for councils, housing associations, and charities to reduce any upkeep required.

– Micro-organisms do not feed off it, nor do their waste products affect its physical properties.

– It does not rot or require preservatives in wet environments. Therefore, does not leach chemicals that can contaminate the environment. This is important in marshlands and sites of special scientific interest.

– Animals do not eat it – for example, horses, livestock, rats and termites. This is important for stabling and grain store floors.

It is selected over concrete for certain applications because it is lighter and chemically inert.

Figure 1.5 Plastic lumber applications – fences, retaining walls, boardwalks, paths, stabling, seating and bollards.

Figure 1.6 Structural applications for composite plastic lumber (top) crib walls and (bottom) railway sleepers.

Acceptance in the UK has grown for particular applications as shown in Figure 1.5. These applications make up the bulk of plastic lumber uses in the UK, however, do not use the material to its full advantage.

Structural applications require qualification testing and guaranteed, consistent, high performance. Crib walls to retain earth embankments and railway sleepers are the most significant structural applications, see Figure 1.6. For crib walling, the major advantage is long life in wet environments. For example, buried softwood timber has been found to be severely rotten within 10 years, even though it was treated to a standard of preservation certified for 50-100 years [17].

Sleepers have been commercially available in America since 1995. Small amounts of composite sleepers are used in other countries including Holland, Germany and Japan. The products in the composite plastic railway sleeper market fall into two categories – metal reinforced and polymer composite. Uptake has been slow due to their extra cost [18]. For Network Rail, composite sleepers were attractive to meet UK Government requirements for use of recycled products, to replace treated softwood in wet and aggressive environments, to minimise contamination in environmentally sensitive areas, and as a substitute for hardwood timbers [19]. This latter reason is a particularly important, because sustainably grown, good quality, hardwood is becoming increasingly difficult to source and very expensive, especially for large cross-sections and long lengths. This is discussed further in Section 6.8.

The project attained two major product approvals in 2012. The British Board of Agrément accredited a crib walling system that utilised the optimised formulations achieved through polymer blending [20]. Network Rail approved sleepers for track trial, that used a formulation optimised for engineering performance. Both products required extensive qualification testing, with the latter application requiring years of qualification testing under a stringent and comprehensive test protocol.

1.6 Summary

Recycled plastic lumber is an important product for the effectiveness of the waste hierarchy because it can use lower grade waste streams by virtue of its significantly thicker cross-section. The aim of this project was to leverage these lower grade waste streams to produce a high performance, higher value product for structural applications.

The material choice was an important decision for the commercial success of the project due to the rising recyclates cost, the change in recyclates available and the volumes of material likely to be required for each product. A plastic formulation tolerant of higher contamination levels was economically very desirable for the project. Particularly considering that good quality material such as LDPE regrind increased in price by 75% over the course of the project [7].

The project was committed to using the production technique of intrusion moulding, due to the major investment in production facilities at the sponsor company.

In Chapters 2, 3 and 4, the blending of different polymers and waste streams are investigated to maximize the advantageous properties of each component polymer in the blend. Optimum thermo-mechanical properties were achieved by phase separated blends. In a second phase, reinforcement was added produce an even higher level of performance.

2 Literature Review

This chapter details the properties of the key thermoplastic polymers and reviews the existing practice in polymer blending research. The purpose of the review was to scope the design of a range of polymer blends that were most suitable for the application. The compounds had to be capable of carrying significant in-service, dynamic loads over a wide spectrum of outdoor temperatures and conditions with a minimum service life of 50 years.

Structural plastic lumber requires a complex range of properties such as strength, stiffness, toughness, suitable operating temperature range within the ambient temperature range of the climate, low creep, fatigue resistance, chemical resistance, good weathering and resistance to microbial attack, and reduced coefficient of thermal expansion (CTE).

When selecting virgin polymers for an application there are many grades, which are suited to specific manufacturing processes and with an array of desirable properties. The different grades are indistinguishable when they are recycled unless the exact source is precisely known. Specific sources are usually only available in limited amounts, which would have been inadequate for this application. With recyclate, the challenges are to overcome the limited range of feedstocks, their variability and any possible contamination. The aim is to make a product with consistently good properties by careful formulation and production method selection.

In the previous chapter it was explained that polyethylene and polypropylene had to be selected for the basis of the formulation, since they were available in sufficient quantities and their mixed blends were relatively inexpensive. Polyethylene and polypropylene alone could not provide the required properties. Blends of polymers and the addition of fillers were investigated to improve the mechanical properties and reduce the effect of feedstock variation.

2.1 Polymers

2.1.1 Polyethylene

Polyethylene (PE) is a semi-crystalline, thermoplastic polyolefin. It is widely used due to its low cost, ease of processing and advantageous properties.

Polyethylene is the simplest polymer structure, which is essentially a long chain aliphatic hydrocarbon:

From this simple chemical structure arises a multiplicity of different polyethylene grades. The common categories with example density ranges are [21]:

– ULDPE – Ultra low density (0.855-0.900 g/cm^3)
– VLDPE - Very low density (0.900-0.910 g/cm^3)
– LLDPE - Linear low Density (0.910-0.925 g/cm^3)
– LDPE - Low density (0.910-0.925 g/cm^3)
– MDPE - Medium density (0.926-0.940 g/cm^3)
– HDPE - High density (0.941-0.969 g/cm^3)
– UHMWPE - Ultrahigh molecular weight (~0.969 g/cm^3)

The different grades vary in the amount of short chain branching; amount of long chain branching; average molecular weight; molecular weight distribution and presence of comonomers [22]. Figure 2.1 gives examples of the different structures.
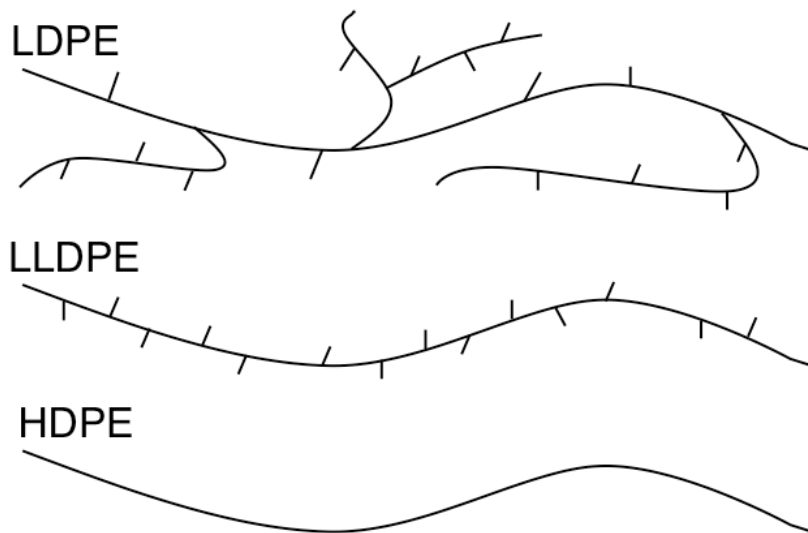
Figure 2.1 A Schematic of the variety of polyethylene molecular structures with short and long chain branching [23].

Polymer structure effects crystallinity and hence the density, because side chains hinder crystal formation. Polyethylene that has a regular chain structure can adopt a planar zigzag conformation [24]. In turn the chains fold to lamellae forming a highly ordered crystal structure, see Figure 2.2. The lamellae consist of many different chains and one chain can be incorporated in different lamellae, which produces a stiff, tough, stable structure. In between the lamellae are amorphous regions of non-crystalline tie molecules. These tie regions provide flexibility and impact resistance [25]. Generally an increase in tie points increases strength, however, too many can cause brittleness and loss of toughness. Long side chains and chains with side branches can also form lamellae, however, the lamellae tend to be smaller, which have lower intermolecular forces and melt at lower temperatures.

HDPE is produced by Ziegler-Natta catalysis, which creates linear chains, high crystallinity (70-80%) and higher densities [26]. HDPE tends to have improved density, heat resistance, creep resistance, stiffness, strength, toughness and chemical resistance, and reduced clarity [22].
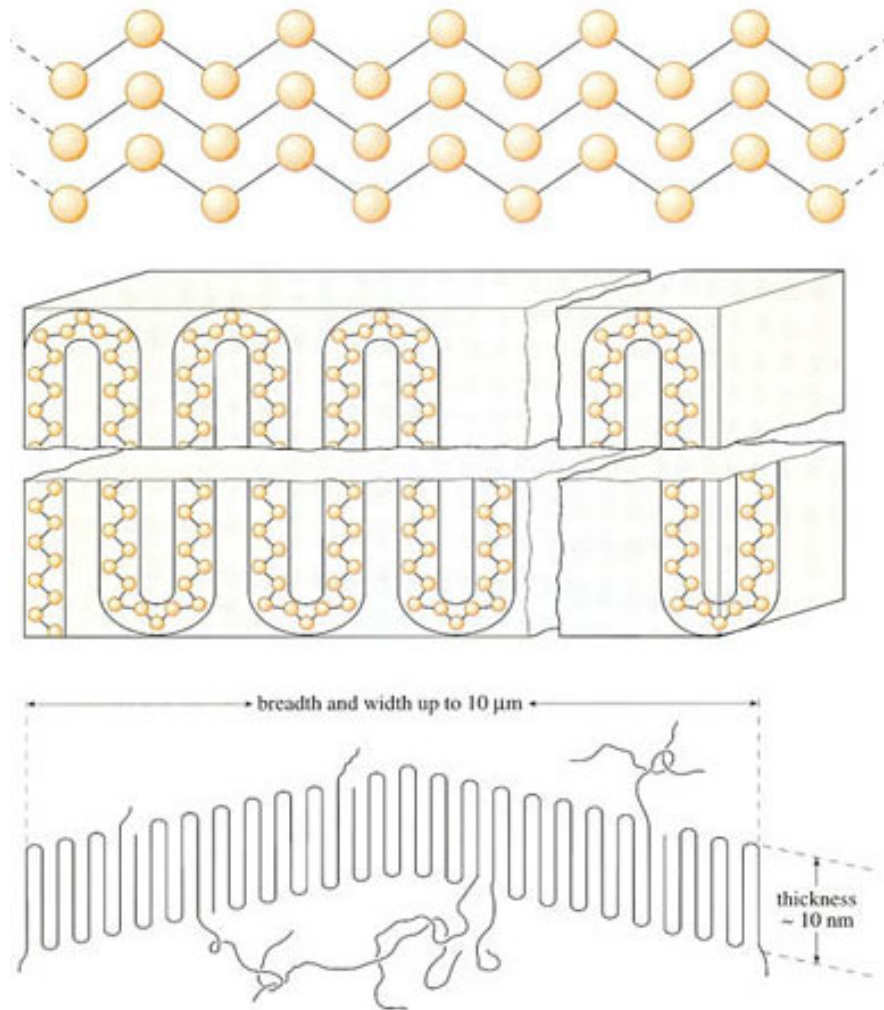
Figure 2.2 Crystal structure of HDPE (Top) Zig-Zag conformation of PE chains stacking within crystal. (Middle) Chain folded model for PE in lamella. (Bottom) Dimension of PE Single crystal showing non-crystalline tie molecules. [24]

LDPE is produced by free radical initiated polymerisation of ethylene under high pressure and temperature. It has a high degree of random short and long chain branching, which limits the crystallinity (44-55%) [26]. It is good for film and shrink wrap, because low crystallinity gives a clear, flexible product and the long chain branches entangle in the melt giving good melt strength [22].

LLDPE has branching of uniform length, randomly distributed along the chain. It is created by adding small amounts of propene, but-1-ene, hex-1-ene or oct-1-ene in a catalysis process. This produces excellent toughness at all temperatures compared to LDPE, however, reduces melt strength. It is used for film and low stiffness injection mouldings [22].

The interplay between molecular weight, structure and morphology produces a complex mixture of properties. There is a significant overlap between the different types of polyethylene. Table 2.1 compares the generic properties of LLDPE and HDPE from the United Laboratories Prospector database.

Table 2.1 Generic properties of Linear Low Density Polythylene and High Density Polyethylene [27, 28]

Property	Standard	LLDPE	HDPE
Specific gravity (g/cm^3)	ISO 1183	0.907-0.935	0.944-0.976
Melt flow rate 190 ^{o}C/ 2.16 kg (g/10 min)	ISO 1133	0.2-6.3	0.03-10
Mould shrinkage (%)	ISO 294-4		1.4-2.0
Tensile yield strength (MPa)	ISO 527-2	7.6-18.5	20.8-31.6
Tensile modulus (MPa)	ISO 527-2	179-494	834-1358
Tensile elongation at yield (%)	ISO 527-2	14-22	2.5-17
Tensile elongation at break (%)		290-540	6-1000
IZOD notched impact (kJ/m^2)	ISO 180	23.1-50.5	1.9-31.5
Brittleness temperature (^{o}C)	ISO 974	-70	-70.5 to -60
Heat Deflection Temperature under load 1.8 MPa (^{o}C)	ASTM D648	34-71	37-82
Vicat softening temperature (^{o}C)	ISO 306	93-117	69-129
Melting temperature (^{o}C)		119-125	127-137
Dielectric constant	ASTM D150	2.1-2.55	2.28-2.31

For standards see [2, 29–36].

Table 2.1 illustrates one disadvantage of semicrystalline polymers such as polyethylene. The maximum load bearing temperature is much lower than the maximum temperature at which the polymer is chemically stable for long periods. The maximum load bearing temperature is also much lower than the softening point where the modulus catastrophically drops [22]. In amorphous materials the softening point is close to the glass transition temperature, T_g. In semicrystalline materials, the modulus changes around T_g followed by a

catastrophic change around the melt temperature, T_m. Higher crystallinity reduces the modulus change at T_g. Many polymers soften progressively between T_g and T_m because the crystalline structures melt at different temperatures. The maximum operating temperature varies considerably depending on the test used. In Table 2.1, heat deflection temperature (HDT) and Vicat softening point are used [1, 34]. The values differ by between 30 and 60 ^{o}C. Vicat softening is a measure at which a material loses its "form stability". In the test, the plastic is heated at a specified rate and the temperature is defined as the point at which a loaded needle penetrates the sample by a specified distance.

HDT is a better measure of when a material loses its load bearing capacity. The sample is heated under load in a three-point bend mode until the sample deforms by a specified amount. The HDT values given in Table 2.1 are within the ambient temperature range for the Northern hemisphere. One option is to use fillers, such as glass fibre, which can change the softening temperature significantly for semicrystalline materials, however, not for amorphous ones [22]. Values close to T_m can then be obtained by increasing the useful operating range.

Polyethylene has very desirable properties for a range of applications [22]. The wide range of molecular structures available means that grades can be tailor-made for different applications and processes. In Table 2.1, it can be seen that the glass transition temperature of polyethylene is very low. This is due to the highly flexible C-C chains. Therefore, polyethylene is tough and flexible at low temperatures, which means it is suitable for freezer and transport containers. Polyethylene is basically a high molecular weight alkane (paraffin), which means it is nonpolar, with low water absorption, and a good electrical insulator. LDPE is used for wire and cable insulation, where it is often crosslinked. Its inert nature causes one major disadvantage in that it is difficult to join using adhesives. The chemical structure also means that it has a very good chemical resistance, low toxicity and low odour. Food contact grades can be produced and it is widely used for food packaging, film, industrial and household chemical

containers, milk containers, bags, fuel tanks, and pipes. The increased crystallinity of HDPE further improves chemical resistance due to its strong molecular packing. Environmental stress cracking resistance varies widely between grades. Resistance to ultraviolet light is also very grade dependent. It has a tendency to embrittle through absorption of 220-320 nm wavelengths by carbonyl groups.

Polyethylene has very good processability [22]. Melt flow and melt strength can be adapted to suit different processing techniques - injection moulding, blow moulding, extrusion and calendaring. No drying is required, because polyethylene is non polar and does not absorb moisture. At 160-190 ^{o}C, process temperatures are comparatively low, due to the flexible backbone and no strong intermolecular forces. However, the stability of the structure produces a high specific heat capacity, which means that high levels of energy are required to melt polyethylene. Care has to be taken, because it can oxidise in air at melt temperatures. The level of crystallinity determines the degree of shrinkage on cooling. Highly crystalline grades shrink significantly.

When polyethylene articles are recycled, they are generally separated into two waste streams – LDPE and HDPE. These may be subdivided into ranges of viscosity by selecting the source.

When the recycled polymer is processed, the morphology determines the effect and degree of degradation. Highly branched polymers become more crystalline, whereas unbranched polymers become less crystalline. With repeated reprocessing, increases and decreases have been observed in MFI, tensile strength and elongation even for the same polymer type [37].

Different grades are not necessarily compatible when recycled, due to their molecular structure and with the presence of photo-oxidative degradation products such as carbonyls, hydroxyls and carboxyls from the polymer and the additives present [38].

For this application, high density polyethylene had some very desirable characteristics, however, relatively low stiffness, strength and operating temperature rendered this material unsuitable for structural applications, unless it was reinforced.

2.1.2 Polypropylene

Polypropylene (PP) is a semi-crystalline, thermoplastic polyolefin with similar properties to HDPE. It is manufactured with Ziegler-Natta or metallocene catalysts [22]. In structure it is a linear hydrocarbon with a methyl group attached to alternate carbon atoms. The position of the pendant methyl group position creates forms of PP with different tacticity, see Figure 2.3. In isotactic PP, the methyl group is on one side of the chain, being the most common commercial form. In syndiotactic PP the methyl groups alternate sides. Atactic has random positioning of the methyl groups.

$$- CH - CH_2 - CH - CH_2 - CH - CH_2 - CH - CH_2 - CH - CH_2 - \quad (a)$$

with CH_3 groups above each CH.

$$- CH - CH_2 - CH - CH_2 - CH - CH_2 - CH - CH_2 - CH - CH_2 - \quad (b)$$

$$- CH - CH_2 - CH - CH_2 - CH - CH_2 - CH - CH_2 - CH - CH_2 - \quad (c)$$

Figure 2.3 Tacticity in polypropylene (a) isotactic (b) syndiotactic (c) atactic [23]

The pendant methyl groups cause the polymer chain to crystallise by twisting in a helix either to the left or the right [22]. One revolution involves three groups and forms a very close packed structure. The helical chains then fold to form lamellae like polyethylene. At ~20 µm/min, the growth rate is far slower than HDPE at ~5000 µm/min [24], hence nucleating agents are often used to encourage crystal formation.

Atactic polypropylene is amorphous with low crystallinity. It is tough and flexible with no defined melting point. It is used for hot melts, adhesives and modifying polyethylene, rubber and other materials [25].

Commercial polymers are 90-95% isotactic [22]. Syndiotactic and atactic can be present as full chains or blocks in the structure. Stereo-block polymers have sections of right hand helix are followed by sections of left hand helix [25].

Polypropylene has very similar properties to polyethylene. The pendant methyl group makes the backbone stiffer and interferes with molecular symmetry [22]. The melting point is raised by about 50 ^{o}C producing higher temperature resistance. Perfect Isotactic polypropylene theoretically melts at 171 ^{o}C. In commercial grades the melting point is reduced to 160-166 ^{o}C. The melting point in syndiotactic polypropylene with 30% crystallinity is even lower at 130 ^{o}C [25]. Commercial isotatic grades can withstand boiling water and sterilisation.

The glass transition temperature is a major weakness as it occurs near 0 ^{o}C. This means it is brittle at subzero temperatures and even at low ambient temperatures. Increasing molecular weight can improve T_g, toughness, and melt viscosity by hindering crystallisation, however, it is at the expense of strength, stiffness, hardness and softening point [22].

Mechanically PP tends to be stiffer, stronger and harder than PE. The fatigue resistance is one of the best compared to other semicrystalline and amorphous polymers. Tolerance to the irreversible microscopic damage caused by the

cyclic loading can be one reason, and this is why generally semicrystalline polymers show better fatigue endurance than amorphous polymers [25, 39].

The chemical resistance of polypropylene is similar to that of polyethylene, and is less prone to stress cracking. However, the tertiary carbon atom makes PP more prone to UV radiation and oxidation at higher temperatures. Polyethylene crosslinks on oxidation, whereas polypropylene undergoes chain scission. Hence, it is not suitable for high energy crosslinking [22]. Stabilisers can be added, however, their functionality may have been exhausted when PP is recycled, hence the molecular mass can be reduced. Recycled material thus can be of lower strength, have lower oxidation stability and become discoloured [38].

Polypropylene can be processed by a wide range of techniques such as extrusion, injection moulding and thermoforming. Polypropylene homopolymer in fibre form is used for fabrics, filters, geotextiles, strapping tape and disposable nappies [25]. In film and sheet form it is used for tapes, shrink film and thermoformable containers. It is also injection moulded into parts for cars, electrical appliances, containers, and other semi-structural applications.

Polypropylene is also produced in a wide variety of copolymer grades to improve toughness and low temperature properties, however, at the cost of strength, stiffness and maximum operating temperature. Copolymers are formed by adding different monomers into the polymer chain. There are two major types shown in Figure 2.4 - random copolymer and block/impact copolymers.

Random copolymers commonly use 1-7 wt% ethylene as a co-monomer. Crystallinity is reduced and chain mobility increases, due to the lower steric interaction of the methyl groups [25]. This produces a material with clarity and reduced density with increased toughness even at low temperatures. Random copolymer is used for films, shrink wrap, blow moulded refrigerated packaging, injection moulded reusable food containers and packaging.

Block copolymer
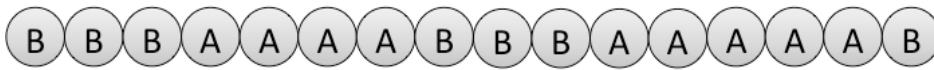
Random copolymer

Figure 2.4 Polypropylene copolymer types – block copolymer and random copolymer [25].

Block copolymers are often called impact copolymers. They are modified with 5-25% of a variety of copolymers such as ethylene-propylene rubber, ethylene-propylene-diene, plastomers, polyethylene, homopolymer and random copolymers [25]. Copolymer is not miscible and phase separates forming evenly distributed, rubbery, amorphous nodules in the semicrystalline homopolymer matrix. These nodules provide impact resistance by absorbing energy instead of allowing crack propagation through the matrix. Block copolymers have far better low temperature impact resistance than homopolymers or random copolymers. Grade selection is a balance between toughness, strength, stiffness, and temperature performance. Using filled grades significantly improves the maximum operating temperature and stiffness. Impact copolymers are used primarily for injection moulding products for appliances, household items, luggage, outdoor furniture and automotive parts such as battery cases and bumpers [25].

A wide range of block copolymers are commercially available, and Table 2.2 shows a comparison between two block copolymers with similar melt flow, injection moulding grades of homopolymer and random copolymer. Sabic PP PHC27 impact copolymer is recommended for crates & boxes, suitcase shells and automotive parts. PP 48M10 impact copolymer is designed for articles with complex shapes, such as crates and boxes, rigid packaging and components for the automotive and electro-technical industries. PP575P homopolymer is typically used for closures and garden furniture. PP670Kh random copolymer is typically used for caps, closures, lids, housewares and appliances [40].

Table 2.2 Comparison in properties of four injection moulding grades: SABIC polypropylene PP575P homopolymer, PP48M10 (Block1) and PPPHC27 (Block2) block copolymers and PP670Kh random copolymer [40].

Property	Standard	Homo	Block1	Block2	Random
Specific gravity (g/cm^3)	ISO 1183	0.905	0.905	0.905	0.905
Melt flow rate 230 ^{o}C/ 2.16 kg (g/10 min)	ISO 1133	11	15	14	11
Tensile modulus (MPa)	ISO 527-2	1700	1400	1000	1050
Tensile yield strength (MPa)	ISO 527-2	36	26	21	27
Tensile elongation at yield (%)	ISO 527-2	9	5	6	14
Charpy notched impact -20 ^{o}C (kJ/m^2)	ISO 179/1eA		6	8	
Charpy notched impact 0 ^{o}C (kJ/m^2)/m2	ISO 179/1A		7	15	2
Charpy notched impact 23 ^{o}C (kJ/m^2)	ISO 179/1A	4	11	60	6.5
IZOD notched impact -20 ^{o}C (kJ/m^2)	ISO 180		5	9	
IZOD notched impact 0 ^{o}C (kJ/m^2)	ISO 180		7	13	2
IZOD notched impact 23 ^{o}C (kJ/m^2)	ISO 180/1A	3	8	No break	6
Deflection temperature under load 0.45 MPa (^{o}C)	ISO 75-2/Bf	90	90	80	75
Deflection temperature under load 1.8 MPa (^{o}C)	ISO 75-2/Af	55	55	50	50
Vicat softening temperature 10 N load 120 ^{o}C/h (^{o}C)	ISO 306/A120	154	151	145	126
Vicat softening temperature 50 N load 120 ^{o}C/h (^{o}C)	ISO 306/B120	95	95	65	69

Table 2.2 gives the impact properties using two different standards – IZOD and Charpy [33, 41]. There is good correlation between the two tests, even though they should not be numerically compared and their test methods are different. IZOD bars are held vertically in a vice. The sample is struck by a pendulum and the energy required to break is noted. In notched samples, the notch is just above the vice and is facing towards the hammer. In Charpy, the sample is horizontal and supported (not gripped) at each end, and a hammer impacts at the centre. In notched samples, the notch is on the opposite side to the hammer blow. Both tests provide useful comparison of data between materials, however, they cannot be used to predict the results for samples of larger cross-sections [22]. Some materials like polycarbonate are very notch sensitive and produce dramatically lower results with a notch.

In terms of the project, the improved temperature resistance, fatigue endurance and stiffness of polypropylene were of benefit. The stiffness alone was not sufficient and the poor low temperature impact resistance was found to be a disadvantage.

2.1.3 Polystyrene

Polystyrene (PS) is an amorphous, substantially linear polymer with the structure shown in Figure 2.5. The pendant benzene ring creates different states of tacticity as described for polypropylene. Commercial polystyrene varies in tacticity sufficiently to prevent crystallisation. The pendant benzene ring stiffens the polymer chain raising the T_g to 90-100 ^{o}C, which gives a rigid, transparent, high refractive index and brittle material at room temperature [22]. The maximum operating temperature is far closer to its T_g, however, other properties drop sharply in this region.
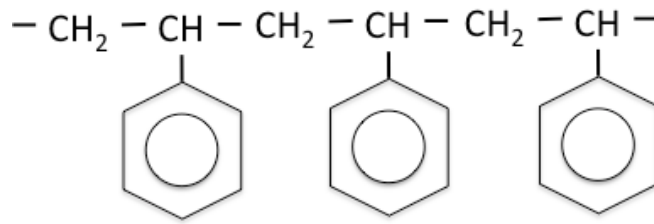
$$- CH_2 - CH - CH_2 - CH - CH_2 - CH -$$

Figure 2.5 Polystyrene molecular structure [22].

Pure polystyrene has some common properties to polyethylene: no taste, odour or toxicity; good electrical insulation; and low water absorption. The benzene rings mean that PS is more reactive than polyethylene to chemicals and UV light. Chemical resistance is good except to hydrocarbons, esters, ketones and essential oils [42]. Also, it burns with a sooty flame compared to polyethylene and polypropylene.

Being amorphous means it has good dimensional stability and low mould shrinkage compared to PE and PP (0.5% mould shrinkage compared to 1.4-2.0% for PE [27, 43]). It is low cost and easily colourable, hence is widely used for injection moulding, extrusion, vacuum forming and foam production.

To improve toughness, high impact polystyrenes (HIPS) are modified during polymerisation with 5-20% of a semi-compatible rubber e.g. styrene grafted polybutadiene rubber or polybutadiene [22, 42]. The rubber forms discrete 1-10 μm droplets in the matrix that are able to arrest the crack propagation. This reduces clarity, softening point and tensile strength, see Table 2.3.

Polystyrene is used for packaging, bottle caps, small jars, containers, housewares, injection moulded parts, electrical appliance housings, foamed packaging, insulation, fridge liners, etc. [42]. The main sources in the waste stream are coat hangers, yoghurt pots, plant pots, packaging and insulation. Foamed polystyrene is difficult to recycle, because it needs to be densified in order to be transported economically.

For the project, polystyrene was interesting as a stiff, amorphous polymer to blend with the semicrystalline polypropylene and polyethylene for reinforcement.

Table 2.3 Comparison in properties of general purpose polystyrene Styrolution PS 124N/L and high impact polystyrene Styrolution PS 454N [43, 44]

Property	Standard	PS	HIPS
Specific gravity (g/cm^3)	ISO 1183	1.04	1.04
Melt flow rate 200 ^{o}C/5 kg (g/10 min)	ISO 1133	12	14
Tensile modulus (MPa)	ISO 527-2	3200	2200
Tensile yield strength (MPa)	ISO 527-2	50	27
Tensile elongation at break (%)	ISO 527-2	2	
Charpy notched impact 23 ^{o}C (kJ/m^2)	ISO 179/1A		16
Charpy unnotched impact 23 ^{o}C (kJ/m^2)	ISO 179/1A	10	
Deflection temperature under load 0.45 MPa (^{o}C)	ISO 75-2/Bf		82
Deflection temperature under load 1.8 MPa (^{o}C)	ISO 75-2/A	78	78
Vicat softening temperature (^{o}C)	ASTM D 1525	87	82
Vicat softening temperature (^{o}C)	ISO 306/A50		91

2.2 Polymer Blends

As discussed in Section 2.1, the individual polymers did not possess the required properties, hence polymer blends were investigated. Blending polymers is a common commercial practice to improve and extend performance or processability of polymer compounds. Blending is a very cost-effective method of developing new materials on relatively low cost equipment compared to developing entirely new polymers [21]. Blends can provide a unique combination of properties not available in one polymer. The properties can be quickly tailored to different customer needs in small to large batch sizes. A large inventory of different materials is not required. Blending creates commercially useful materials when using recycled materials or for batches that have failed to meet the required specification.

About 36 wt% of polymers used commercially are some form of miscible or immiscible blend, i.e. at least 2 wt% of another polymer or copolymer [21]. Commercial polymers blends are mostly designed to be compatible or have some degree of compatibility, in order that they remain ductile and do not delaminate. In this case compatible polymers are either molecularly miscible or are morphologically distinct phases that are interfacially stable [21]. The miscibility of polymers is dependent on the balance of small enthalpic and non-configurational entropic effects. Compatibility can arise from: thermodynamic miscibility; segmental miscibility (there is an adequate level of interfacial adhesion even between separate phase); or by using compatibilising additives such as block or graft copolymers that reduce interfacial tension, stabilise the morphology and strengthen adhesion at the interface. It was a project requirement to investigate the limits of polymer blends without the added cost of compatibilisers. For example, elastomers such as SBS (styrene-butadiene-styrene) and SEBS (styrene-ethylene-butadiene-styrene) were not available as a waste stream and virgin costs were prohibitive.

The physical properties of the blend are altered by the blend composition, phase morphology and their relative crystallisation behaviour [21].

The morphology of a polymer blend depends on: the proportion of each polymer, the process conditions, the individual and comparative polymer flow characteristics and, interactions in the melt phase and during solidification [21]. At low concentrations, the dispersed phase forms nearly spherical droplets in the matrix of the other polymer. At higher loadings, the dispersed phase can form cylinders, fibres or sheets. When proportions are similar, a co-continuous structure can be formed, which is also called an interpenetrating network, see Figure 2.6. Synergism of properties can arise in this region such as high modulus with good impact performance.
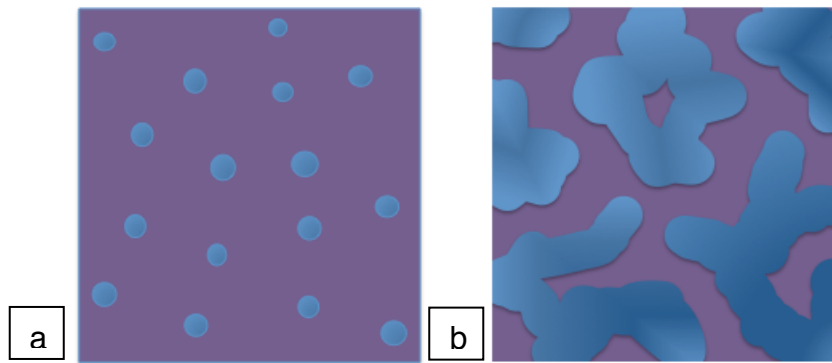
Figure 2.6 Schematic of blend morphology types (a) dispersed phase (b) co-continuous structure

The degree and nature of crystallisation in the phases may greatly influence the mechanical behaviour, and particularly, the fracture mechanisms. In an immiscible blend the phases are physically separated in the melt. The crystallisation process is influenced by molecular composition and molecular mass of the components, blend composition, type and degree of dispersion of the phases in the melt, interactions between phases, melt history, crystallisation conditions (e.g. cooling rate), and physical crystallisation conditions (e.g. second phase molten or solidified) [21]. In a blend with two semi-crystalline polymers, the phases crystallise separately around their characteristic bulk crystallisation temperature, T_c. T_c is altered by primary nucleation on heterogeneities and at the interface between phases. Heterogeneities are residual catalysts, fillers, impurities, crystalline residues, etc.. These migrate between phases depending upon their relative interfacial free energy. This changes the nucleation density in each phase and, hence, the spherulite size of the phase compared to crystallisation in the pure polymer. The nature of the spherulites is also effected i.e. shape, spherulite texture and interspherulitic boundaries. In blends with two semicrystalline polymers, the crystallisation behaviour of one phase depends whether the other phase is molten or already crystallised. It has been observed in HDPE/PP blends, the PP nucleation rate decreases when the melt is held at a temperature above above T_c of HDPE, however, it increases when the melt is below T_c of HDPE [45]. In the former case, heterogeneities migrate from PP to HDPE reducing the number of nucleation sites. In the latter case, HDPE crystals act as nucleation sites for PP.

When amorphous PS is dispersed in semi-crystalline PP, heterogeneities have been observed to move from PS to PP [46]. This increases the nucleation density in the PP, and is more significant than the nucleation on the very sharp interface between the phases. Increased crystallinity and reduced spherulite size improves impact strength, stiffness and yield strength [47–49].

In the next section the effect of polymer selection, sample manufacture method and test parameters are compared for polyethylene and polystyrene blends. Following this blends of polyethylene, polypropylene and polystyrene are discussed.

2.2.1 Polyethylene and Polypropylene Blends

In commercial grades, polyethylene is only added to polypropylene at low concentrations to improve low temperature impact strength. These are immiscible blends, or are compatibilised with Ethylene-Propylene rubber (EPR) or EPDM (Ethylene Propylene Diene terpolymer rubber) by reactive blending or post-blending co-crosslinking [21].

The prevalence of mixed PE and PP waste has led to a large amount of academic research to understand and improve the properties. The results have been very mixed. Results vary with the polymers used, compounding methods, sample preparation and test speeds. To investigate the affect of these factors, four studies are compared in Table 2.4 and Table 2.5. Table 2.4 compares three studies where 70 wt% PP was blended with either 30 wt% HDPE or post consumer resin (PCR). The PCR contained equal proportions of LLDPE, HDPE and PP. Table 2.5 compares studies where 70 wt% HDPE was blended with either 30 wt% PP or PCR. The tables do not give the actual values because each study used different test regimes, which make the values not comparable.

Table 2.4 Comparison of blend studies using 70 wt% PP with either 30 wt% HDPE or 30 wt% post consumer resin (PCR). Percentage deviation from values predicted by rule of mixtures is provided [50–52].

Property	Deviation from rule of mixtures (%)		
	Greco[50]	Jose[51]	Blom PCR[52]
PP MFI (g/10 min)[1]	3.9	3	20
HDPE MFI (g/10 min)[2]	3.7	20	34[3]
Test speed (mm/min)	5	50	254
Flexural modulus			0
Tensile Modulus	0	+40	
Yield strength	+28	-25	[4]
UTS	-30	-20	+10
Impact[5]		-75	+40

[1] Standard conditions are 2.16 kg 230 $^\circ$C. Only confirmed by Blom.

[2] Standard conditions are 2.16 kg 190 $^\circ$C. Only confirmed by Blom.

[3] weight and temperature not specified

[4] PCR did not yield.

[5] IZOD notched impact in kJ/m^2 for Jose study. Charpy unnotched in J/m in Blom study.

Displayed is the percentage deviation of the result from that predicted by the rule of mixtures. For a blend, the rule predicts the value of property, Y, from the values of the component parts according to the proportions of the volume fractions, Φ, [21]:

$$Y = \Phi_1 Y_1 + \Phi_2 Y_2 \qquad \text{Linear rule of mixtures} \qquad 2.1$$

For miscible or well-compatibilised blends, modulus and yield stress are additive, however, maximum strain at break, ε_b, follows the inverse rule of mixtures [21].

$$1/\varepsilon_b = \phi_1/\varepsilon_{b1} + \phi_2/\varepsilon_{b2} \qquad \text{Inverse rule of mixtures} \qquad 2.2$$

Table 2.5 Comparison of blend studies using 70 wt% HDPE with either 30 wt% PP or 30 wt% post consumer resin (PCR). Percentage deviation from values predicted by rule of mixtures is provided [50–53].

Property	Deviation from rule of mixtures (%)				
	Greco	Jose	Blom HDPE5	Blom HDPE65	Blom PCR
HDPE MFI (g/10 min)[2]	3.7	20	5	65	5
PP MFI (g/10 min)[1]	3.9	3	20	20	34
Test speed (mm/min)	5	50	254	254	254
Flexural modulus			+25	-8	+18
Tensile modulus	0	+21			
Yield strength	0	-2	0		[4]
UTS	-38	-25	-5	+5	0
Impact[5]		-45	-45	-65	-60

[1] Standard conditions are 2.16 kg 230 $^{\circ}$C. Only confirmed by Blom.

[2] Standard conditions are 2.16 kg 190 $^{\circ}$C. Only confirmed by Blom.

[3] weight and temperature not specified

[4] PCR did not yield.

[5] IZOD notched impact in kJ/m^2 in Jose study. Charpy unnotched in J/m in Blom study.

Interactions between the component polymers and heterogeneities present can cause synergistic or antagonistic deviations from these rules.

The test parameters used in each study were substantially different. Fast speeds of 254 mm/min were used in one study, whereas ISO 572-1 recommends testing at 1% of gauge length per minute for modulus measurement i.e. 0.5 mm/min with 50 mm gauge [54]. Polymers are viscoelastic in nature, which means their response varies depending upon the strain rate used [39]. At low strain rates, the polymer chains have sufficient time to flow giving higher elongations, lower modulus and lower strength. At high strain rates the material does not have time for viscous deformation. Low strain rate mechanical testing is commonly used to investigate formulations [21].

Blend morphology, crystallinity and the nature of the interphase boundaries will affect the behaviour of the blend at different strain rates. In the 70 wt% PP blends, each study observed a synergy in a different property: an increase in tensile modulus was observed at 5 mm/min [50]; an increase in yield strength was observed at 50 mm/min [51]; and an increase in the ultimate tensile strength (UTS) with no yielding was observed at 254 mm/min [52].

Trends in impact strength gave examples of test method and material related differences. In 70 wt% PP blends, impact strength decreased in one study [51] and increased in the other [52]. However, notched samples were used in the first study, and un-notched samples in the latter. Notch sensitive materials, such as incompatible polymer blends may be more notch sensitive, and produce far lower impact values, as reported by Jose [51]. For 70 wt% HDPE, the decrease in impact strength varied between 45% and 65%. The least reduction in impact strength was seen in the blend, which contained the HDPE grade with the highest impact strength.

The study by Greco [50] blended virgin materials of similar low melt in a single screw laboratory extruder and tested the extrudate. Without added mixing elements, a single screw extruder does not provide very good distributive mixing (creating an even distribution of the minor phase in the major phase) or dispersive mixing (breaking the minor phase down into small droplets). The compositions ranged from 100 wt% PE to 100 wt% PP. The study characterised the blends by their fractional crystallinity and tensile mechanical properties. By applying techniques, such as DSC and wide angle x-ray diffraction, it was deduced that the blend consisted of two crystalline phases and at least one amorphous phase with no co-crystallisation. PP formed spherulites before PE. At over 50 wt% PP, PP and PE fractional crystallinities were nearly constant, because the presence of PP spherulites hindered crystallisation of PE. This reduced the fractional crystallinity of PE to 0.7 compared to 0.8 in the pure polymer. The fractional crystallinity of PP increased significantly from 0.4 to 0.58, when PP was present as the minor phase. The authors proposed the latent heat of crystallisation of the PE was absorbed by the crystalline PP, which partially

melted, recrystallised thereby increasing crystallinity [49]. Microsocopy was not used to measure the size of the dispersed phase nor the size and nature of the spherulites in the extrudrate or the DSC samples. Coalesence of the minor phase was not considered, with its affect on interface area, and PP nucleation rate. The DSC test included a 10 minute melt anneal at 190 ^{o}C to ensure the polymers were fully melted, before cooling at a rate of 20 ^{o}C/min. In a PS/PP blend study, PP nuclei were observed after 5 minutes melt annealing at 190 ^{o}C, which significantly increased PP nucleation rate compared to 5 minutes anneal at 220 ^{o}C [46].

The study by Greco observed a decrease ultimate tensile strength by 50-65% compared to the pure polymers. Melting temperature, density and Young's modulus showed a linear, additive trend over the composition range. A non-linear synergy was found for tensile yield strength and elongation at yield above 25 wt% PP with a maximum at 80 wt% PP for yield strength. At the peak, yield strength increased by ~7 MPa compared to the predicted value of 26 MPa and elongation increased by 0.05 from a predicted value of 0.17. It was reasoned that PP reinforced PE delaying necking and producing higher yield values. Where PE was the major phase, small amounts of PP did not reinforce the blend in a similar way. The observed trends in mechanical properties did not agree with other studies [55], leading the authors to concluded that such properties were very strongly dependent on the process conditions and crystallinity of the phases not only the chemical nature of the component polymers.

The study by Jose found that mechanical properties were intimately dependent upon morphology as well as crystallinity [51]. Blends ranging from 100 wt% HDPE to 100 wt% PP were tested. Low melt PP was blended with moderate melt HDPE in a Brabender plasticorder, which provided good distributive mixing [56]. Tensile specimens were punched out of compression-moulded plaques. Using SEM, it was found that as the proportion of HDPE increased in PP matrix, there was increasing coalescence of the HDPE particles. Coalescence occurs in the melt phase driven by diffusion and collision. This reduces the dispersion

of the minor phase in the major phase. After a maximum point a co-continuous morphology forms, in this case at 40 wt%. The minimum point for coalescence is affected by viscosity and interfacial tension. PP and HDPE are incompatible, which produces high interfacial tension and a weak interface. Coalescence was lower in the blend with viscous PP as the major phase compared to the blend with less viscous HDPE as the major phase. DSC was used to measure percentage crystallinity of the phases. The samples were rapidly heated at 40 ^{o}C/min to 200 ^{o}C then measured whilst cooling at a rate of 10 ^{o}C/min. There is no mention of a holding time at 200 ^{o}C, therefore, self seeding PP nuclei may have been present. In the study by Jose, pure HDPE was 63% crystalline and PP 44%, because HDPE has faster nucleation and growth rates (see Section 2.1.2). In the blend, the crystallinity of the major phase was not appreciably reduced (~6%) by the presence of the minor phase, except in the co-continuous region where the crystallinity of both phases decreased by ~16-20%. In the dispersed phase, crystallinity remained at the low levels of the co-continuous region. The study by Greco measured a linear change in the crystallinity of the blend over the entire range of compositions, which suggests that a co-continuous morphology did not form.

The study by Jose found a synergy in Young's modulus peaking at 80 wt% PP with a value of >1800 MPa compared to the predicted 1220 MPa. However, all other properties were negatively affected with their minimum values in the co-continuous region [51]. It was reasoned that Young's modulus was measured at low strain, where the crystalline structure dominated. Yield strength was measured at high strains where the incompatibility of the blends had more effect. The addition of HDPE increased the percentage crystallinity of the blend compared to 100 wt% PP, which increased Young's modulus. Jose proposed that HDPE reduced the PP spherulite size by acting as a nucleating agent and hindering growth by occupying the interspherulite region. This increased the interfacial area present. At low strains the stress was transferred between the regions. At high strains, the poor interfacial adhesion meant that there was cracking and fracture at the interphase boundaries. The effect peaked, because at lower concentrations there was insufficient HDPE and at higher

concentrations there was more coalescence. A HDPE/PP and LDPE/PP studies by Bartczak and Galeski [45, 57] observed three phenomena used in this explanation. Significant nucleation of PP on HDPE caused PP spherulite size to decrease. The spherulite growth front did not reject HDPE inclusions, and grew around them. At the interface between phases, PP volume decreased as it crystallised, so that LDPE flowed into the gaps between PP spherulites, these influxes created thick interfacial region and improved mechanical properties. Microscocy was not used in the study by Jose to verify change in spherulite size.

The study by Greco did not observe a synergy in Young's modulus. A tensile test speed x10 slower than the study by Jose was used, which makes it difficult to compare the actual values. Increased strain rate generally increases strength and modulus [26]. For example, in the study by Greco the component polymers are quoted as having tensile strengths 20-25% lower (24-28 MPa) than the study by Jose (29-36 MPa). The component polymers also had very different properties. The study by Jose used component polymers with similar Young's modulus of ~1200 MPa. However, in the study by Greco, the PP modulus was 30% lower than the HDPE value of 1080 MPa. The study by Greco used a compounding method with less efficient distributive mixing, however, the component polymer viscosities may have been better matched to produce good distributive mixing. The final mechanical properties of the blend would have been effected by properties of the component polymers, morphology, crystallinity, sample preparation and testing. A lower strain rate could have delayed the point at which poor interfacial adhesion would have an over-riding affect. Research papers could not be found to verify this proposition.

One study by Blom investigated the effect of different viscosities in virgin materials [53]. Moderate melt PP was mixed with HDPE of either low melt (HDPE5) or very high melt (HDPE65). Blends were mixed on laboratory Buss Ko-kneader, then samples were injection moulded. Buss kneader is a single screw type machine, which oscillates axially once per revolution in a sinusoidal motion [56]. It introduces low shear and provides good distribution. The mechanical properties of PP/HDPE5 blend were superior to the properties of the

PP/HDPE65 blend, for example, flexural modulus was 1500 MPa compared to 1100 MPa even though both HDPEs had flexural modulus of ~900 MPa. From consideration of the viscosities at the injection pressures, it was concluded that the difference in viscosities produced different dispersion morphology and hence caused the difference properties. PP and HDPE5 were well matched in viscosity. This was presumed to produce good dispersion and superior properties. Whereas PP and HDPE65 were poorly matched in viscosity, which was presumed to produce poor dispersion. Given the observations in the study by Jose, the high melt flow HDPE65 matrix would have also permitted more coalesence further reducing the dispersion.

The studies showed that the results of blending formed a complex picture even for virgin thermoplastic polymers. The property changes with different sample production techniques have been confirmed in studies by Xanthos and Tzandkova Dincheva [58, 59]. Final blend properties were dependent upon the actual and comparative differences in material properties and flow characteristics, effectiveness of mixing, sample preparation technique and test conditions. This comparison has demonstrated that the project needed to test a range of different waste streams using actual production techniques and full profile tests that were representative of final use. Testing standard test bars in the laboratory could not be presumed representative of the final product.

Blending PP and PE alone would not provide adequate properties for the final product. The lowest tensile modulus value measured in the studies was ～700 MPa, which was insufficiently stiff for railway sleepers. Additionally the softening temperatures of the polymers quoted in Section 2.1 were too close to room temperature. A third component was required for the blend.

2.2.2 Polystyrene, Polyethylene and Polypropylene Blends

Polystyrene was the next abundant recycling stream to mix with a polyolefin blend. PS is amorphous, therefore, it is much stiffer than PE and PP.

The only significant commercial grades of polystyrene polyolefin blends are expandable beads to make cellular foams. These form an interpenetrating network of PE and PS. PS gives rigidity and HDPE gives solvent and abrasion resistance. In the past polyethylene has been used to improve impact resistance of polystyrene. Other formulations were developed for: plastic paper (uncompatibilised); blister packaging (significantly compatibilized with SEBS); and thermoformable sheet for fridge liners (highly compatibilised) [21].

The AMIPP Advanced Polymer Centre at Rutgers University has extensively investigated immiscible blends of recycled polystyrene, polyethylene, polypropylene and other polymers. The formulation and technology has been patented and licensed to Polywood Inc., where it is used for structural plastic lumber applications, including the substructure for decks, railway sleepers and the first vehicular bridge made from plastic lumber [60]. The material has a flexural strength of 21 MPa and a flexural modulus of 1378 MPa minimum and 1516 MPa average [61]. For plastic lumber, a moulding or extrusion grade polyolefin (HDPE bottles of MFI = ~0.35 g/10 min 2.16kg 190 ^{o}C) is mixed with recycled polystyrene of 7 g/10 min 5kg 200°C [62, 63].

In the late 1980's, the group studied kerbside tailings, which were the remains of recycling household collections after PET bottles and milk bottles had been removed. The tailings contained 80-90% HDPE bottles plus low levels of other polyolefins. To create a high stiffness and high strength material, they created a polymer/polymer reinforced composite using 35 wt% recycled polystyrene. PS was used because, it is a rigid, glassy polymer at room temperature that can be processed at similar temperatures as tailings (220 °C) [61]. Trials were completed with polystyrene from two sources post consumer waste and pelletised, namely insulation and industrial scraps [64].

The fundamental concept was to produce a three dimensional interpenetrating co-continuous network. Both phases remain continuous, which restricts phase mobility. The polystyrene glass transition temperature occurs at the same temperature as polyolefin crystallisation, ~125 ^{o}C. On crystallisation HDPE

naturally shrinks by as much as 15% by volume. The PS is amorphous, therefore, has only a small volume change at T_g. With correct mixing, the phases are interlocked, which prohibits HDPE from shrinking and polymer chain mobility is reduced, thus hindering crystallisation. There is a drop in the amount of crystallinity (also observed by Jose in PP/PE blends [51]). On further cooling, the effect is amplified because the polystyrene is rigid and glassy. The HDPE phase contracts around the rigid PS phase resulting in tighter packing than would normally occur in a dispersed phase-continuous morphology [61].

Conventional opinion is that a compatibiliser is required in immiscible blends to improve interfacial adhesion thus improving the stress transfer between phases and hence the mechanical properties [21, 51, 52]. AMIPP found the interpenetrating, co-continuous network morphology produced good, reproducible, mechanical properties without the need for compatibilisers, because imposed stresses are shared equally [61].

Strict control of the processes and material ratio is required to obtain the co-continuous morphology. The volume ratio required for co-continuity is predicted using a semi-empirical relationship discovered by Jordhamo et al [65]:

$$\eta_1/\eta_2 \approx \varphi_1/\varphi_2 \qquad\qquad 2.3$$

Phase inversion occurs when the viscosity, η, and volume fraction, φ, ratios of the two components, 1 and 2, are approximately equal.

The Jordhamo equation only predicts where co-continuity will occur. Co-continuity alone does not produce synergy. In some cases, the synergy raises values above the rule of mixtures, in others the peak value is only at the level expected by the rule of mixtures. A study by Joshi compared virgin PS/PP and PS/HDPE by mixing in a Brabender then testing the extrudate [66]. Around 40 wt% PS, a decrease in crystallinity and a synergy in flexural modulus occurred that peaked at a level predicted by the rule of mixtures. Later, Joshi compared virgin PS/HDPE blends with recycled blends by injection moulding sample blends [63]. A crystallinity decrease and property synergy was only observed

with the recycled blend. Again the synergy was near rule of mixtures values. Viratyporn also showed synergy is not always present in co-continuous virgin materials [62]. Virgin PS/HDPE and PS/PP were mixed in a Brabender then injection moulded. The PP blends had a finer dispersed phase and performed better than PS/HDPE. PS/HDPE had low impact resistance, which was attributed to the coarse, non bonded interface providing limited crack deflection and minor energy absorption. The best properties were seen with a dispersed morphology at 20wt%PS/80wt%PP, which produced 127% increase in notched impact resistance and 32% increase in tensile modulus. This 20wt%/80wt% synergy and having improved properties with finer dispersion correlates with the PE/PP blends previously discussed.

The interconnecting co-continuous network and synergy in properties are pivotal to the patents held by the inventors [67]. It covers compositions of 20-50 wt% PS, 50-80 wt% polyolefin with at least 75 wt% HDPE in polyolefin component. The material has a minimum modulus of 1186 MPa and minimum strength of 20.7 MPa with co-efficient of expansion 1.08×10^{-4} mm/mm $^{\circ}$C. The preferred composition is 35wt%PS/65wt% polyolefin with 1379 MPa modulus and 24 MPa yield stress. The US version of the patent describes the polystyrene forming elongated fibres of mean length to diameter ratio of >5 (and preferably >8), with a typical mean diameter of <15 microns [68]. The polyolefin kerbside tailings are described as having a bimodal distribution of 10 and <3 (preferably <1) g/10 min 190°C 2.16kg.

These studies showed that there was a real possibility of synergy in incompatible blends, however, the concept was very sensitive to the materials used and processing conditions. Continuity of supply and material consistency would need to be guaranteed to reliably maintain enhanced properties from interpenetrating co-continuous networks. The high quality waste streams used by AMIPP were not available to the project, because the recycling industry had changed very significantly since the late 1980s, see Chapter 1. A variety of polystyrene/polyolefin blends were evaluated and are presented in the next chapter.

2.3 Reinforcement Additives

An alternative method of reinforcement is the use of fillers and additives [69]. The effect of a filler on the mechanical properties will depend upon its chemical composition, particle shape and size, size distribution, specific surface area, surface chemistry, interparticle spacing and extent of agglomeration [70]. As with unfilled blends, the method of production also has an impact on the microstructure and resulting properties. A study by Tzankova Dintcheva compared injection moulded and compression moulded samples of a polyethylene rich polyolefin blend with 20 wt% wood fibre. The injection moulded samples had vastly improved properties [59].

There are three main types of filler – spherical, plate and fibre. Higher aspect ratio fillers produce greater reinforcement, however, there is a limit to their size in some processing methods.

Typical spherical fillers are calcium carbonate, clay, glass beads, carbon black and alumina trihydrate. Among these, calcium carbonate ($CaCO_3$) is the most widely used filler as it is readily available at low cost [70]. It reduces warpage, increases modulus and, in virgin materials, reduces the cost of the material. In such applications, strength is normally reduced slightly. Impact toughness is also reduced, with the exception of very fine additive grades, which can act as impact modifiers [70]. Stearate coatings are often used to improve surface bonding and dispersion. The type of polymer is also important where filler/matrix interfaces are considered. For example, the coated filler increased the impact toughness in PP homopolymer; however, it decreased the toughness in HDPE and PP copolymer [71].

Plate-like fillers are better reinforcements than spherical fillers. Examples are talc, mica and kaolin [72]. Modulus, shrinkage, warpage and heat distortion temperature have been improved by the addition of all these fillers to polymers. However, tensile strength, impact strength and elongation at break tend to decrease [73]. Mica has an aspect ratio only rivalled by fibrous materials. For good bonding to non-polar plastics, it needs to be silane treated or mixed with

maleic anhydride modified polymers. Most commercial applications do not justify the expensive silane treatment [73]. Mica has low co-efficient of thermal expansion (CTE) and good weathering performance [72]. A synergy was found by some authors [74, 75] when adding low quantities of mica to glass fibre reinforced polyolefins to increase modulus, improve dimensional stability and reduce cost. The increase in properties was attributed to a positive effect of mica on the fibre–matrix adhesion.

Fibre fillers have the highest aspect ratio and provide significant reinforcement. Examples are glass, carbon, straw, flax, and hemp. The degree of reinforcement is significantly affected by fibre modulus, aspect ratio, length and orientation in the product. Glass fibre is the most common reinforcement for polymers. As reported by several industrial and academic studies, it can be used to upgrade recycled thermoplastics into long life products [76]. It improves strength, stiffness, fracture toughness and heat resistance [70, 74]. An increase in the heat deformation temperature from 60 to 150 ^{o}C for a 40 wt% loaded PP has been reported [70]. Titanate or silane coatings and maleic anhydride or acrylic acid coupling agents are required for optimum fibre–matrix bonding. Fibre lengths >0.5 mm are required for optimum strengthening, and the properties are dramatically improved above 1 mm. A study on 30 wt% long glass fibre PP showed that the addition of 20 wt% $CaCO_3$ to the PP matrix gave an increase of 10% in tensile modulus. Such an increase exceeded the modulus enhancements predicted by the rule of mixtures and was therefore attributed to synergistic interactions between the glass fibres and $CaCO_3$. However, tensile strength and fracture toughness decreased [74]. Glass fibre and mica have been shown to increase stiffness and reduce warpage [75, 77, 78]. In a study of mica filled PP based glass mat thermoplastic, the addition of up to 15 wt% mica enhanced the fibre–matrix adhesion while improving the tensile, flexural and impact properties [75].

Fillers naturally have a lower co-efficient of thermal expansion (CTE) than polymers. The CTE of filled compounds can depend upon particle size, distribution and specific surface area [79]. Increasing the interfacial area

increases the constriction of the matrix and decreases the CTE. However, poor adhesion between filler and matrix can lead to an increase in the thermal expansion coefficient [80]. For some systems (e.g. silica filled epoxy composites), decreasing the filler crystallinity decreases the CTE [79].

There are many patent applications for varieties of reinforced recycled plastic lumber and manufacturing processes. Patents tend to give a formulation that is as wide ranging as possible, which makes it difficult to ascertain the exact formulation used. A patent from Tietek contains the example formulation of 60 wt% polyolefin, 14 wt% crumbed (tyre) rubber of less than 100 mesh, 12 wt% expanded mica and 12 wt% glass fibre. The product was twin screw compounded and directly extruded into a mould with the rubber off-gassing to foam the product. This produced a stiffness of 992-1133 MPa [81]. Axion International manufacture a glass fibre reinforced product under licence from AMIPP at Rutgers University [82, 83]. The example formulation in the patent contains kerbside tailings (>90 wt% HDPE from bottles) with polypropylene car bumper scrap with a minimum fibre length of about 0.1 mm, preferably ~0.5-~10.0 mm. 35 wt% coated fibre produced a 100x100x2.43 mm profile with 13 wt% glass fibre (foaming would reduce the profile weight). This formulation gave a flexural modulus of 2496 MPa and a flexural strength of 29 MPa. The inventors claimed that using coated fibres caused greater alignment and a greater increase in properties than would be expected for the fibre content. Other patents contain a range of formulations with reinforcing additives such as nylon carpet fibre, carbon fibre, metal fibre, recycled glass fibre from thermosets, talc and mica [84–87].

In the next chapter, trials are described that compare different types of fillers and levels of glass fibre.

2.4 Flame Retardants

Reduced flammability is desirable for many building applications and is often mandatory for products designed for indoor use. The majority of plastics are inherently flammable, and some produce dense black smoke e.g. styrenics.

Polyolefins are inherently high molecular weight waxes hence are flammable and burn with a relatively clean flame. Flame retardants work by delaying ignition, slowing flame spread, reducing smoke or moderating heat generation [72]. The selection of flame retardants for blends can be difficult, because different flame retardants systems are more effective for certain polymers.

Halogenated flame retardant systems have been traditionally used, because they are effective at low concentrations hence have little effect on physical properties [72]. They work by interfering with the chain reactions of flame spread. However, certain systems are banned in many applications due to high smoke production and smoke toxicity [70]. Halogenated systems could not be considered in this application.

Zero halogen systems are available, such as alumina trihydrate and magnesium hydroxide. These act by releasing water in an endothermic reaction, which removes heat from the system, dilutes the combustion gases and the remaining metal oxide forms a char [70]. They are better smoke suppressants than halogenated compounds. Loadings of 60 wt% are required to produce the same level of flame retardancy to the detriment of strength and impact resistance [70].

Phosphorous based systems are often intumescent and form an insulating char that acts as a barrier between the heat source and the polymer fuel [72]. Their smoke suppression is also reasonably good. A loading of 20-40 wt% loading is required in PP to obtain UL-94 V0, which affects the mechanical properties [70, 88].

Assessing a material's suitability for an application can be difficult, because a fire is a very complex process. Many factors affect the result such as sample size and geometry, proximity of other combustible materials, prevailing temperatures, wind speed and direction, and the scope for rapid heat dissipation vary with the circumstances [72]. There are many international standards for electrical appliances to building materials, with assessments ranging from small labscale materials tests to full room product tests. Often a

range of tests is used to assess many the aspects of fire – heat release, flame spread, smoke and ignitability.

Flame retardancy was a requested attribute. Five blends with flame retardant were made to judge the impact on properties, the efficacy of the flame retardant in a mixed plastics system and the additional cost.

2.5 Conclusion

A promising range of recycled polymer blends was highlighted by the review, which could produce the demanding range of properties required for structural plastic lumber applications.

The literature review showed that there would be a variety of challenges to be overcome. The polymer grades present in different waste streams would produce different results. Hence, careful selection of polymer waste streams would be required to obtain the specific, well-controlled properties needed for structural applications. However, finding a robust formulation that could use a wide range of polymers would be important for the economic success of the project. The sample production method and test method could significantly influence the results. The morphology was affected by production method as well as the polymer grades used. The test method, in particular speed, affected how the component materials and morphology reacted in a test. This was taken into consideration when planning the manufacturing route and test regimes.

On the basis of the literature review a range of polymer blends with reinforcement and flame retardants were trialed and tested. These are described in Chapter 3.

3 Materials Selection and Experimental Evaluation

This chapter describes the laboratory scale testing of a range of formulations. The purpose was to select recycled plastic waste streams and determine a formulation suitable for production trials. Different waste streams were evaluated separately and in combination. A formulation matrix was designed based on the review in Chapter 2, industry experience and knowledge of the recycling streams. The formulations were iteratively developed using combinations of the three preferred recycled polymer types along with selected additives. Production trials and product tests of the optimised blends are described in Chapter 4.

Different formulations needed to be compounded and tested on a laboratory scale, because information on the processability and material properties for different recycled waste streams was not available. Five separate trials were completed using different blend ratios, additives, and polymer waste streams. The trials were conducted at different stages of the project over the course of several years. Each investigation will be discussed here separately. They are not discussed in historical order.

Some of the data from Trials 1, 3 and 4 have been published [69]. The optimised formulations, selected for scaled-up manufacturing, were not included in the published results.

3.1 Selection of Compounding and Testing Methodology

The first stage in experimental work was to evaluate a range of formulations to understand the effect of the polymers and their potential mechanical properties. A method was required for fast production and testing in order to screen a wide variety of formulations.

It was decided to prepare formulations using laboratory scale, twin screw compounding that extruded strands, which were cut into pellets. These were

injection moulded into standard ISO and ASTM test bars. This process route produced homogeneous, good quality samples for standard ISO and ASTM testing using a small amount of raw materials in a fast process. The equipment required high quality recyclate streams with low levels of contamination, to prevent the strands breaking prior to pelletisation and for consistent mouldings. The morphology of the mouldings was not necessarily representative of the final product, because mixing was better than that achieved in Production and cooling was much faster. However, testing to ISO and ASTM standards was relatively efficient and the results could be compared directly with other published data.

Sample size, process conditions and test parameters can have a large influence on the final properties. ISO 178 warns that results may not be comparable from mouldings of different sizes or even samples of the same size with different moulding conditions [89]. This is especially seen in semi-crystalline polymers, where flexural properties are affected by the thickness of the orientated skin layer. The thickness of this layer is dependent on moulding conditions and thickness [89].

Ideally profiles for testing would have been manufactured using the standard intrusion production equipment. This would have ensured that the measured properties were comparable to use of the final product. However, the production machinery was not suitable for loose fibres and powders, and large quantities of raw materials were required with a lengthy production time. Three polymer reinforced blends were made for comparison to the injection moulded samples. Standard test bars were machined from the profiles. Any test bars with particles of contamination were rejected, because the contamination would have had a significant effect on results. Machining of samples is not ideal, because it can introduce surface flaws that fail at lower stress compared to moulded samples [90].

3.2   Sample Manufacture

The injection moulded test bars were made at J.G.P. Perrite Ltd in Warrington, a commercial compound manufacturer and toll compounder.

Materials were weighed, tumble mixed, then compounded and pelletised. The additive trial used a Berstorff ZE25 co-rotating twin screw extruder with a temperature profile of 180–210 ^{o}C and a speed of 430 rpm. The other trials used a TSA EM 26-30 twin screw extruder with 26 mm co-rotating twin screw of 30:1 length/diameter ratio. The temperature profile was 210-220 ^{o}C used with a speed of 425 rpm.   Contaminants and volatiles in some waste streams produced a strand with a rough surface that picked up moisture.   These compounds were dried before moulding at 80 ^{o}C overnight.

Standard test specimens were injection moulded using a Negri Bossi V55-200 with 32 mm screw and 62 ton maximum clamp force. The temperature profile was 200–230 ^{o}C. The mould was not cooled.

In Trial 1, certain formulations were also intrusion moulded into profiles on a production machine at the sponsor company, see Section 1.4 for a description of the process. Flex and compression samples were machined from the solid outer wall of the profile.

3.3   Test Methods

This section details the test methods used to evaluate samples. All blends were tested in flexure. Then additional tests were used depending on the focus of the trial - tensile, charpy impact, compression, melt flow index, filler content, co-efficient of thermal expansion, flammability and scanning electron (SEM) micrographs.

3.3.1 Flexural Properties

Three point flexural testing was the key mechanical test, because it is the most common mode of loading in service. Flexural strength, modulus and breaking strain were measured.

Samples in Trials 1-4 were tested on a Hounsfield HK100-S with a 1 kN load cell in the Department of Engineering Materials, University of Sheffield. Trial 5 used a Tinius Olsen H5KS with 5 kN load cell in the LEA laboratory, Department of Mechanical Engineering, University of Sheffield. Both machines used the same three point loading jig with support noses of 5.95 mm diameter and loading nose of 6.3 mm diameter, see Figure 3.1. ASTM D 970 flexural bars (127x12.7x3.2 mm) were used [91]. Test procedure and analysis followed ISO 178 at a span of 51.2 mm and a speed of 2 mm/min [89]. Five samples were tested for each blend.

Figure 3.1 The three point bend jig for flex testing.

3.3.2 Tensile Testing

Tensile testing was used for comparison purposes in early trials. The Hounsfield HK100-S with a 10 kN load was used from the Department of Engineering Materials, University of Sheffield. Injection moulded, Type 2 ISO 3167 dog bone specimens were tested and data analysed with reference to ISO 527-1

and ISO 527-2 at a speed of 5 mm/min [32, 54, 92]. Five samples were tested for each blend. Strain values were taken from crosshead position not using an extensometer.

3.3.3 Compression Testing

Compression was a very important loading mode in product use. The Hounsfield HK100-S with a 10 kN load cell was used from the Department of Engineering Materials, University of Sheffield. The standard test samples were too thick to be injection moulded. Samples were 40x12.5x12.5 mm in size. They were machined from intrusion mouldings 48x48 mm in cross-section. Testing was in accordance with ISO 604 at a speed of 5 mm/min [93]. Five samples were tested for each blend. Compressive strength and modulus were measured.
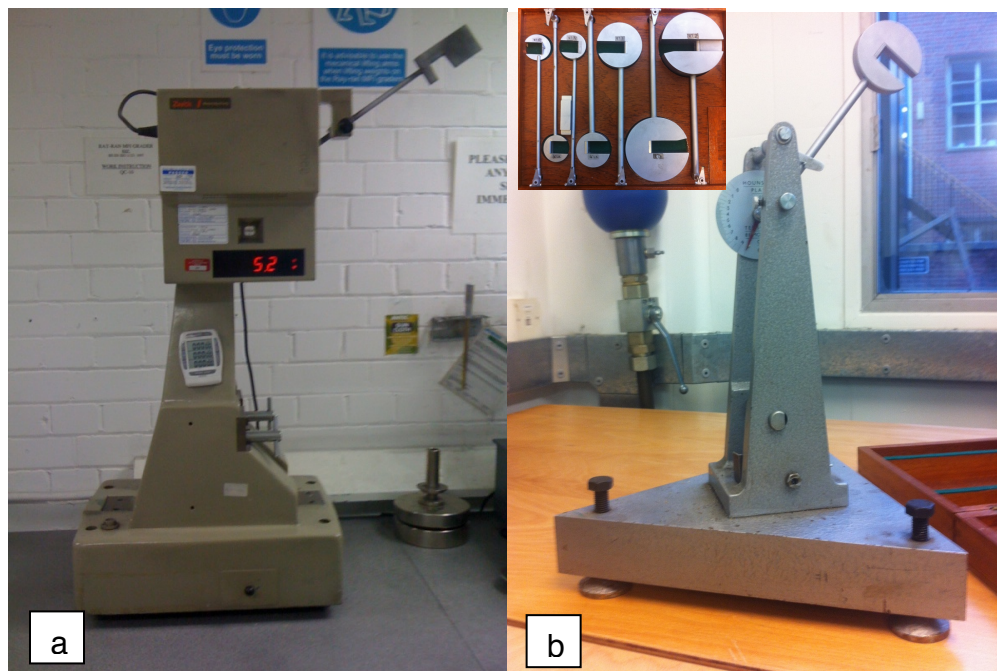
3.3.4 Impact Resistance

Figure 3.2 Charpy impact Testers (a) Zwick 5100 (b) Tensometer H.20 Plastic Impact Machine. Inset shows the impact hammer (Tup) set.

Impact testing (especially at cold temperatures) was used as an indicator for resistance to crack propagation and damage.

Charpy impact testing samples were tested edgewise at room temperature and -30 ^{o}C. ISO 179 test standard was followed for unnotched samples and type A notched samples [41].

The samples were notched after moulding using a Rayran Polytest motorised notching machine at J.G.P. Perrite, Warrington. The test machines are shown in Figure 3.2. Room temperature impact testing was carried out on the Zwick 5100 s/n 112026 at J.G.P. Perrite. Cold temperature impact used a Tensometer H.20 Plastic Impact Machine from the LEA laboratory, Department of Mechanical Engineering, University of Sheffield. The machine had changeable hammers (Tups) to ensure the energy measured was between 0.3 and 0.7 on the dial scale. The Tups ranged from 1/32 lb – 2 lb (14 - 908 g). The standard test bars had to be cut down to 58 mm in length to fit into the machine.

Samples were conditioned at the test temperature for 24 hours. The cold temperature samples were cooled in an ESPEC ET34 environmental chamber in the Department of Electrical Engineering, University of Sheffield. The chamber was calibrated using a ThermaData Humidty-Temperature logger HTD D09490530. The impact tester was set up next to the environmental chamber. Samples were removed five at a time and tested immediately. Ten samples were tested from each batch.

3.3.5 Melt Flow Index

Melt flow was a key quality control tool to ensure grades were suitable for intrusion. Additionally the previous research review showed that the blend morphology was effected by the interplay between different viscosities, see Section 2.2.1 and 2.2.2 [53, 65].

Melt flow index was measured to ISO 1133 using a Ray-Ran Melt Flow Indexer 6MBA at I-Plas Ltd, Halifax [30]. Flakes or pellets of the sample were rammed into a barrel that was heated to the required temperature. The sample was left to warm for 6 minutes. A specified weight was placed on the sample, which pushed the molten polymer through a die. The amount of material pushed

through the die in a set time was collected and weighed. The weight of material in grammes that would be extruded in 10 minutes was calculated and reported.

3.3.6 Filler Content

Filler content of the mouldings and waste stream were analysed to ensure that the formulations were correct. A sample was heated in a crucible in an 850°C furnace for 15 minutes. The filler content was calculated from the difference in weight.

3.3.7 Softening Temperature

Heat Deflection Temperature (HDT) and Vicat softening temperature are a good indication of the maximum safe operating temperature. They were measured using a HDT/Vicat Standard from Zwick at J.G.P. Perrite, Warrington. HDT was measured following ISO 75-1 [1]. Vicat softening temperature was measured following a test method based on ISO 306 [34]. A description of the tests was given in Section 2.1.1.

3.3.8 Co-efficient of Thermal Expansion

The linear co-efficient of thermal expansion (CTE) is critical for maintaining the distance between the rails on a railway track. The CTE also is important for determining expansion gaps and distance between fixing points for applications such as retaining walls, decking and cladding. CTE was measured using two different methods.

A Perkin Elmer Diamond thermo-mechanical analyser was used over the range of -20 – 60°C at a ramp rate of 2 ^{o}C/min. Secondly, the change in length of the flexural test bars was measured after conditioning at -18 and 55 ^{o}C using a standard laboratory oven and freezer. Vernier callipers were used to measure the change in dimensions.

3.3.9 Scanning Electron Microscopy

The effectiveness of the mixing technique was ascertained from the morphology of the material examined by scanning electron microscopy (SEM). Flexural test bars were dipped in liquid nitrogen, clamped in a vice and fractured by a hammer blow. The fracture surfaces were carbon coated and examined in secondary electron and backscattered electron modes using a Philips XL 20 at the Department of Biomedical Sciences, University of Sheffield.

3.3.10 Fire Resistance

Fire resistance is a desirable attribute for use in buildings and tunnels. A standard laboratory test, UL 94 vertical burn, was used to evaluate the effectiveness of the flame retardant additives. UL 94 rates plastics used for electrical devices and appliances [21, 88]. Tests were conducted in the UL 94 chamber at J.G.P. Perrite Ltd, Warrington.

A vertical test bar (127x12.7x<12.7 mm) was supported at its upper end and was ignited at its bottom edge for 10 s, by Bunsen burner, in a draft-free area. The flame duration was timed. The specimen was re-ignited for 10 s if flaming or glowing combustion stopped within 30 s after removal of the flame. If flaming particles dripped from the specimen, they were collected by falling on to a layer of surgical cotton 0.3 m below the sample. Ignition of the cotton was considered to be a fail in the test. There were three levels for fire resistance V0, V1 and V2.

3.4 Trial 1 – PSPPPE Polymer Blends

This trial investigated the tensile and flexure properties of polystyrene mixed with PE, PP and in combination. Machined intrusion samples were tested in flexure and compression to compare the different methods of manufacture.

3.4.1 Materials

High quality waste streams with low levels of contamination were selected. Table 3.1 gives the melt flow index of the materials. The PE was high density

polyethylene. The PS was high impact polystyrene. The PP was copolymer. The PS, PE and PP grades flowed relatively easily and were suitable of injection moulding. PPP was an extrusion grade polypropylene. The MFI of the PPP is very low, because extrusion grades require high melt strength and are not required to have long flow paths.

Table 3.1 Melt Flow index of the Trial 1 component polymers

Material	MFI at 230°C 2.16kg (g/10 min)	MFI alternative conditions (g/10 min)
PS	5.7	5.2 at 200°C 5kg
HDPE	18.5	9.8 at 190°C 2.16kg
PP	16.5	
PPP	0.34	

Table 3.2 lists the compositions for Trial 1. The formulations contained 35 wt% polystyrene to compare to previous work. A 50:50 split of PE:PP was used to mimic a potentially good source of material (latterly this source did not make it to market). The PSPEPP blend was the base formulation for Trials 3 and 4.

Table 3.2 Trial 1 polymer blends

Material (wt%)	PSPE	PSPP	PSPPP	PSPEPP	PSPEPPP
PS	35	35	35	35	35
HDPE	65			32.5	32.5
PP		65		32.5	
PPP			65		32.5

All formulations were compounded and injection moulded. PSPE and PSPP were also intrusion moulded using the same raw materials.

3.4.2 Flexure and Tensile Testing Results and Discussion

The injection moulded samples were tested in flexure and tension. The results are given in Table 3.3.

Table 3.3 Average flexural and tensile properties of Trial 1 injection moulded polymer blends samples ± standard deviation.

	Flexural		Tensile	
	Strength	Modulus	Strength	Modulus
Compounds	(MPa)	(MPa)	(MPa)	(MPa)
PSPE	26.2±0.1	902±32	16.5±0.2	851±47
PSPP	33.4±0.2	1350±24	21.5±0.8	694±101
PSPPP	31.8±0.2	964±19	19.3±0.4	861±57
PSPEPPP	29.5±0.2	947±43	18.7±0.3	760±67

PSPP gave the highest strength and stiffness, except for tensile modulus. Mixing PE and PPP in a blend was detrimental to properties. PSPPP had better strength and stiffness than PSPEPPP. However, PSPEPPP still had improved strength and flexural modulus than PSPE.

Table 3.4 presents the flexural results from the machined intrusion samples. The intrusion results have been labelled with an "i" in order to differentiate with the injection mouldings. POi was a polyolefin, packaging waste stream containing low density polyethylene, medium density polyethylene, high density polyethylene and polypropylene. A UK equivalent of the AMIPP kerbside tailings discussed in Section 2.2 [61]. Flexural samples were cut in the longitudinal direction i.e. parallel to the flow direction along the length of the profile.

Table 3.4 Average flexural properties of Trial 1 machined, intrusion moulded polymer blends samples ± standard deviation.

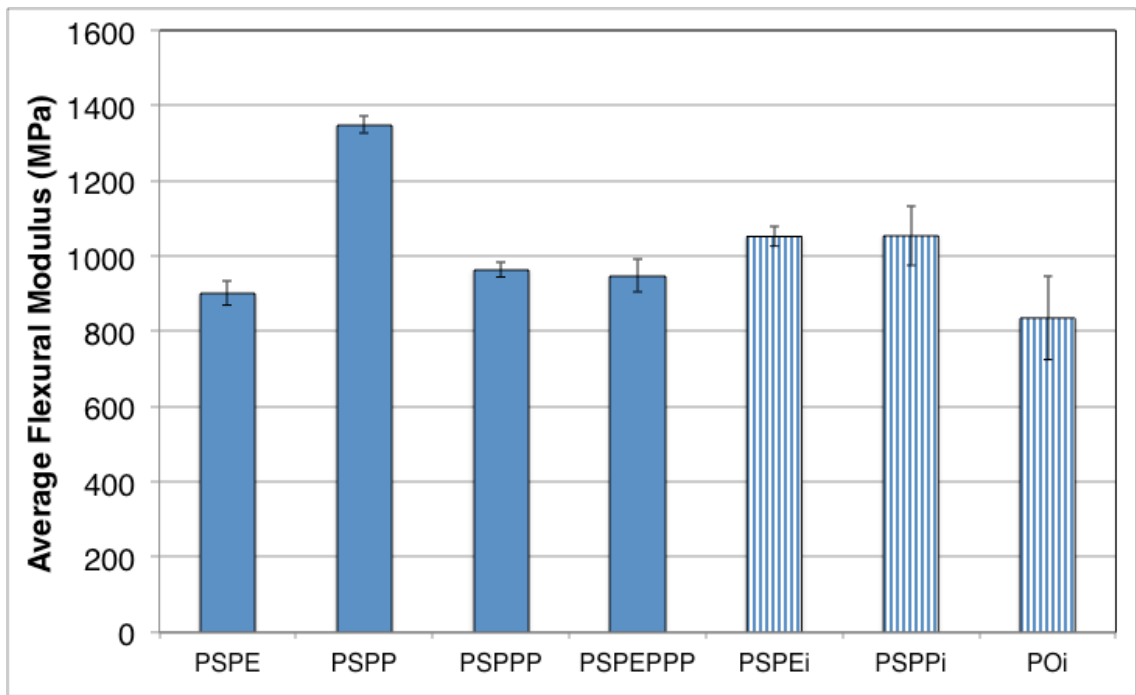|	Flexure - Average ± standard deviation	
	Strength	Modulus
Compound - Longitudinal	(MPa)	(MPa)
PSPEi	19.7±1.1	1052±26
PSPPi	18.5±2.2	1054±80
POi	18.3±0.5	835±110

Figure 3.3 Average flexural modulus of Trial 1 blends. Injection moulded samples (solid bars) compared with intrusion moulded samples (striped bars). ± standard deviation included.
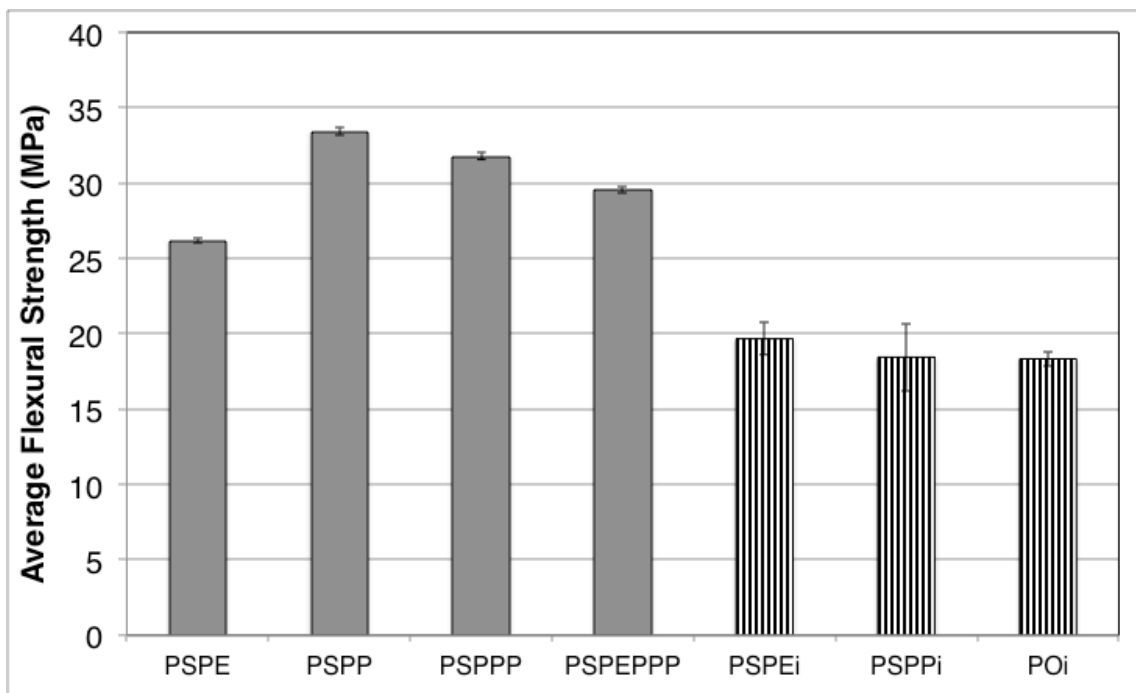

Figure 3.4 Average flexural strength of Trial 1 blends comparing injection moulded samples (solid bars) with machined intrusion moulded samples (striped bars). ± standard deviation included.

The machined, intrusion moulded test bars gave conflicting trends in flexural modulus compared to the injection moulded test bars. PSPEi had a higher modulus. PSPPi had a significantly lower modulus. The flexural strengths were all lower.

Machining produced a higher standard deviation than injection moulding, as shown in Figure 3.3 and 3.4. The random nature and variability in surface flaws would be expected to increase variation in failure.

There are two sources that can be used to evaluate the results, the draft ISO standard for plastic railway sleepers and AMIPP/Polywood product described in Section 2.2 [61, 94]. The values in these sources were only used as an indication, because they did not use standard injection moulded test bars.

The ISO standard had pass values of 13.8 MPa flexural strength and 1170 MPa flexural modulus [94]. These values were based on testing larger samples machined from a railway sleeper. Both injection moulded and machined intrusion samples passed the minimum ISO strength. The strengths of the machined samples were much reduced compared to the injection moulded, see Figure 3.4. Machining introduces small surface flaws that can cause early failure. This was confirmed in a study of glass filled PA66 [90].

Only PSPP in injection moulded samples passed the minimum ISO flexural modulus. Intrusion moulding of the same formulation produce a lower flexural modulus, see Figure 3.3. The intrusion machine had a single screw extruder, which would not produce significant dispersive nor distributive mixing. The twin screw process had far better dispersive and distributive mixing. This may have broken the PS into a fine, well distributed dispersion that provided better reinforcement of the PP matrix in the injection moulded samples.

AMIPP/Polywood formulation used the same ratio of polymers as the PSPE blend, however, the waste streams were different. The Polywood product published properties were a minimum flexural modulus of 1379 MPa and

flexural yield strength of 21 MPa [61]. The values were obtained in accordance with ASTM test standards that use full size plastic lumber profiles [95]. The profile size used was not stated. The results in injection moulded samples had a comparable or higher yield strength. Only PSPP had a comparable flexural modulus, however, this had a low modulus under tensile testing. The difference between injection moulded test bars and full profiles will be discussed in Chapter 4.

The PSPPP did not provide the expected improvement in properties compared to the PSPP mix. The PPP was an extrusion grade with far lower viscosity than the PP injection moulding grade. The MFI of the component polymers in the PSPPP blend was similar to the MFI of the component polymers in the AMIPP mixes, see Section 2.2.2 [62, 63]. Microscopy was not used to compare the morphologies or spherulite size. Section 2.2.1 discussed the affect of melt viscosity, dispersion, melt morphology, crystallinity and spherulite size on the mechanical properties of PE/PP blends. Based on this discussion, the lower melt flow PSPPP was expected to produce a finer dispersed morphology compared to PSPP. This morphology has a higher interfacial area, on which PP crystallites can nucleate and form a fine spherulitic structure. A study on PSPP blends showed significant heterogeneous nucleation on the phase interface [46]. This study observed heterogeneities migrating from PS to PP due to the interfacial free energies of the impurities with respect to the two molten phases. PSPP modulus was 1350 MPa compared to 964 MPa for PSPPP. From the literature, an increase in modulus suggests an increase in crystallinity or decease in spherulite size from increased nucleation rate. In recycled materials the level and type of such impurities and additives will vary with waste stream and batch. Microscopy to observe the spherulite size would have been required to verify this. Viratyaporn proposed that the presence of atactic polypropylene would improve mechanical properties. Atactic polypropylene is miscible with polystyrene and can have a compatibilising effect, which improves load transfer and hence the modulus [62].

The extrusion grade polypropylene was discounted for further work, because it was too stiff for the intrusion process.

3.4.3 Compression Testing Results and Discussion

Machined, intrusion moulded samples were compression tested. Compression samples were machined longitudinal and transverse to the flow direction. The results are tabulated in Table 3.5 and shown as a graph in Figure 3.5.

Table 3.5 Average compressive properties of Trial 1 machined, intrusion moulded polymer blend samples in longitudinal and transverse directions. ± standard deviation.

Compounds	Compression - Average ± standard deviation	
	Strength (MPa)	Modulus (MPa)
Longitudinal		
PSPEi	22.3±1.9	759±44
PSPPi	26.3±1.9	822±96
POi	21.4±1.0	725±53
Transverse		
PSPEi	20.1±1.0	599±24
PSPPi	19.5±2.9	696±29
POi	18.4±1.6	550±12

The longitudinal compression values were better than the transverse values. This is to be expected, because the polymer molecules are orientated in the direction of intrusion.
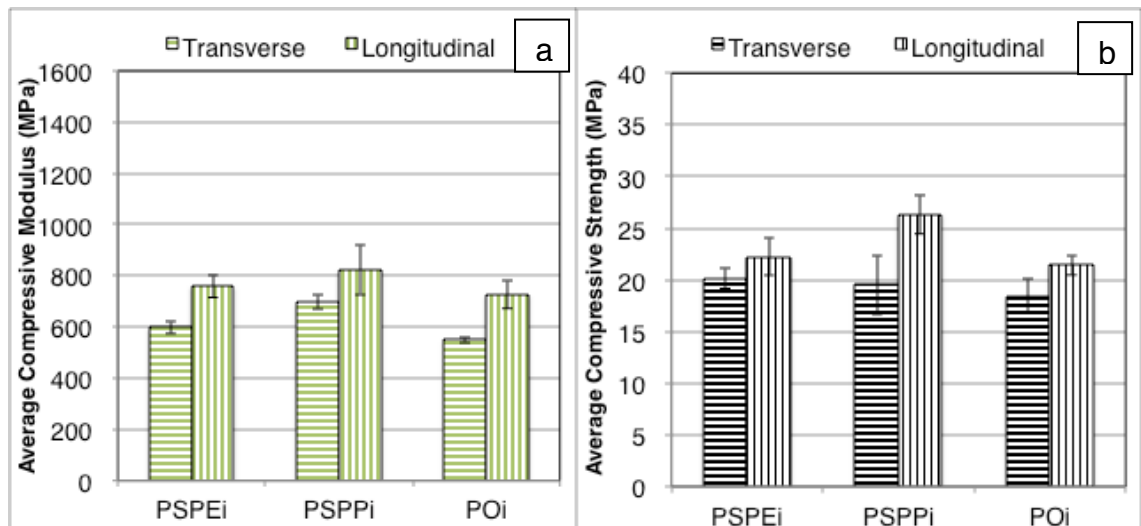
Figure 3.5 Trial 1 intrusion moulded, machined samples in longitudinal and transverse directions of the profile (a) average compressive modulus (b) average compressive strength. ± standard deviation included.

The AMIPP/Polywood plastic lumber product claimed a compressive modulus of 1172 MPa (direction not specified), a longitudinal strength of 29.6 MPa and a transverse strength of 8.3 MPa [61]. These values were based on ASTM plastic lumber tests [96]. Compared to these AMIPP values, the current trial was stronger in the transverse direction, weaker in the longitudinal direction and the modulus was half. The reason for the difference in results is due to the size of sample when testing profiles. This is explained in Chapter 4, where profiles are tested in compression.

3.4.4 Conclusion

This trial confirmed that the method used to manufacture samples affects the material properties. The blends had better flexural strength than the benchmark profile standards, however, the stiffness was inadequate. Injection moulding produced higher flexural strength values than machined intrusion samples. The effect of manufacturing method on modulus was inconclusive. Machining produces surface flaws, which reduces strength and increase variability. The flexural results showed that a synergistic co-continuous morphology was not produced. Compression properties of machined intrusion samples was stronger along the profile compared to transverse to the profile. Polymer molecules are orientated along the direction of flow giving improved properties.

3.5 Trial 2 – Effect of Polypropylene Waste Stream on a Blend

This trial investigated the effect of using different polypropylene waste streams in a model blend. Flexure and impact properties of the blends were compared.

3.5.1 Materials

The polypropylene and polyethylene waste streams used are given in Table 3.6. All materials were recycled, intrusion quality materials with the exception of one virgin grade. The virgin grade was Ineos PP 400-NA01, which was high impact, sheet grade copolymer.

Table 3.6 Trial 2 details of polypropylene and polyethylene waste streams

Polymer	Source	Code	Characteristics
Polyethylene	Bulk containers	HDPE	0 - 4.1 g/10min 190 $^{\circ}$C/ 5 kg
Polypropylene	Agglomerated film	F	5.7 - 6.5 g/10min 230 $^{\circ}$C/ 2.16 kg 7.5% filler
	Bulk Bag	BB	2.5 g/10min 230 $^{\circ}$C/ 2.16 kg
	Sheet	S	0.8 - 1.9 g/10min 230 $^{\circ}$C/ 2.16 kg
	Bumper	B	12 g/10min 230 $^{\circ}$C/ 2.16 kg
	Virgin	V	1.5 g/10min 230 $^{\circ}$C/ 2.16 kg

The MFI of each material reflected the manufacturing process for which it had been used. Bumper had the highest melt flow, because it was an injection moulding grade that had to fill a large mould. Sheet, fibre and film had lower MFI, because they needed good melt strength and did not require long flow paths [26]. Bulk containers are thick wall containers made by rotational moulding.

3.5.2 Properties of the Individual Waste Streams

The waste streams came in the form of jazz flake or pellets. Test bars were injection moulded from each waste stream. They were tested in flexure and for impact strength at room temperature and -30 $^{\circ}$C. Table 3.7 gives the measured properties.

Table 3.7 Average flexural and impact properties of Trial 2 waste streams. ± standard deviation is quoted. See Table 3.6 for waste stream codes. NB = No Break.

Waste Stream	Flexural (MPa)		Unnotched Impact Strength (kJ/m^2)		Notched Impact Strength (kJ/m^2)	
	Strength	Modulus	RT	-30°C	RT	-30°C
F	25.2±0.3	866±63	NB	13±2.3	4.1±0.7	1.6±0.2
BB	31.7±0.2	1041±23	NB	17±3.2	5.3±0.5	2.0±0.3
B	24.8±0.4	1291±125	NB	26±8.6	40±3.2	5.7±0.9
S	36.1±0.4	1185±82	NB	NB	40±5.2	5.9±1.0
V	36.6±0.2	1250±81	NB	NB	25±12	6.9±0.7
HDPE	19.6±1.2	714±58	NB	NB	41±7.8	7.2±0.7

The HDPE had the best impact properties, though it had low stiffness and strength. Bulk containers have thick walls that compensate for the low strength and stiffness. HDPE is used because it has good chemical resistance and good impact properties at high and low ambient temperatures.

Agglomerated film (F) had acceptable strength, however, it had low modulus, poor notched and low temperature impact properties. A notched impact strength of above 10 kJ/m^2 was considered reasonable. Agglomerated film was likely to be random copolymer from a range of sources contaminated with other polymers, low levels of anti-blocking fillers, inks and adhesives. Random copolymer is used to produce a clear, flexible, tough film.

Bulk bag (BB) was woven polypropylene fibres, which was likely to be homopolymer. Homopolymer would be expected to have the highest stiffness and strength, however, it was contaminated with nylon stitching, films and other debris. The quality of the material can be seen in Table 1.4, which has an inset picture of agglomerated film and fabric.

Bumper (B) and Sheet (S) were highly modified block copolymers to give very good impact properties at low temperatures. They were much stiffer and stronger than bulk bag and film. The sheet and virgin (V) sheet grade materials had very similar properties. Contamination such as paint flakes, may have caused the reduced strength of the bumper material.

3.5.3 Formulation Details

The formulation blended polystyrene, polypropylene and polyethylene. The exact formulation cannot be divulged due to the proprietary nature of the blends. The level of polystyrene was lower than in Section 3.4. The percentage of HDPE also differed. The polypropylene portion of the formulation contained 30 wt% agglomerated film and 70 wt% of one of the alternative polypropylene waste streams.   The agglomerated film was a cheap, abundant source of material, though with poor mechanical properties. The aim of the trial was to improve mechanical properties by blending the agglomerated film with a higher quality polypropylene waste stream.

Table 3.8 The component plastics present in Trial 2 blends.

Component Plastic	Blends							
	FF	FBB	FB	FS	FV	FR	F2	F4
Polystyrene	✓	✓	✓	✓	✓	✓	✓	✓
HDPE	✓	✓	✓	✓	✓	✓	✓	✓
Agglomerated film (F)	✓	✓	✓	✓	✓	✓	✓	✓
Bulk bag (BB)		✓						
Bumper (B)			✓					
Sheet (S)				✓				
Virgin (V)					✓			
Crumb rubber (R)						✓		
Impact modifier							2%	4%

Samples were prepared using twin screw compounding and injection moulding. Two alternatives to blending were also trialed impact modifier and crumb rubber. PA93022 impact modifier from Wells Plastics was trialed at 2 wt% and 4 wt%.

Rigoprene R151 supplied by Verneos was very fine crumbed rubber in a 50 wt% polyolefin carrier. This was diluted in 4:1 ratio with agglomerated film. The compound compositions and nomenclature are given in Table 3.8.

3.5.4 Blends Results and Discussion

Table 3.9 gives the flexural and impact properties of the blends. The properties of the blends were lower than the individual polypropylenes as illustrated in Figure 3.6 and 3.7.

The rule of mixtures predicts the value of property, Y, from the values of the component parts according to the proportions of the volume fractions, see Section 2.2.1 [21]. By rule of mixtures, the strengths were 3-8% lower and the moduli were 13-22% lower. This is comparative to published literature, which showed a 10-20% reduction in modulus for PSPP and PSHDPE blends [63, 66]. These studies measured a synergistic increase in properties in specimens with co-continuous morphology, however, the maximum values did not exceed the rule of mixtures value.

Table 3.9 Average flexural and impact properties of Trial 2 blends ± standard deviation. See Table 3.8 for blend codes.

| Blend	Flexural (MPa)		Unnotched Impact Strength (kJ/m^2)		Notched Impact Strength (kJ/m^2)	
	Strength	Modulus	RT	-30 ^{o}C	RT	-30 ^{o}C
FF	23.4±0.8	749±29	52±5.3	17±3.5	5.8±0.3	2.6±0.7
FBB	26.2±0.3	870±59	49±8.0	19±4.1	7.0±0.6	3.2±0.6
FB	23.4±0.1	894±31	46±6.8	24±6.0	9.9±0.6	4.8±1.3
FS	28.2±0.0	953±17	39±2.7	23±3.5	11±0.8	4.3±0.6
FV	28.8±0.2	963±53	36±5.0	17±2.3	10±0.7	4.3±0.6
FR	23.2±0.0	817±18	17±1.8	11±1.5	4.9±0.4	2.3±0.8
F2	23.3±0.1	807±35	34±7.8	13±6.2	5.7±0.3	3.0±0.7
F4	22.9±0.1	839±52	39±7.6	13±4.8	6.0±0.3	3.1±0.3
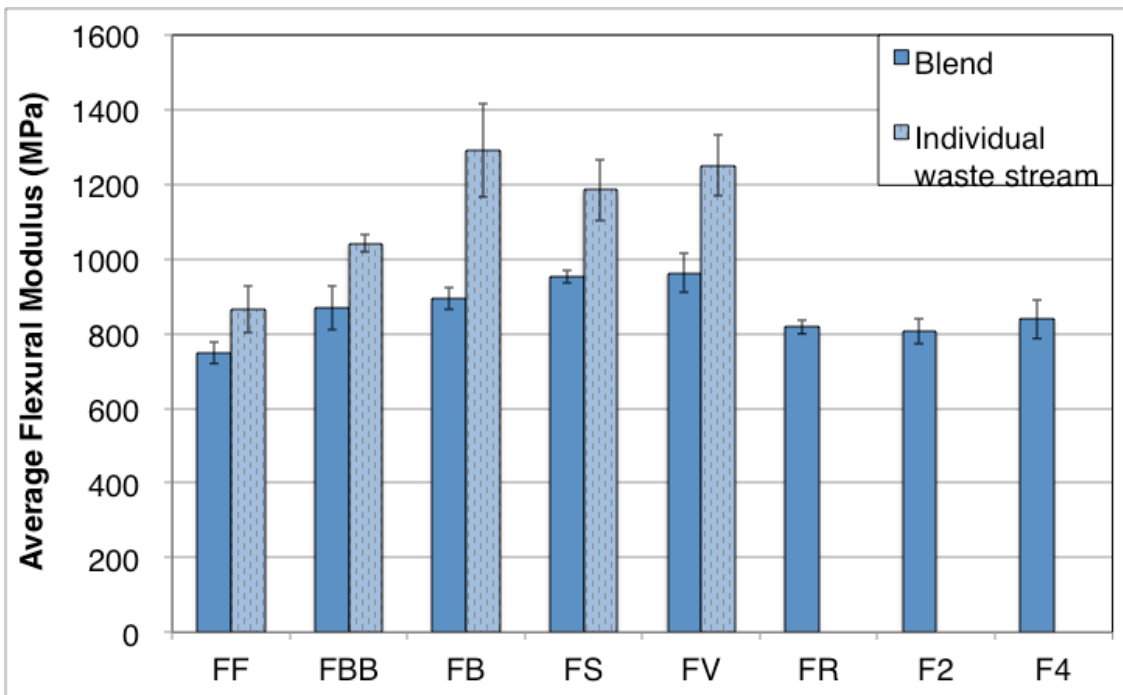
Figure 3.6 Average flexural modulus of Trial 2 individual waste streams compared to their associated blend. ± standard deviation included. See Table 3.8 for blend codes.
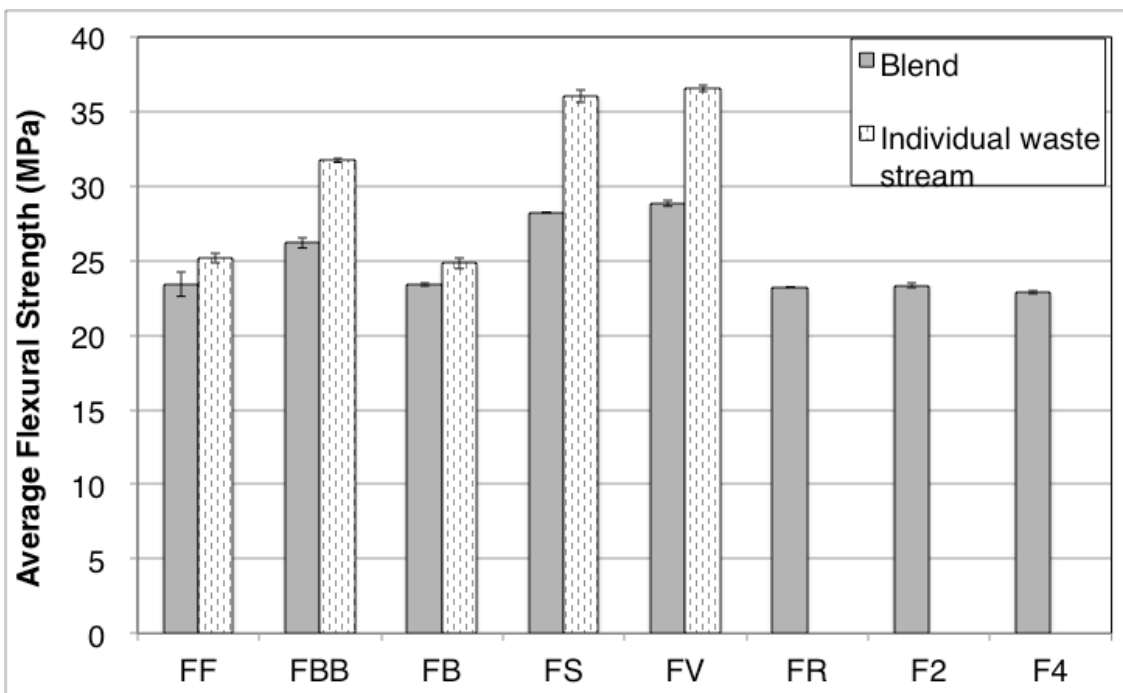

Figure 3.7 Average flexural strength of Trial 2 individual polypropylenes compared to their associated blend. ± standard deviation included. See Table 3.8 for blend codes.
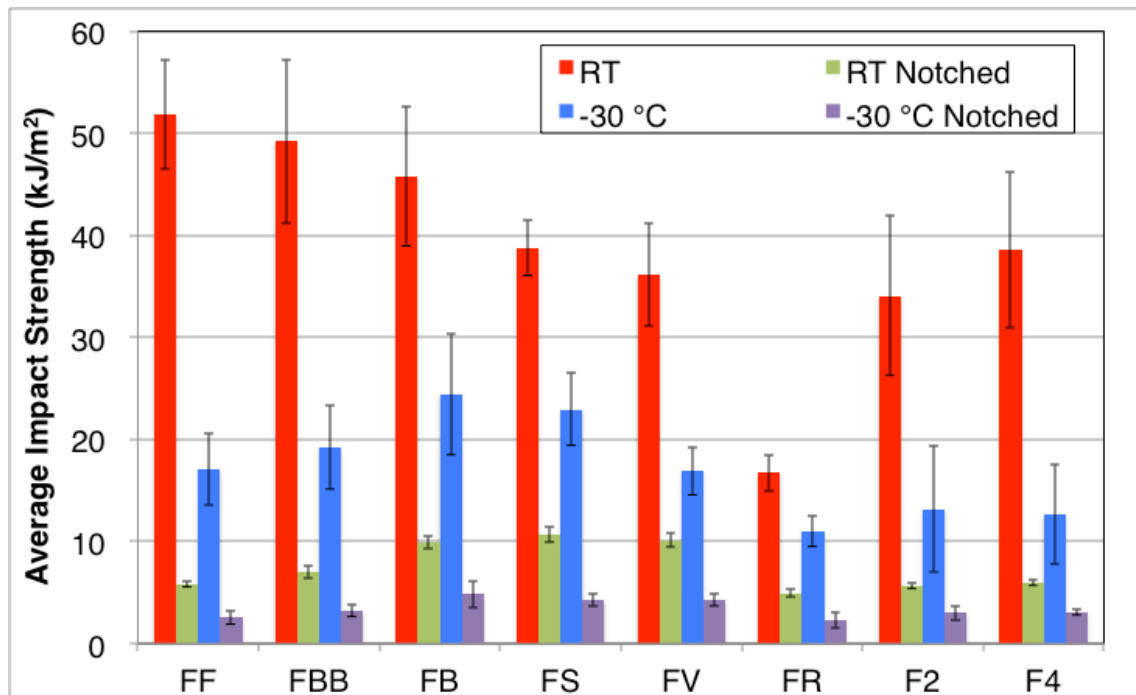
Figure 3.8 Average impact strength of Trial 2 blends. ± standard deviation included. See Table 3.8 for blend codes.

Blending waste streams improved the stiffness compared to the baseline, FF. The improvement in properties tracked the performance of the individual waste streams. The improvement in properties was 2-14% above that expected by the rule of mixtures. The impact modifier did not give a significant benefit. However, the best performing FS and FV were 200 MPa still below the 1170 MPa machined railway sleeper benchmark [94]. These sheet grade materials gave the best improvement in modulus, strength and notched impact properties.

The rubber compound had a significant deleterious effect on impact properties. Ground tyre rubber is documented to reduce mechanical properties even at low loadings [42]. The rubber is a lightly crosslinked thermoset, that does not molecularly interact or flow during moulding. Any bonding is mechanical due to surface roughness and particle shape, unless compatibilisers and surface treatments are used. 0.1-5 μm particle size is optimum for toughening brittle polymers. At 20 μm size, rubber particles are generally not detrimental. However, the smallest size that is economically viable to produce is 100-400 μm [42]. The rubber used had a surface area to volume ratio of 15-18:1 and did not have surface treatment. Particle size was not divulged by the supplier.

The impact strength of the individual waste streams was better than that of the blends with the exception of film and bulk bag notched impact. The improvement in blend cold impact properties followed the ranking of the individual waste streams, except that the values for B (bumper blend) were the highest, see Figure 3.8. The room temperature notched values were about a third of the value expected by rule of mixtures for all the polypropylene blends. This suggests an increased notch sensitivity of incompatible polymer blends as discussed in Section 2.2.1. A study by Viratyaporn found PS/HDPE notched impact strength plummeted with the addition of PS, reaching 25% of the expected value at 20 wt% PS [62]. In the same study, PS/PP had double the expected impact strength for the same level of PS.   The reason for this difference in behaviour was not clear. It was suggested that the presence of atactic PP acted as a compatibiliser with the PS.

3.5.5   Conclusion

The mechanical, notched impact and cold temperature properties were improved by blending waste streams compared to the film grade waste stream. The properties of the block copolymer polypropylenes were better than that of the blends. Film is a widely available, cheap source of PP. Bulk bag is an adequately available and reasonably priced source of material. Sheet is too specialised to be available in sufficient quantities and has an MFI that is too low for the intrusion process. Bumper had been widely available due to the car scrapage scheme, however, availability shrunk significantly when the scheme stopped March 2010.

3.6   Trial 3 - Effect of Flame Retardants

Flame retardancy is a desirable, if expensive property. Five formulations were trialed to see if adequate flame retardancy could be achieved in a complex polymer system with little effect on the mechanical properties.

3.6.1 Materials

The trial used the PSPEPP blend from Section 3.4 as the base blend. The flame retardants were added at a suitable level to give UL 94 V0 rating [88]. The flame retardants were:-

– Smoke suppressant - 60898-M1-300 Superex ZB Smoke Suppressant masterbatch for polyolefins from Americhem, supplied in a LDPE carrier.

– Wells masterbatch - FR93039 Low Smoke/Zero Halogen masterbatch supplied by Wells Plastic, supplied in a universal carrier.

– Americhem masterbatch - 58578-M1-300 Superex POV0-HF flame retardant masterbatch from Americhem. A proprietary halogen free intumescent flame retardant in low density polyethylene carrier.

Table 3.10 gives the compositions.

Table 3.10 Flame retardant compositions for Trial 3.

	wt% Material		
Blend code	WFR	AFR	SS
PSPEPP	70	60	85
Smoke Suppressant			15
Wells Masterbatch	30		
Americhem Masterbatch		40	

3.6.2 Flammability Results

All samples failed UL 94 V0, V1 and V2 [88]. The smoke suppressant did not have a significant affect on smoke generation. 40 wt% of the Americhem intumescent flame retardant was required to give a significant improvement in flammability properties, however, it still failed V0. This high level would be expected to have a significant effect on mechanical properties.

3.6.3 Mechanical Properties Results and Discussion

Table 3.11 and Figure 3.9 give the results of the mechanical testing. The blend values are the PSPEPPP blend from Section 3.4, because PSPEPP was found to be contaminated.

Table 3.11 Flexural and tensile properties of Trial 3 flame retarded blends giving average value with standard deviation. See Table 3.10 for blend codes.

	Flexural		Tensile	
Compounds	Strength (MPa)	Modulus (MPa)	Strength (MPa)	Modulus (MPa)
Blend	29.5±0.2	947±43	18.7±0.3	760±67
WFR	21.3±0.1	937±19	11.7±0.1	832±43
AFR	21.9±0.2	897±24	12.3±0.1	780±38
SS	25.9±0.1	824±36	16.2±0.2	791±37

The effect on mechanical properties was similar for all materials. Tensile modulus increased, though strength decreased and there was an unexpected decrease in flexural modulus. Intumescent flame retardant systems are not reported to have a reinforcing effect, plus their hydrophilic nature creates a poor interfacial bond with hydrophobic polymers. Studies have reported an increase in modulus and heat deflection temperature, with a decrease in impact strength and other mechanicals [70]. Coupling agents have been studied, showing improvements in mechanical properties without a detrimental effect on flammability [97, 98]. Reinforcement additives and impact modifiers could also be added to counterbalance the property reduction [70].
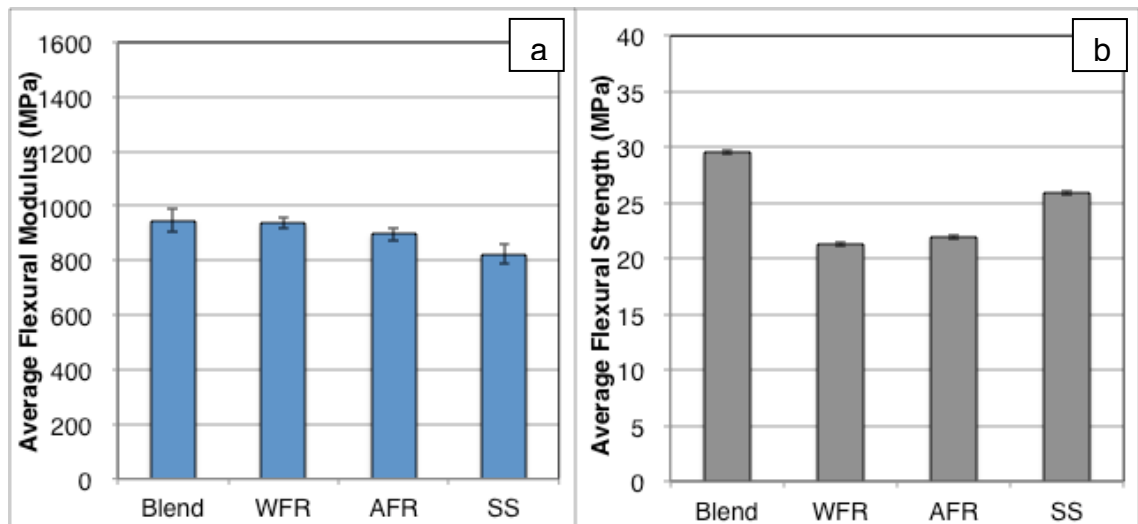
Figure 3.9 Trial 3 flame retarded blends (a) average flexural modulus (b) average flexural strength. ± standard deviation included. See Table 3.10 for blend codes.

3.6.4 Conclusion

The use of flame retardants was judged undesirable due to the high loadings required, the reduction in mechanical properties and the high cost.

3.7 Trial 4 - Effect of Reinforcement Additives

The effect of reinforcing additives on a model polymer blend was investigated. One particulate, two plate-like and one fibrous filler were added to the PSPEPP blend from Section 3.4. Combinations of fibre and particulate fillers were also explored to further enhance the structural properties.

3.7.1 Materials

The particulate filler was Omyalene 102M calcium carbonate from Omya UK. An 86 wt% stearic acid coated chalk whiting in a polyolefin carrier. The particles had an aspect ratio of 1 and an average particle diameter of 2 μm. The specific surface area was 2.5 m^2/g according to BET ISO 4652.

The plate-like fillers were both mica:

–   Micro Mica W160 from Norwegian Talc AS and distributed by Omya. A muscovite with aspect ratio 20:1 and a median particle size of 13.5 μm (wet analysis Malvern Mastersizer X) or 4.2 μm (X-ray analysis Sedigraph 5001). The specific surface area was 6.8 m^2/g according to BET ISO 4652.

–   Mica MKT from Imerys and distributed by Richard Baker Harrison: a white micronized, muscovite, with aspect ratio 20:1 and average particle size d_{50} 4.5 μm. The surface area was 7.2 m^2/g (BET). Example uses were in paint, varnish, rubber, plastics and adhesive industries.

The fibre was 3299 EC13 chopped strand glass fibre from PPG Industries. The silane treated filaments had a fibre diameter of 14 μm, and an average length of 4.5 mm. 2 wt% Bondyram 1001 maleic anhydride modified homo-polypropylene from Polyram was added to the matrix to act as a coupling agent and compatibilise to the polypropylene.

Table 3.12 shows the additive combinations used with a base polymer blend of polystyrene, polyethylene and polypropylene with a melt flow of 11.1 g/10 min 230 ^{o}C 2.16 kg. The base blend was the same PSPEPP that was used for Section 3.4.

Table 3.12 Compounds trialed with a proprietary recycled plastic blend in Trial 4 (G: glass fibre, OM: mica from Omya, IM: Mica from Imerys, C: calcium carbonate $CaCO_3$)

Additive (wt%)	20C	20IM	20OM	15G	15G5OM	15G5C	30G	30G5OM
PSPEPP	80	80	80	85	80	80	70	65
Glass				15	15	15	30	30
Mica Imerys		20						
Mica Omya			20		5			5
$CaCO_3$	20					5		

The mixing efficiency was checked by using scanning electron microscopy. It showed a well dispersed blend of different polymers. The orientation of the

fibres in the direction of process flow (perpendicular to the fracture surface) can be observed at the fractured surface, see Figure 3.10. The calcium carbonate addition showed good distribution with little agglomeration, see Figure 3.11. The maximum agglomerate size observed was below 10 µm, see Figure 3.11b.
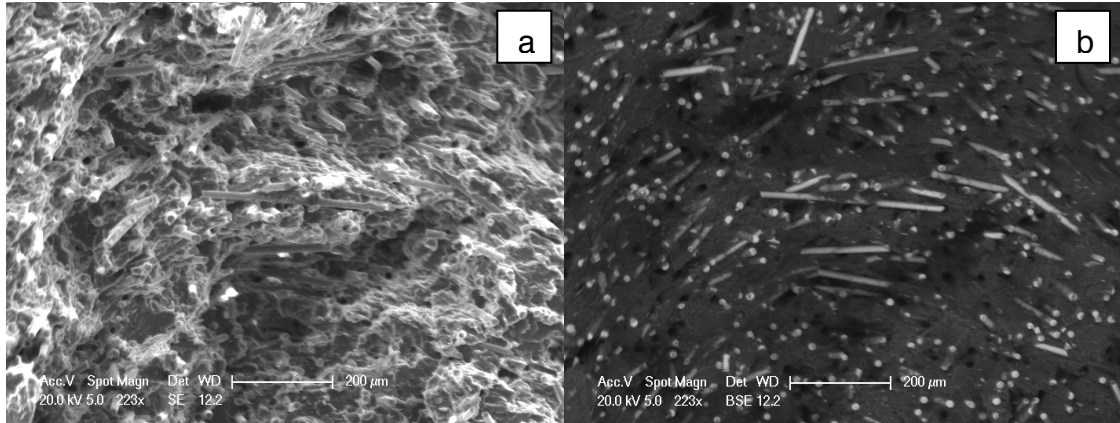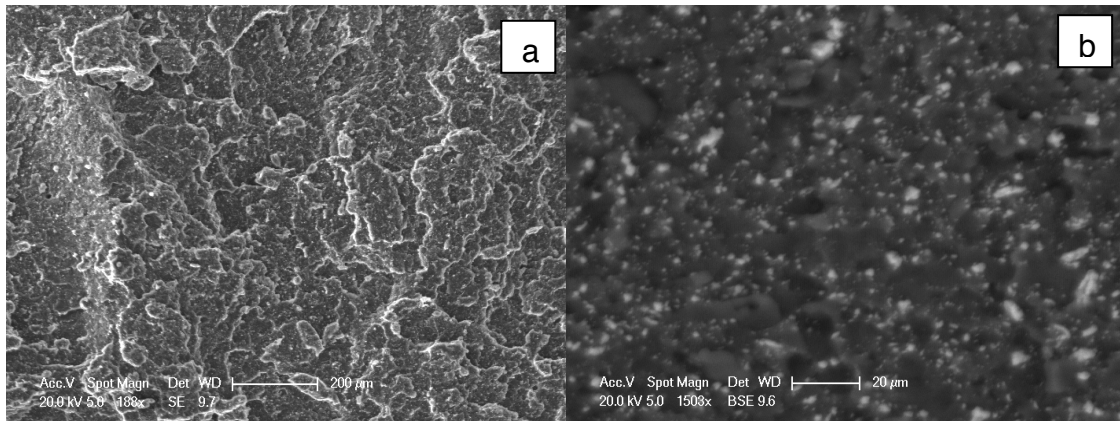

Figure 3.10 SEM micrograph showing the fracture surface morphology of 30 wt% glass fibre 5 wt% mica filled compound. (a) secondary electron mode (b) back scattered electron mode showing filler distribution.

Figure 3.11 SEM micrograph showing the fracture surface morphology of 20 wt% calcium carbonate filled compound. (a) secondary electron mode (b) back scattered electron mode showing calcium carbonate distribution.

3.7.2 Mechanical Properties Results and Discussion

The test results are given in Table 3.13, Figure 3.12 and 3.13. The effect of each filler was dependent on the aspect ratio of the filler, level of filler and the mode of loading. Loading in flexure produced higher strength and modulus values than in tension. In flexure, the stress is maximum at the surfaces. The force is compressive on the loaded surface with an equal and opposite tensile

stress on the opposite surface [39]. The increase in flexural strength for both particulate filled systems was attributed to the compressive component of the mechanical response. The compressive strength of filled systems tends to increase even for uncoupled systems. This was consistent with other studies, which report that compressive strength is directly proportional to Young's modulus [80]. The flexural and tensile modulus increased with aspect ratio of the filler – particulate, followed by plate-like, with fibrous producing the best enhancement. The addition of a second type of filler further improved the modulus. Flexural and tensile strength followed the same general trend as modulus.

Table 3.13 Average flexural and tensile properties of Trial 4 reinforced polymer. ± standard deviation. See Table 3.12 for blend codes.

| Compound	Flexural		Tensile	
	Strength (MPa)	Modulus (MPa)	Strength (MPa)	Modulus (MPa)
Blend	29.5±0.2	947±43	18.7±0.3	760±67
20C	32.0±0.3	1500±39	17.1±0.3	907±53
20IM	30.0±0.3	1912±49	15.1±0.1	1026±91
20OM	31.8±0.5	2137±30	18.0±1.1	1278±184
15G	48.1±0.5	3156±20	32.0±0.9	1287±153
15G5C	49.5±0.6	3350±49	27.8±1.2	1681±90
15G5OM	50.9±0.5	3662±13	33.8±1.3	1680±498
30G	63.3±0.6	5577±47	35.7±2.1	2411±209
30G5OM	64.5±0.7	5966±48	41.5±5.3	3122±304
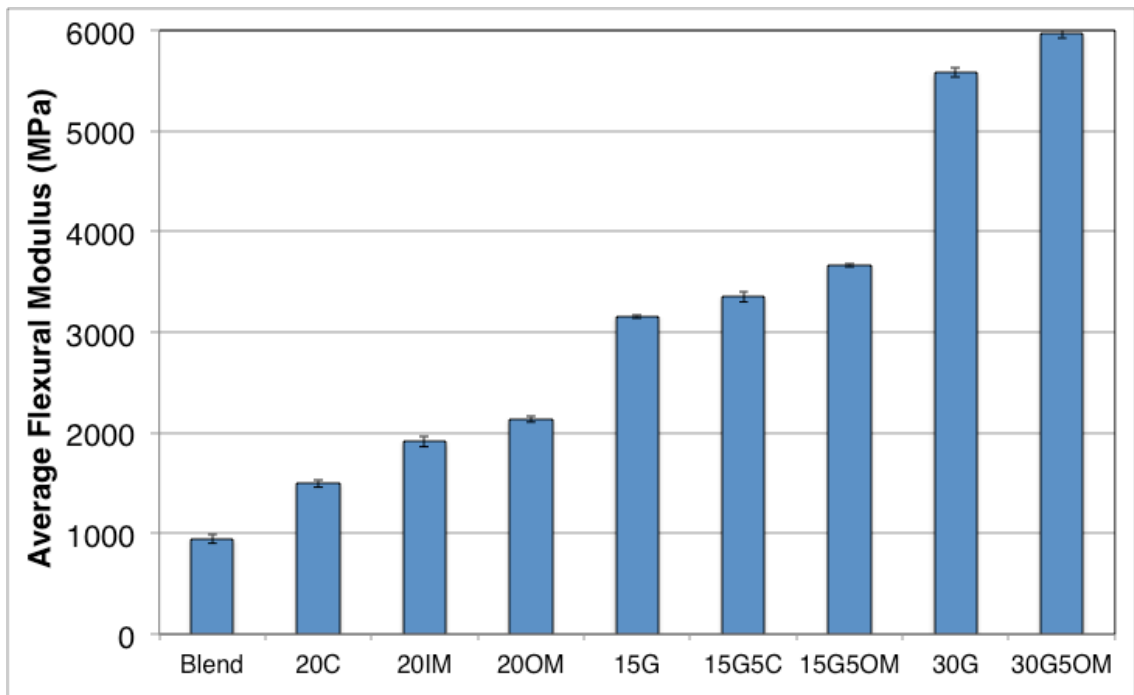
Figure 3.12 Average flexural modulus of Trial 4 reinforced blends. ± standard deviation included. See Table 3.12 for blend codes.
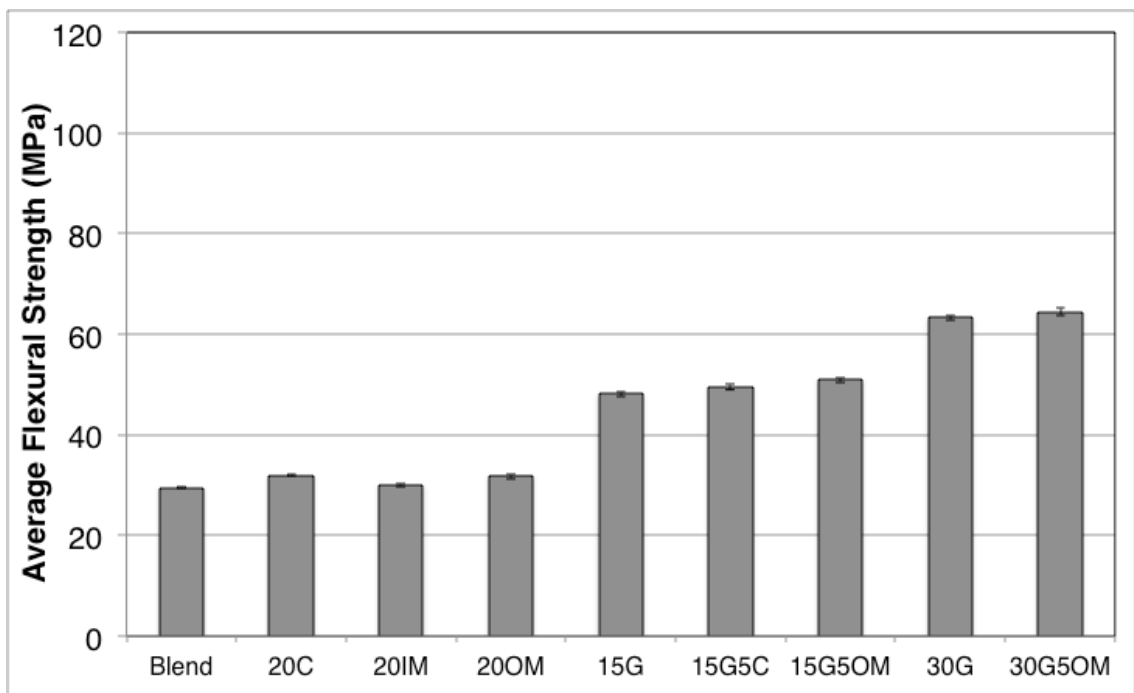

Figure 3.13 Average flexural strength of Trial 4 reinforced blends. ± standard deviation included. See Table 3.12 for blend codes.

Stearate coated calcium carbonate behaved as predicted from the reported literature [70, 79]. The modulus increased by 20%, and the strength decreased slightly. In flexural mode, the modulus was increased by 50%, and the strength increased slightly. Calcium carbonate is known to lower tensile strength and impact properties, to a degree dependent on the grade and surface treatment used [25]. The reduction in tensile strength indicates poor interfacial adhesion, which at high strains, causes debonding at the polymer/filler interface followed by cavitation [79]. The stearic acid improves dispersion because carboxylate functional groups anchor to the filler surface. However, the coupling effect is low, because it has limited ability to bond or entangle with the polymer [70].

In the mica filled systems, the tensile strength decreased for the Imerys mica and was practically unchanged for the Omya Mica. The reduction in tensile strength was expected to be less than for calcium carbonate, because mica has a higher reinforcing effect [70, 79]. Greater agglomeration of the Imerys mica may have caused the larger drop in tensile strength, unfortunately SEM was not used to verify this [79]. The flexural modulus doubled and tensile modulus increased 35-70%. The higher modulus for mica filled systems is consistent with the increase in aspect ratio, as observed in other studies that report a 50–100% increase compared to talc or calcium carbonate, with little or no reduction in impact strength [70, 79]. Mica has a far higher aspect ratio than calcium carbonate, which increases the contact area between the mica and the matrix and leads to a more significant effect on properties. The increased surface area improves stress transfer from the matrix to the filler [79]. In addition, mica has a higher tensile modulus (172 GPa) compared to $CaCO_3$ (35 GPa) [80].

The mica from Omya gave better reinforcement that the mica from Imerys. The two types of mica were expected to give similar results as their specifications were similar [99, 100]. In reality, there may have been significant differences in aspect ratio, particle size and size distribution. The aspect ratios were quoted as "typical" values not precise measurements. Wypych in the "Handbook of Fillers" regards aspect ratio as the most important single property characterising the quality of micas, because a high aspect ratio contributes greatly to polymer

reinforcement [80]. The particle size distribution is not sufficiently described on the Imerys datasheet to compare with the Omya datasheet [99, 100]. The Imerys datasheet does not provide a test method for measuring particle size. Whereas, the Omya specification quoted median values of 13.5 µm using a laser diffraction method and 4.2 µm using a sedimentation technique. In a comparative study of particle size measuring techniques, laser diffraction gave larger values than sedimentation, and that the difference was larger for flaky particles [101]. In fact the researchers found the flatness of flaky particles could be characterized by the ratio of median diameters. The literature gives conflicting opinions on whether small or large particles give better reinforcement. A study in nylon, PA6, found an improvement in reinforcement for 75 µm diameter mica compared to 37 µm, [102]. The difference in particle size was inconclusive in a study of biodegradable poly(ester-urethane) with standard talc of particle size below 10 µm (85%) and fine talc below 5 µm (80%) [103]. However, aspect ratio of the particles was not considered in either study.

The silane treated glass fibre with maleic anhydride polypropylene compatibiliser significantly improved the strength and modulus of the blend, as expected in a well oriented and consolidated glass fibre composite. 15 wt% glass fibre increased the tensile strength and the elastic modulus by 70%. The flexural strength was increased by 60% and the flexural modulus by 210%. 30 wt% glass fibre increased the tensile strength by 90% and the modulus by 215%. The flexural strength was increased by 115%, and the flexural modulus by 490%.

The 20 wt% mica increased the tensile modulus to the same degree as 15 wt% glass fibre, however, without the same increase in strength or flexural modulus. Mica could be used as an alternative to glass fibre for certain applications.

Calcium carbonate had a similar effect in the glass filled blend as with the pure polymer blend. In both cases, the addition of calcium carbonate caused a slight increase in the mechanical properties, except for the tensile strength.

The addition of mica to the glass fibre blend resulted in an increase in tensile and flexural properties. The addition of 5 wt% mica to glass fibre blend had a far greater effect on tensile strength than 20 wt% mica in the polymer blend. This synergism was observed in tensile strength at 15 wt% glass fibre and was particularly marked at 30 wt% glass fibre with a 16% increase in strength. A similarly remarkable effect has been observed for silane coated mica filled glass fibre mat reinforced PP [75]. The authors found that the addition of 10 wt% mica to 12.5 vol% glass fibre mat reinforced thermoplastic PP led to a substantial increase in tensile and flexural modulus (in the order of 100%), combined with a moderate improvement of strength. This synergy was explained by the mica increasing the radial compressive stress of the matrix on the glass fibres, which produced an increase in interfacial shear strength. The study by Zhao used SEM micrographs to demonstrate the increase in interfacial shear strength. Pulled out fibres had higher surface roughness when mica was present in the matrix.

The interfacial shear strength, $\tau = \rho_s \sigma_R$ where ρ_s is the static friction co-efficient and σ_R is the radial stress due to thermal shrinkage of the matrix [104]. Using the equation proposed by Dilandro [105]:-

$$\sigma_R \quad = \quad \frac{(\alpha_m - \alpha_f) \, \Delta T \, E_f \, E_m}{(1 + v_f + 2V_f)E_f + (1 + v_m)E_m} \qquad\qquad 3.1$$

Where α is the thermal expansion co-efficient; ΔT the difference between the matrix solidification temperature and the testing temperature; v is poisson's ratio; and E is Young's modulus. The subscripts are f for fibre and m for matrix. From the equation the fibre radial compressive stress depends upon the modulus and the co-efficient of thermal expansion (CTE) of the matrix. Mica increased the modulus of the matrix substantially, however using the rule of mixtures, the authors calculated there would be a 3% decrease in the co-efficient of thermal expansion. Lee measured an 8% decrease in bulk CTE in a 10 wt% mica filled polypropylene, though calculated values varied depending upon the ellipsoid orientation [106]. A CTE for a 10 wt% mica polypropylene

commercial grade could not be found, for 20 wt% mica filled PP values of 1-5x10^{-5} cm/cm/^{o}C were quoted compared to a generic value of $\sim$10x10^{-5} cm/cm/^{o}C for unfilled polypropylene [107–109]. The flexural modulus of these filled compounds was over double that of the unfilled grade. In a study by Nairn, the residual interfacial forces of unidirectional graphite fibres in PP and epoxy matrices were modeled and mechanical properties measured [110]. A significant change in modulus with moderate decrease in CTE was also measured. Their model included a similar equation to Dilandro. The authors proposed that during solidification, the difference in co-efficient of thermal expansion (CTE) between polymer matrix and glass fibres generated a compressive radial stress at the interface, which was proportional to the difference in thermal expansion co-efficient and dependent upon the elastic modulus of the matrix.

The untreated mica used in this study tended to increase the CTE of the polymer blend (see Section 3.7.3), which could lead to a further increase in compressive stress at the interface and a more significant improvement in the elastic modulus. It is expected that the fibre–matrix adhesion strength would be significantly decreased in the presence of higher loadings of mica because of the contact of the glass fibres and the mica flakes at the interface [75, 110]. However, it is still unclear why this synergy was observed only for 30 wt% and not for 15 wt% glass fibre loading and why similar trends have not been previously reported [77, 78]. The studies used a single virgin polymer matrix. The combination of recycled polymers and fillers may produce a complex synergistic morphology, such as Jackson described for recycled PE, PP and glass fibre [111]. It is also documented that recycled blends produce different results to virgin materials in some cases [63].

3.7.3 Co-efficient of Thermal Expansion

The co-efficient of thermal expansion, CTE, was measured for selected blends. Thermomechanical analysis measurements produced complex results due to the number of transitions for the separate polymers. Direct measurement of the test specimens produced reasonably consistent results, see Figure 3.14. The

standard deviation was appreciable due to the small changes in size and limited sample size. Particulate fillers appeared to increase the linear CTE, while it was significantly reduced in the presence of fibre reinforcement. The increase in CTE for the particulate systems can be attributed to the poor adhesion between these fillers and the polymer matrix [80]. However, one study measured a 12% reduction in a 40 wt% $CaCO_3$ filled PP blend [79]. The level of agglomeration and dispersion could also account for the difference in results.
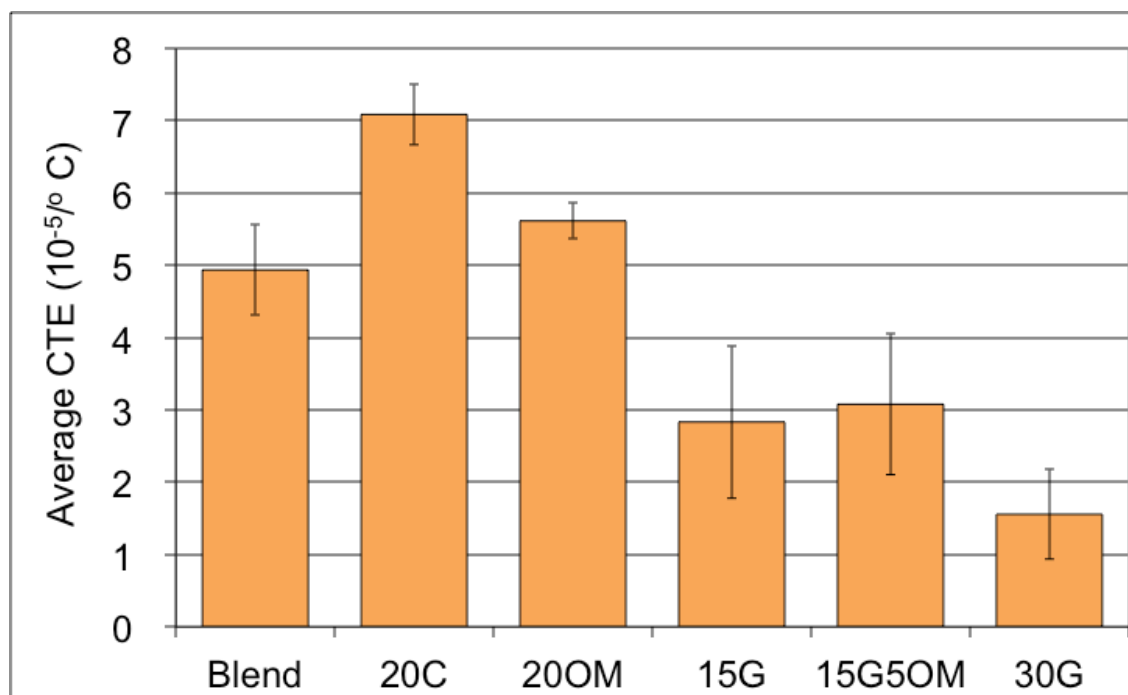

Figure 3.14 Average co-efficient of thermal expansion of selected blends by measurement of moulded bars . ± standard deviation included. See Table 3.12 for blend codes.

The reduction in CTE for the glass fibre reinforced systems was consistent with a strong coupling between glass fibres and the polymer matrix, which was achieved by the addition of silane coating and maleic anhydride grafted PP. The 15 wt% glass fibre had a CTE of 30×10^{-6} $^{\circ}C^{-1}$, which is close to that of wood across the grain [112]. The 30 wt% glass fibre gave 18×10^{-6} $^{\circ}C^{-1}$, which is in line with steel, concrete and wood along the grain [112–114]. The fibres were oriented parallel to the direction of the flow, therefore, there was a large interfacial area to constrict the expansion of the matrix.

3.7.4 Conclusion

Trial 4 confirmed the effectiveness of using plate-like and fibre reinforcement, and that synergy can occur when used in combination. Fibre reinforcement is particular of interest, because it also reduces co-efficient of thermal expansion.

3.8 Trial 5 - Different Glass Fibre levels in Intrusion Quality Material

The level of glass fibre was varied in an intrusion grade polyolefin blend to investigate the change in properties with glass content.

3.8.1 Formulations

Formulations were compounded at J.G.P. Perrite, Warrington as described in previous trials. In this trial, a commercial 30 wt% glass fibre PP compound was blended with a mixed polyolefin waste stream and recycled PP bulk bag. The glass fibre compound was a blend of recycled glass fibre filled PP, recycled PP and virgin glass fibre of 4.5 mm average length. The recycled PP was blended from post industrial and post consumer sources to produce consistent batch-to-batch properties. The polyolefin blend contained 20 wt% PP mixed with 80 wt% HDPE, MDPE and LDPE.

Formulations were designed to contain 0, 5, 10, 15 and 30 wt% glass fibre (GF). 0 wt% GF was 100% mixed polyolefin waste stream. 30 wt% GF was the undiluted commercial compound. 5, 10 and 15 wt% GF maintained a constant level of PP through the addition of the recycled PP bulk bag.

Samples were ashed to determine their glass fibre content. The results were acceptably close to target – 0, 4.5, 8.5, 16 and 28 wt%.

3.8.2 Results and Discussion

The mechanical test results are given in Table 3.14. The flexural strength and modulus followed the same rising, non linear trend with increased glass content,

see Figure 3.15. The un-notched impact dipped at intermediate glass levels, see Figure 3.16. Notched impact was significantly lower than un-notched impact.

Table 3.14 Average flexural properties and impact strength for Trial 5 variation of glass fibre content. ± standard deviation included.

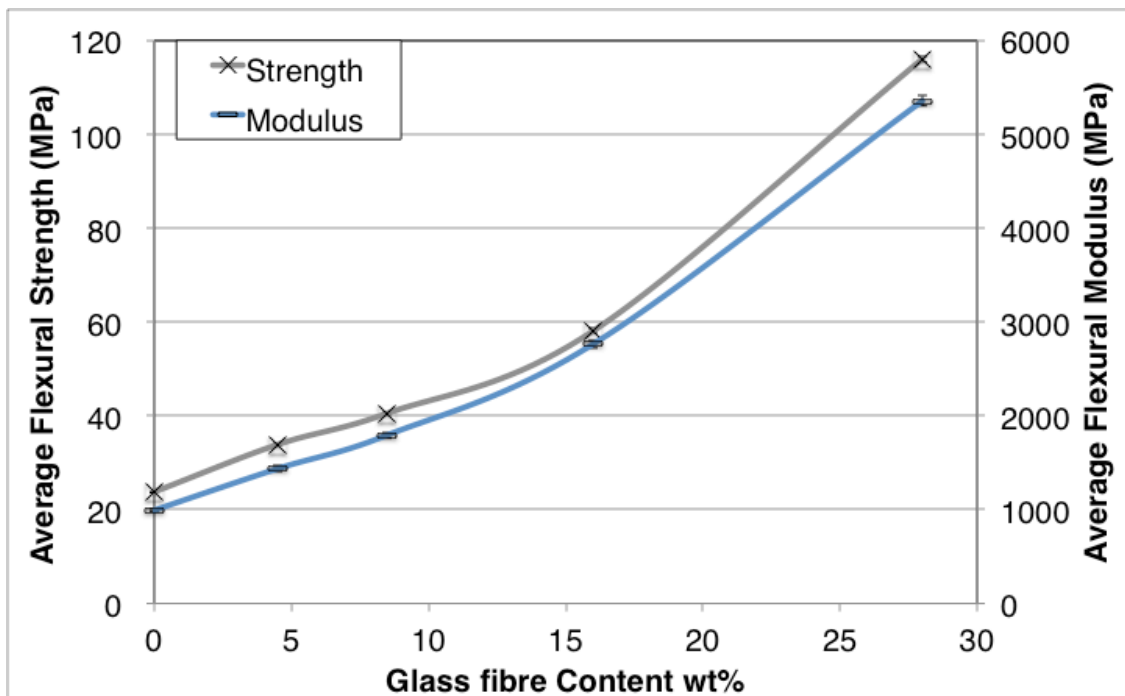| Compound	Flexural (MPa)		Unnotched Impact Strength (kJ/m^2)		Notched Impact Strength (kJ/m^2)	
	Strength	Modulus	RT	-30°C	RT	-30°C
0 wt% GF	23.8±0.1	995±16	NB	NB	4.0±0.3	3.1±0.3
5 wt% GF	33.9±0.3	1437±38	48±0.5	34±3.9	3.9±0.5	2.8±0.3
10 wt% GF	40.6±0.3	1796±34	31±0.5	27±1.8	3.1±0.5	2.9±0.3
15 wt% GF	58.1±0.5	2765±42	30±0.5	27±1.7	3.4±0.5	3.4±0.2
30 wt% GF	116±0.6	5357±52	44±2.8	38±4.6	6.7±0.5	6.7±0.4

Figure 3.15 Average flexural strength and modulus plotted against glass fibre content blend for Trial 5. ± standard deviation included.
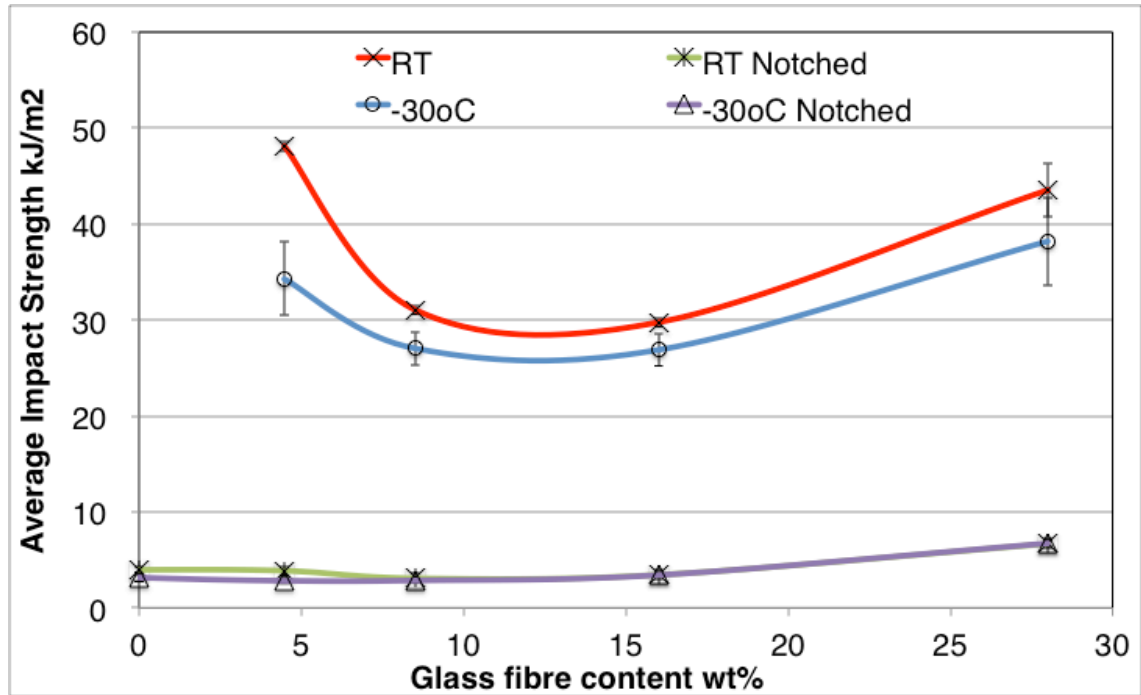
Figure 3.16 Average Charpy impact strength against glass fibre content for Trial 5. ± standard deviation included.

Glass fibre filled PP systems have been reported as having a linear dependence of modulus with glass content [115]. The non-linear increase in modulus of the current study was due to matrix composition. 30 wt% GF matrix only contained polypropylene, which would be expected to have better properties than the immiscible blend of polyethylenes and PP present in 5 wt% GF and 10 wt% GF.

Trial 4 Section 3.7 had similar levels of glass fibre in a PSPEPP matrix. At 15 wt% GF, the current trial had 20% higher strength with 15% lower modulus than Trial 4. The presence of PS would contribute to the higher modulus in Trial 4. The presence white pigmented material in Trial 4 may have resulted in the decreased strength. Titanium dioxide is a common white pigment that is very abrasive. It is known to attack glass fibre [116] and reduce mechanical properties.

At 30 wt% GF, a much larger difference was seen between the immiscible blend in Trial 4 and the homogeneous blend in the current trial. The flexural strength was almost double for the homogeneous blend, however, the modulus was

slightly lower. The comparative modulus value and significant difference in strength could be due to the phenomenon observed in a study by Jose as discussed in Section 2.2.1 [51]. The modulus was measured at low strains, where stress in transferred between the phases. The strength was measured at high strains where poor interfacial adhesion meant that instead of stress transfer there was cracking and fracture at the interphase boundaries in the immiscible blend causing reduced strength in Trial 4.

In a review of glass fibre loading studies, the level of increase in modulus and strength was dependent on the system, production technique and test method [76]. The rise in modulus and strength in this experiment was comparable of the highest rises seen in the reviewed studies. Several factors may account of this.

Some authors propose the glass fibres act as a compatibiliser, because the fibres cross through and bind to regions of dissimilar resins [76]. This has been used to explain the improvement in performance of immiscible polymer blends.

Using recycled fibre reinforced materials, instead of virgin glass fibre, was not as detrimental to mechanical properties as might be expected. Fibres breakdown to an ultimate length ($\approx$0.3-0.8 mm) that is dependent on the matrix, glass fibre content and method of processing [117–119]. Attrition is faster with longer fibres, higher concentrations of glass fibre and in higher shear processes. A study found after three extrusions, tensile strength and modulus were reasonable constant [118].

Mechanical properties are better with good distribution and alignment of fibres, however, this involves more shear and leads to fibre breakage [117–119]. Twin screw compounding with injection moulding as in this study should have produce well distributed, aligned short fibres.

A decrease in impact strength at low glass fibre content, was also observed in glass fibre filled PP [115]. In the study, un-notched charpy impact strength proceeded to peak at 30 wt% GF. Notched impact tests did not produce the

same trend and strengths peaked at 40-50 wt% GF. The current study had similar un-notched impact strength with lower notched impact strength values. In Scelsi's review [76], impact strength increased in some systems and decreased in others. It is unclear if notched impact or unnotched impact was used. A drop in impact performance was attributed to the incompatibility of the matrix in some studies [120, 121].   Certainly, the use of compatibilisers improved unnotched impact strength in other studies [122, 123].

3.8.3 Softening Temperature

Softening temperature of the blends was measured to gauge the improvement in maximum operating temperature.

Table 3.15 Vicat Softening ISO 306 B50 of the Trial 5 glass filled blends.

	0 wt% GF	5 wt% GF	10 wt% GF	15 wt% GF	30 wt% GF
Vicat (^{o}C)	69	74	76	86	>120

Glass fibre improved the maximum operating temperature measured by Vicat Softening ISO 306/B50 shown in Table 3.15.   As discussed in Section 2.1.1, Vicat is a good indication where form stability is lost, whereas HDT is a better indication of maximum load bearing temperature. The reference blend had a HDT of 52 ^{o}C at 1.8 MPa, unfortunately the other blends could not be measured using this technique. Adding 5 wt% GF and 10 wt% GF increased the Vicat slightly.   Whereas, 15 wt% GF increased by 17 ^{o}C and 30 wt% GF increased over 50 ^{o}C.   The effect of adding the fibre was important, because it raised the maximum operating temperature under load above maximum ambient temperatures.

Softening temperature is a test that is very dependent on the test type, load and heating rate.   It is difficult to make comparisons between with commercial grades, because most companies quote only one value and use a variety of tests.   Glass filled PP grades are commercially very common, filled HDPE grades are rare. Analysis where a range of tests is quoted, showed that the effect of changing load or technique was inconsistent. For example, PP

copolymer from J.G.P. Perrite had Vicat values that were similar (130 to 144 ^{o}C) whether 0, 10 or 20 wt% fibre filled, however, HDT at 1.8 MPa increased from 45 ^{o}C to 120 ^{o}C and 135 ^{o}C respectively [124]. HDPE has similar or lower values to PP. 10 wt% glass fibre HDPE is quoted as having 88 to 104 ^{o}C HDT at 1.8 MPa, and 116 to 121 ^{o}C at 20 wt% glass fibre [125–129]. The Trial 5 blends had lower values than commercial blends, this could be attributed to the mixture of polyethylenes in the blend.

3.8.4 Summary

In summary, Trial 5 confirmed glass fibre efficiently reinforces a mixed polymer blend and increases the maximum operating temperature, however, it showed that impact properties are not improved significantly.

3.9 Conclusion

The five trials reported in this chapter explored polymer blends a range of PSPEPP and PEPP polymer blends with different waste streams, fire retardants and reinforcing additives. It can be concluded that:

– the manufacturing method affects the final material properties. Intrusion moulding produced higher modulus values than twin screw compounding and injection moulding. Machining of specimens tends to a reduction in the measured flexural strength.

– blending immiscible plastics generally produced lower mechanical properties than those of pure polymers.

– careful selection of plastic waste stream and processing technique is essential to ensure the correct morphology for appropriate mechanical properties.

– poorer quality polypropylene waste stream was enhanced with the addition of higher quality polypropylene waste stream.

– glass fibres and plate-like mica efficiently reinforced a mixed polymer blend.

– a synergistic increase in tensile strength was observed when glass fibre was used in combination with mica, as mica enhances the matrix and hence increases the forces constricting the glass fibre.

–   glass fibre reinforcement reduced the co-efficient of thermal expansion.

–   glass fibre reinforcement raised the maximum operating temperature.

–   glass fibre reinforcement did not improve impact properties significantly.

Full scale intrusion trials were carried out on polymer blend and glass fibre reinforced blends, that had formulations designed from these trials.

4   Large Scale Experiments and Results

Chapter 3 described standard testing of the injection moulded test bars. These trials gave valuable information about the factors to be considered when designing formulations. However, a uniform, thin injection moulded sample cannot reflect the thick outer walls and foamed core of the intruded profiles. This Chapter details testing of the full size, intruded profiles from 100x50 mm to 250x130 mm in cross-section and up to 2.6 m in length.

Profiles were made using the standard manufacturing process on the production machines as described in Section 1.4. Samples of two production grades were collected randomly over the course of 18 months from four production machines. This ensured that a distribution in properties, which arose due to the variation of materials used, was effectively measured. Four trial grades were also made, where possible, two-three batches were manufactured of each trial grade. Profiles were tested at the end of the collection period. The only exception was 250x130 mm sleeper profiles, which were tested over the course of four years.

The samples were tested under three-point bend, four-point bend, and compression loading conditions. These load configurations were the most representative of the in-service conditions.
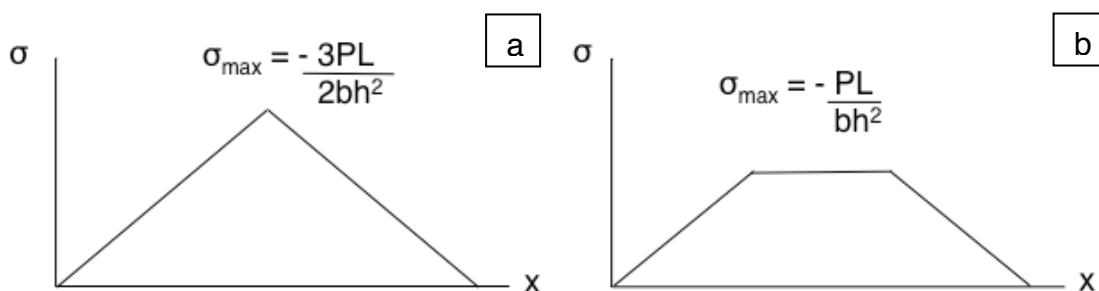

Figure 4.1 Comparison of stress distribution in (a) three and (b) four point bend, where σ = stress, x = the distance between support points, P = force, L = span, b = specimen width, h = specimen thickness [130].

Figure 4.1 shows the difference in stress distribution between three point and four point bend. In three point bend, the maximum load is concentrated at one point. In four point bend, the stress is constant between the loading noses, which puts a higher proportion of the sample under maximum stress and means that flaws are more likely to be detected [131]. Hence for quality control and structural applications, the value given by four point bend would be a more realistic "safe" lower boundary limit for strength [131]. Another benefit of four point bend is the reduction in interlaminar shear, which means that it is suitable for long fibre reinforced and composite materials e.g. wood [89, 132]. However, three point bend is usually favoured by industry, because it is an easier test to set up [133].

The co-efficient of thermal expansion was also measured. This is an important property for the following reasons: to calculate expansion gaps; determination of fixing points to prevent warping; compensation requirements when installing at temperature extremes; and the maintenance of gauge on railway sleepers.

4.1 Profile Structure, Sizes and Orientation Nomenclature

Intrusion moulded profiles have a solid outer walls and foamed core, see Figure 4.2. Blowing agent is used to foam the centre to counteract shrinkage on cooling, so giving a product with flat outer surfaces.

Profile sizes are defined by the cross-section dimensions, for example, 50x100 mm, see Figure 4.3. Dimensions are quoted in millimetres using the convention length x width x thickness.

The profile was tested in two orientations – plank and joist. In plank orientation the largest dimension of the cross-section was horizontal. In joist orientation the shortest dimension of the cross-section was horizontal. Joist orientation is called edgewise in some International standards [95]. When profile cross-section is quoted, the orientation of a profile is reflected in the dimensions given, see Figure 4.3. A 100x50 mm profile is in plank orientation. 50x100 mm profile is in joist orientation.
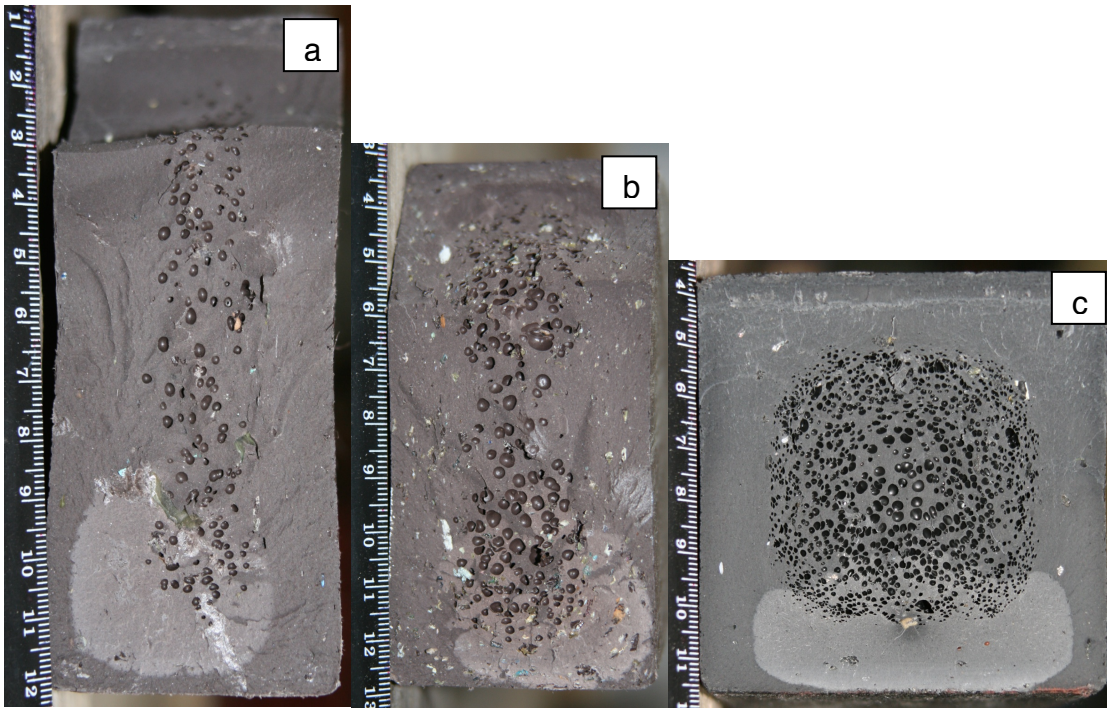
Figure 4.2 The fracture surfaces of four point bend test profiles tested in joist position. The load was applied on the top surface. Each appears to have a different proportion of foamed core, pore size and "white" ductile fracture region (a) 50x125 mm Standard grade (b) 50x100 mm Standard grade (c) 80x80 mm Impact grade.
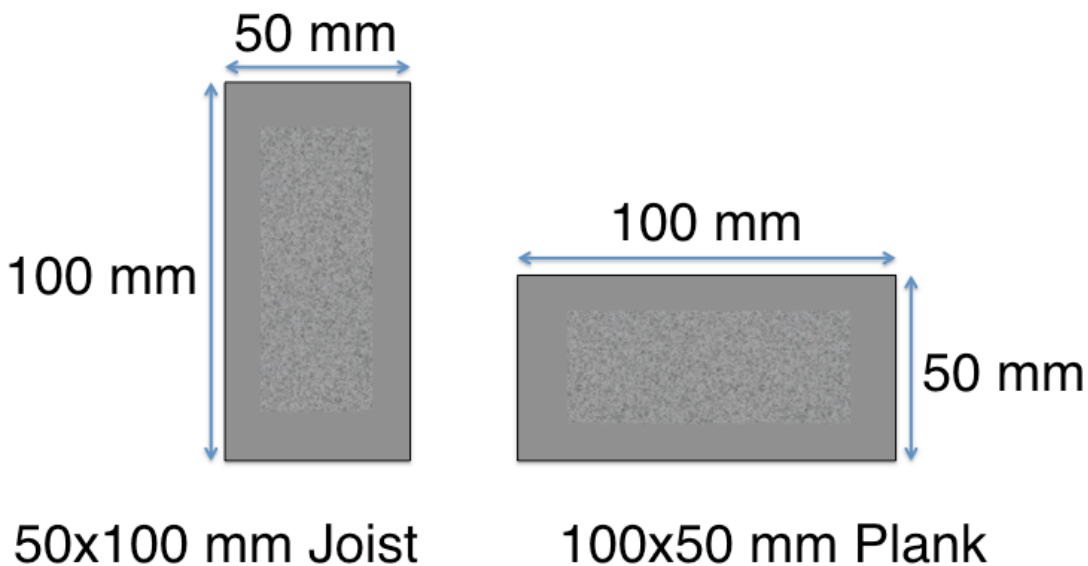

Figure 4.3 A schematic showing profile naming convention for orientation and size.

4.2 Formulation Selection

Six different formulations were tested. Two were standard production grades – Standard and Impact. One trial grade was a polymer blend - BP. Three trial grades were glass fibre reinforced – GL, GM and GH.

The production grades were blends of recycled polystyrene, polypropylene and polyethylene. The ratio and type of each polymer were tailored to suit the application. Impact grade (I) had lower stiffness with higher impact resistance for use in posts, moulded shapes and bollards. Standard grade (S) needed to be higher modulus for use in boardwalks, furniture, decking, tongue and groove, and fencing. The formulation did not change between batches, however, the specific waste recycling streams changed depending on availability. In addition a percentage of regrind was used from shredded rejected profiles.

The polymer blend trial grade (BP) included polystyrene, polypropylene and polyethylene blend. The polystyrene content was less than 35 wt%, because these formulations had been found to be very brittle in profile form. Using the rule of mixtures, a level of polystyrene was selected that gave the required stiffness with higher toughness. The PP:PE ratio was selected using the rule of mixtures, and industrial experience. Section 3.5 used the same formulation with a variety of different waste streams.

When production samples were taken in 2011, the standard production grade was very close in formulation to the polymer blend trial grade. This was because the results from the project had been used to improve the production formulations since project began in 2008. The major difference was in the waste streams used and the lack of regrind in the trial blend.

Glass fibre reinforcement was selected because it was the most cost effective, efficient reinforcement solution and was available in a recycled form. Powder and plate-like fillers were not deemed necessary in this first trial. The glass fibre levels were selected using the rule of mixtures with reference to published information for standard virgin grades. The published information was based on

injection moulded samples with good glass fibre alignment and longer glass fibre lengths.   Whereas, the intrusion moulded sample would have limited alignment and use recycled fibre. This was factored into the glass fibre content calculations. The highest glass fibre blend, GH, was used in the 250x130 mm sleeper testing.   The blends with lower levels, GM and GL, were made to explore possible applications requiring slightly greater stiffness than the standard production grade. Section 3.8 had the same target glass fibre levels with a different PP:PE ratio due to the polyolefin waste streams used.

4.3   Test Methods

4.3.1   Three Point Bend Test

The three point bend test was specified by Network Rail for 250x130 mm cross-section sleeper profile.   Network Rail did not have a specification for the recycled composite railway sleeper, therefore, a specification was defined as a part of the project. There was no international standard for the three point bend testing of plastic lumber railway sleepers. A test method was devised based on: ASTM D6109 "Flexural Properties of Unreinforced and Reinforced Plastic Lumber", ISO 178 "Plastics - Determination of flexural properties" and a proposed ISO standard for Plastic railway sleepers [89, 94, 95].

Samples were tested on a bespoke rig on the Schenk SNK2/25 hydraulic test machine located in the LEA laboratory, Department of Mechanical Engineering at the University of Sheffield. A schematic and a photograph of the test is shown in Figure 4.4.

The profile was tested in plank orientation. It rested on two cylindrical supports spaced 1435 mm apart. (1435 mm is standard gauge (spacing) between the rails on a railway track.) The central load was transferred to the sample through a cylindrical loading nose and a spreader plate. The loading nose and supports were 60 mm diameter; these needed to be sufficiently large to prevent excessive indentation of the sample. The spreader plate was 260x150x10 mm. The profile was loaded at a rate of 10 mm/min until rupture occurred.   The

sample had to strapped down, because the energy at break was very large. Three samples were tested from every batch when possible.
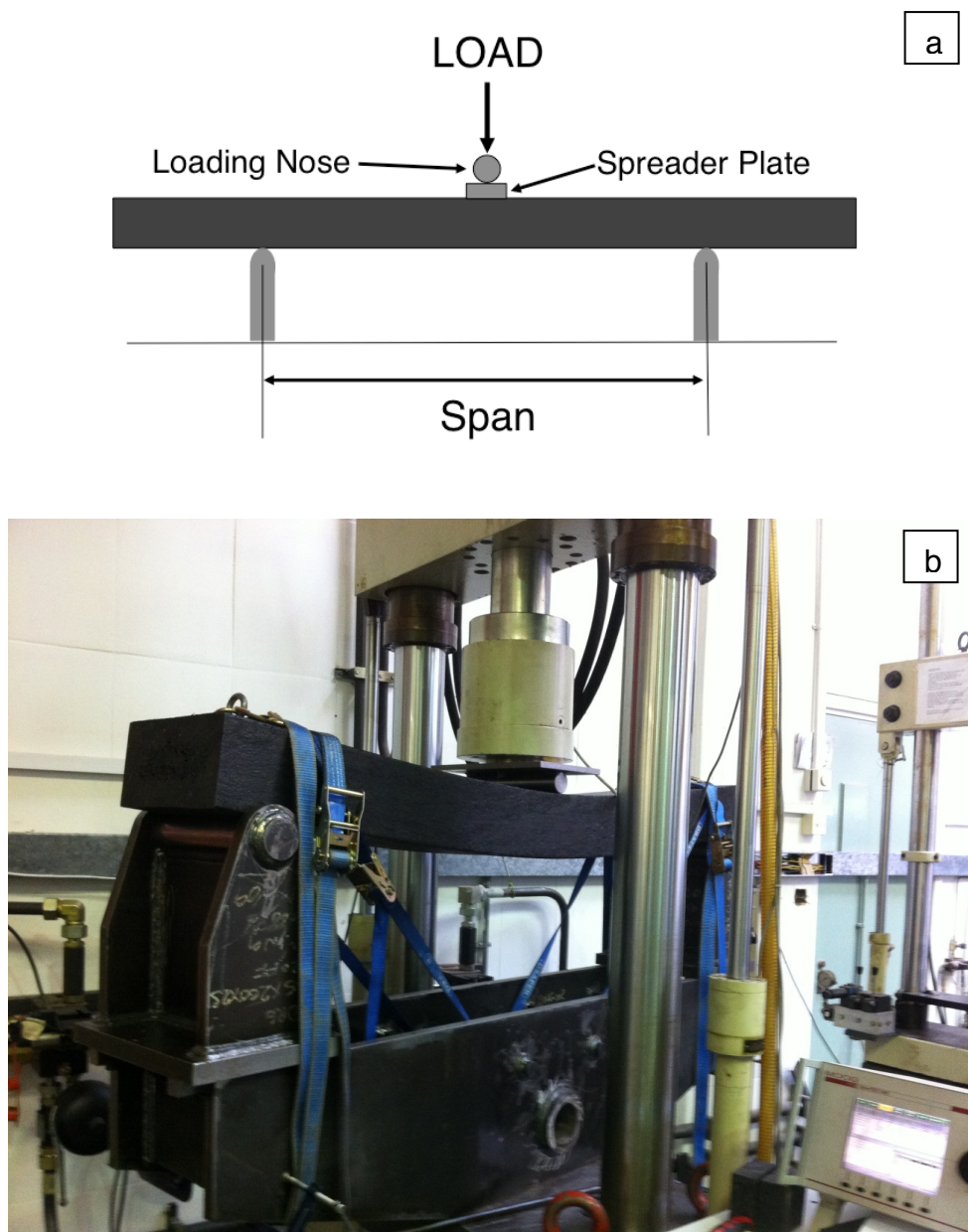

Figure 4.4 Three point flex test (a) schematic (b) photograph of a sleeper being tested in plank orientation.

The flexural stress and flexural strain was calculated using the following formula. All measurements are in Newtons and mm [89].

$$\sigma = \frac{3\,P\,L}{2\,b\,h^2} \qquad\qquad 4.1$$

$$\varepsilon = \frac{6\,s\,h}{L^2} \qquad\qquad 4.2$$

Where σ in the flexural stress (MPa), P is applied force (N), L is the loading span (mm), b is specimen width (mm), h = specimen thickness (mm), ε = flexural strain, s = deflection (mm).

The flexural modulus was the gradient for the linear portion of the stress-strain curve preferably between 0.0005 and 0.0025 strain. Some graphs started with a curved "toe" region due to the take up of any slack, alignment or sample settling [91]. For these samples, the gradient was taken from the linear portion of the graph, and the line was back extrapolated to calculate a corrected zero strain point.

4.3.2 Four Point Bend Test

Four point bend testing was conducted on a range of profiles of differing cross-sections, made from the production formulations and the glass reinforced trial formulations. The same profile size could not be made in all formulations, because formulations were only run on particular production machines, which had a different range of mould sizes.

The purpose of the testing was to compare formulation properties, quantify batch-to-batch variation and to measure the effect of different profile shapes and orientations. The ratio of thick outer wall to blown centre varied between profiles, see Figure 4.2.

The four point flex test method was based on ASTM D6109 "Flexural Properties of Unreinforced and Reinforced Plastic Lumber" and ISO 178 "Plastics - Determination of Flexural Properties". The number of samples was taken from ASTM D6662 "Polyolefin-Based Plastic Lumber Decking Boards" [89, 95, 134].
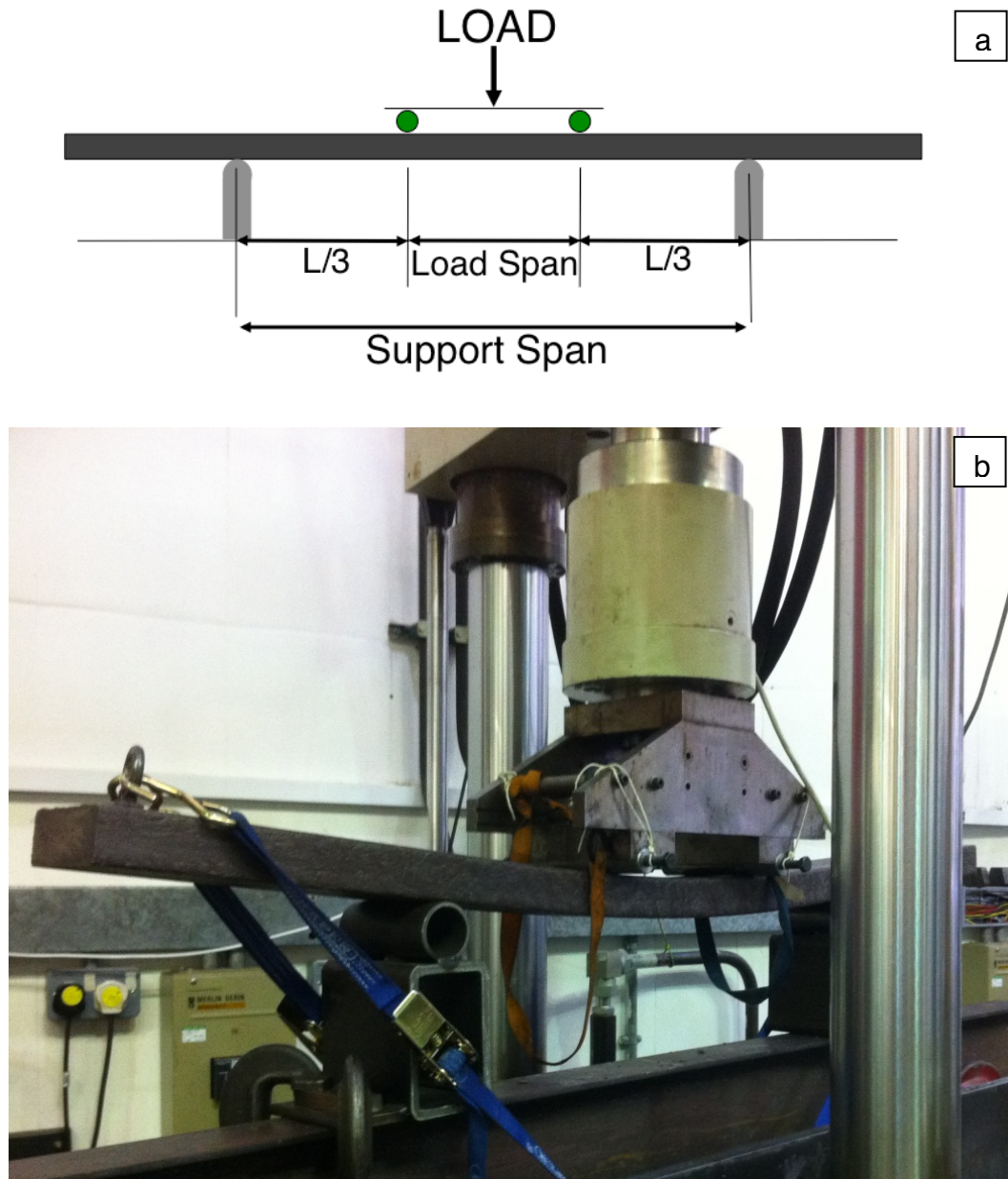

Figure 4.5 Four point bend test (a) schematic (b) photograph of a profile being tested in plank profile.

The four point flex rig was built on the Schenk SNK2/25 hydraulic test machine located in the LEA laboratory, Department of Mechanical Engineering. A schematic and a photograph of the test is shown in Figure 4.5. The load span was one third of the support span. The support span was 14-15 times the profile thickness. The support noses were 60 mm in diameter and loading noses were 30 mm in diameter, which were sufficiently large to prevent excessive indentation of the sample. At least 10 samples were tested and where possible 30 samples. The crosshead speed was calculated to produce 0.01 mm/mm/min strain rate on the outer fibres for plank orientation and 0.003 mm/mm/min for joist orientation. The ASTM D6109 used different strain rates to ensure that the sample broke by 3% strain for valid comparison with specifications and other materials. The flexural strength equation assumes stress is linearly proportional to strain until break. This creates a slight error, because the materials are not linear at high strains. ASTM 6109 deems these errors acceptable up to 3% strain.

The flexural strength and flexural strain were calculated using the following formulae [134]. All measurements are in Newtons and mm.

$$\sigma = \frac{P\,L}{b\,h^2} \qquad\qquad 4.3$$

$$\varepsilon = \frac{4.70\,s\,h}{L^2} \qquad\qquad 4.4$$

Where σ in the flexural stress (MPa), P is applied force (N), L is the loading span (mm), b is specimen width (mm), h = specimen thickness (mm), ε = flexural strain, s = deflection (mm).

The flexural modulus was the gradient for the linear portion of the stress-strain curve preferably between 0.0005 and 0.0025 strain [89]. Toe correction was applied where necessary as described in Section 4.3.1.

The deflection at the load points was measured not the deflection at the midpoint of the beam as specified by the standards. The midpoint deflection was calculated as being 1.15 times the deflection at the load points, by using the standard beam equations from Machinery's Handbook [135], see Appendix 1. Measurement of midpoint deflection was not possible because of time constraints, insufficient budget and practical issues such as strain gauges would not reliably adhere to the surface, and the energy release of a large sample braking could have damaged valuable measuring equipment in close proximity to the sample.

4.3.3 Compression Testing

Compression testing was completed on three formulations in transverse and longitudinal orientation. For each test, five samples were tested, which were selected from different production runs. Testing was completed on the bottom actuated Schenk SNK2/25 hydraulic test machine located in the LEA laboratory, Department of Mechanical Engineering.

The test was used based on ASTM D6108 "Standard Test Method for Compressive Properties of Plastic Lumber and Shapes" and ISO 604 "Plastics — Determination of compressive properties" [93, 96].

Samples were lengths of profile that had flat, parallel ends. The height was equal to twice the minimum cross-sectional dimension. For example, in 100x100 mm profile: the longitudinal sample was 200x100x100 mm and the transverse sample was 50x100x100 mm, see Figure 4.6 and 4.7. In use profile is compressed in the transverse direction, however not in a thin section. For comparison with the thin transverse samples, a metal block of area 80x40.5 mm was indented into the centre of a face 250x130 mm profile in the transverse direction. In this case, the foamed core was restrained by the solid walls of the profile.
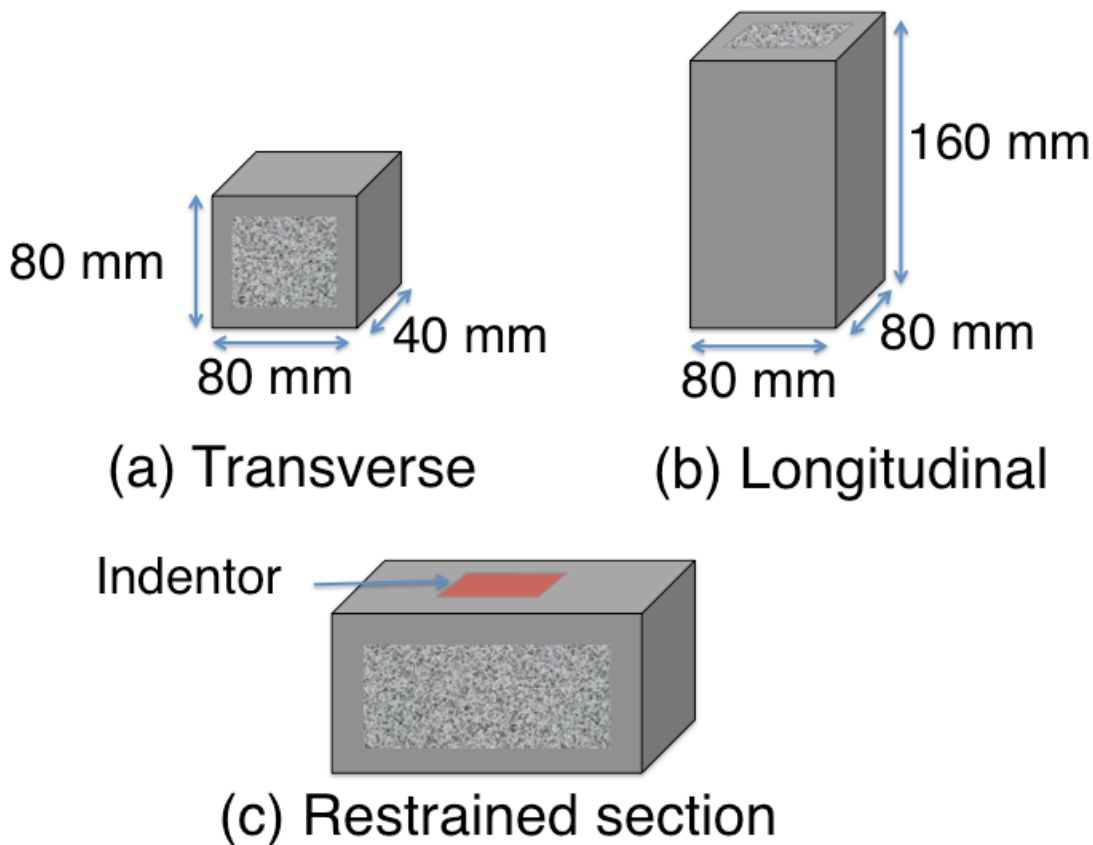
Figure 4.6 Schematic of the profile samples samples for compression testing (a) transverse, (b) longitudinal and (c) restrained section.

The cross-sectional area of the samples was measured in three places. Samples were compressed between two platens at a strain rate of 0.03 mm/mm/min.

The compressive strength was calculated by dividing the maximum load with the minimum cross-sectional area. The compressive strain was calculated as the decrease in length per unit length. The compressive modulus was the gradient for the linear portion of the stress:strain curve preferably between 0.0005 and 0.0025 strain [89]. Toe correction was applied where necessary, see Section 4.3.1.

Figure 4.7 Compression testing of profile in (a) transverse, (b) longitudinal and (c) restrained section.

4.3.4 Co-efficient of Thermal Expansion

The co-efficient of thermal expansion was measured using the method in ASTM D6341 "Standard Test Method for Determination of the Linear Co-efficient of Thermal Expansion of Plastic Lumber and Plastic Lumber Shapes" [136]. Five lengths of profile were cut at least 300 mm long and with flat, parallel ends. These were conditioned for 48 h at at the test temperature, after which the length was measured in three places within 1 minute of removal from the test

chamber. The test chamber used was the ESPEC ET34 environmental chamber in the Department of Electrical Engineering. Vernier measurements were taken between -30 and 55 ^{o}C. Using linear regression, the gradient of the best fit line was calculated for the change in sample length against change in temperature. The co-efficient thermal expansion, α, is the gradient divided by the sample length at room temperature (20 ^{o}C).

$$\alpha \;=\; \frac{1}{L_o} \;.\; \frac{L_2 - L_1}{T_2 - T_1} \;=\; \frac{1}{L_o} \;.\; \frac{\Delta L}{\Delta T} \qquad\qquad 4.5$$

Where L_o is specimen length at the reference temperature of 20 ^{o}C and, L_1 and L_2 are specimen lengths at temperatures T_1 and T_2 respectively.

4.4   Test Results and Discussion

4.4.1   250x130 mm Profile

The 250x130 mm railway sleeper was the largest profile tested. Five formulations were three point bend tested – Impact grade, polymer blend trial grade and the three reinforced trial grades. 3-6 samples of each grade were tested. Table 4.1 and Figure 4.8 show the results from this section.

The BP had significantly better properties than I. BP was formulated for stiffness and strength. The Impact grade was tailored for toughness with lower polystyrene levels, lower polypropylene levels and different waste streams of polyethylene. These formulation changes would explain the difference in properties.

Table 4.1 Average three point bend test results for 250x130 mm profile with ± standard deviation.

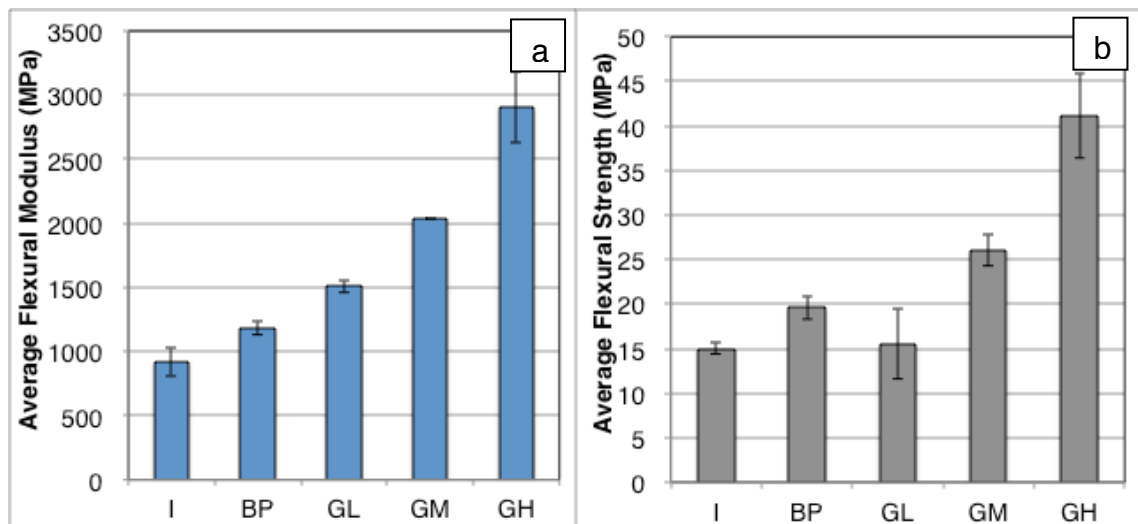| Compound		Number of Samples	Flexural Strength (MPa)	Flexural Modulus (MPa)	Strain at break
Impact	I	6	15.0±0.6	920±114	0.028±0.004
Polymer blend	BP	6[1]	19.6±1.3	1187±56	0.026±0.004
5% GF	GL	3	13.5±4.4	1511±50	0.010±0.004
10% GF	GM	3[1]	26.1±1.8	2034±0	0.017±0.002
20% GF	GH	5	41.1±4.7	2905±279	0.019±0.003

[1] one modulus measurement deleted due to test issue.

Figure 4.8 Three point bend of 250x130 mm profile (a) average flexural modulus (b) average flexural strength with ± standard deviation. See Table 4.1 for grade definitions.

The addition of glass fibre significantly improved the strength and stiffness of the profiles. The flexural strength of GL profile was a far low than expected, in fact it was lower than BP. Three samples were tested, which produced results of 18.3, 12.7 and 9.5 MPa. In the last sample, the fracture surface was very straight, which indicates a more brittle failure than the other samples. The shape of fracture surfaces are discussed in Section 4.5. The trial compound was tumble blended in one batch, and the samples were run sequentially. The

material may have degraded through prolonged residence time in the machine. Such material should have been purged before the mould was filled.

Table 4.2 compares the results from the current trial with those obtained for the injection moulded blend samples in Section 3.5 and Section 3.8. The Table also compares the results to predicted values calculated using the rule of mixtures.

Table 4.2 Percentage difference in flexural strength and modulus compared to injection moulded samples in Section 3.5 and Section 3.8. Plus rule of mixtures predicted values calculated from the injection moulded component materials. See Table 4.1 for grade definitions.

Blend	Compared to Injection Moulded (%)		Compared to Rule of Mixtures (%)	
	Strength	Modulus	Strength	Modulus
BP	-25	36		
GL	-54	5	-64	-4
GM	-36	13	-50	-11
GH	-29	5	-46	-15

The profile strengths were significantly lower than the injection moulded values. The moduli were not significantly different according to the Welch's t test for independent samples of unequal sample number and unequal variance in a normal distribution [137]. A much larger sample size would be required to have confidence in measured differences between the production methods. Only BP had a significantly higher modulus than FBB of Section 3.5. The decrease in strength is in agreement with the results from Section 3.4, where the same formulation was tested as injection moulded samples and intruded samples that had been machined to standard sample bars. In this case, the injection moulded samples were 25-45% stronger, though the modulus was 14% higher for one blend and 22% lower for the other. The lower than expected failure strength was due to premature failure caused by inclusions and contamination. All flexural samples had a whitened area (see Figure 4.2), which often contained an inclusion. The white areas were the location of crack initiation, which will be discussed in Section 4.5.

The rule of mixtures calculations used strength and modulus values of the injection moulded component polypropylene, polyolefin blend and 30 wt% GF filled compound. GL and GM had a lower PP content than the injection moulded component materials used in the calculations, because a more concentrated glass fibre compound was used. The calculations again show a significant reduction in strength, with similar or marginally low modulus.

An alternative method to predict the modulus is to consider the glass fibre geometry and orientation in the matrix. Halpin Tsai equations are semi-empirical and are widely used to predict the elastic properties of short fibre reinforced composites [138–140]. The equations have been found to fit some data very well at low fibre volume fractions, but under predicts some stiffnesses at high volume fractions [115, 138]. The model assumes that the fibre and the matrix are isotropic, linearly elastic and are well bonded at the interface [141]. The modulus E is calculated by:

$$E = E_m . \frac{(1 + \xi \eta V_f)}{(1 - \eta V_f)} \qquad 4.6$$

$$\eta = \frac{(E_f / E_m) - 1}{(E_f / E_m) + \xi} \qquad 4.7$$

V is volume fraction. The subscripts are designates for fibre, f, and matrix, m. ξ is a measure of the geometry (aspect ratio of the reinforcement phase). For circular fibres orientated parallel to the direction of mechanical loading, ξ_1 is given by equation 4.8, where L is the fibre length and D is the fibre diameter:

$$\xi_1 = 2 . \frac{L}{D} \qquad 4.8$$

For fibres orientated perpendicular to the loading direction, ξ_2 is:

$$\xi_2 = \sim 2 \qquad 4.9$$

The modulus parallel to the fibre direction, E_{11}, and the modulus perpendicular to the fibre direction, E_{22}, are given by equations 4.10 and 4.11.

$$E_{11} \; = \; E_m \, . \; \frac{(1 + \xi_1 \eta_L V_f)}{(1 - \eta_L V_f)} \qquad\qquad 4.10$$

$$E_{22} \; = \; E_m \, . \; \frac{(1 + \xi_2 \eta_T V_f)}{(1 - \eta_L V_f)} \qquad\qquad 4.11$$

$$\eta_L \; = \; \frac{(E_f / E_m) - 1}{(E_f / E_m) + \xi_1} \qquad\qquad 4.12$$

$$\eta_T \; = \; \frac{(E_f / E_m) - 1}{(E_f / E_m) + \xi_2} \qquad\qquad 4.13$$

For fibres orientated in different directions an orientation parameter, n, is used [115]. For random 3D fibres n= 0.2. The modulus then becomes:

$$E_n \; = \; n \, . \, E_{11} + (1\text{-}n) \, . \, E_{22} \qquad\qquad 4.14$$

For the Halpin Tsai calculations, values needed to be selected for fibre dimensions, fibre modulus and modulus of the PP in the compound. 81 GPa is a standard value for glass fibre modulus [80]. 1.2 GPa was selected as typical PP flexural modulus [124]. Fibre dimensions of 0.34 mm length and 14 µm diameter were used. Studies of fibre length reduction have found the final length is dependent on fibre concentration, matrix and the method of compounding [119, 142]. A study of 10-30 wt% glass fibre in a PSPP matrix found that single screw compounding reduced 4.5 mm length fibres to 1.1-0.72 mm with the lower value for 30 wt% glass fibre. In comparison twin screw compounding produced values of 0.33–0.35 mm for the same compounds. Other studies have found that after repeated reprocessing the fibre length plateaus, however, the final value is dependent on the technique used [118, 143, 144].
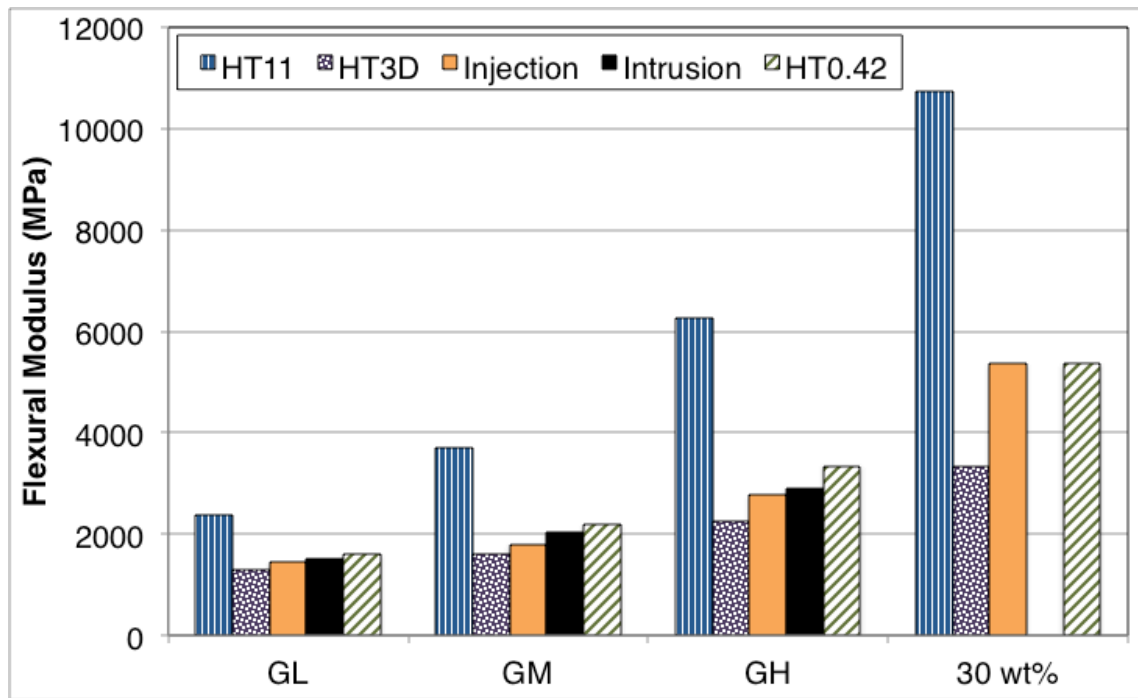
Figure 4.9 Comparison of Halpin Tsai modulus predictions with injection moulded and intrusion test data. The predicted moduli are HT11 for aligned fibres, HT3D for random fibre orientation and HT0.42 for orientation factor, n = 0.42. See Table 4.1 for grade definitions.

Figure 4.9 compares three Halpin Tsai predicted moduli with results for the injection moulded from Section 3.8 and the intrusion results from this section. Compared to the predicted modulus for random orientation, actual results were 10-30% higher (30 wt% GF was 60%). Compared to the predicted value for fully orientated fibres, actual results were 35-55% lower. Injection moulded tensile test bars, have been reported to produce an orientation factor, n, close to 1 in recycled PET with 20-40 wt% GF with good interfacial bonding [139]. The formulations in Figure 4.9 are far more complex with immisicible polymers and the moulded structure.

The 30 wt% GF injection moulded samples had the simplest system with a PP matrix. A n=0.42 matched the actual values for this compound. With n=0.42, injection moulded samples were 10-18% lower than predicted and the intrusion samples 5-13% below expectation. This deviation is similar to the actual difference between injection moulded and intrusion moulded (see Table 4.2), which was calculated to be statistically insignificant due to small sample size.

In a study of 10-70 wt% GF PP, n was measured optically plus was calculated to fit the experimental data [115]. With increasing glass content, n increased in optical measurements, though apparently decreased in calculations. In the same study, n was calculated to be higher for flexural modulus (0.8-0.6) compared to tensile modulus (0.64-0.5) for the same samples. This demonstrates that other factors change the apparent orientation parameter in addition to the actual orientation of the fibres. For example with increasing glass content, crystallinity can increase, interaction between fibres increases, packing structure can change and fibre length tends to decrease [139].

Similar effects would affect the apparent orientation parameters in this study. The matrix is inhomogeneous. The injection moulded samples were expected to have better properties than intrusion moulded, due to a greater glass fibre alignment. Injection moulded test bars are designed to have laminar flow and, therefore, high fibre orientation in the direction of flow. In intrusion, the material fans out and touches the colder mould walls. This cools the materials, which becomes more viscous. The material rolls down the mould pushed by the pressure of new material entering the mould. This flow pattern was observed in X-ray radiography of profiles. Additionally, the intrusion moulded profiles have the foamed core structure and the core could remain molten for a long time depending on cross-section size. The slow cooling would promote higher crystallinity. The profile used for the small machined, intruded samples was only 50x50 mm, which would cool relatively quickly. This may explain the lower modulus values in this case. Differential Scanning Calorimeter measurements would be required to measure the change in crystallinity with profile size.

From this trial it can be concluded that the modulus of intrusion moulded glass reinforced profiles was higher than predicted for fibre reinforced blends with randomly orientated fibres as calculated by Halpin Tsai equations. The modulus of a polymer blend was higher when intrusion moulded compared to injection moulded samples. The profile strength was significantly lower than predicted. Low contamination levels are required to obtain maximum strength and

minimize the premature failure due to inclusions. This is explored further in the later trials.

4.4.2 80x80 mm Profile Four Point Flexure

The purpose of this trial was to obtain statistically significant four point flexure data on Impact grade and the three glass reinforced trial grades. Manufacture and testing of 250x130 mm sleepers was very time consuming and expensive, hence, 80x80 mm glass reinforced profiles were made at the same time as the 250x130 mm sleepers. Ten samples of GL and GM grade were made during one trial. Thirty GH samples were made in three production trials. Thirty-five impact samples were taken from ten different production runs. Samples could not be obtained for Standard grade, because the trial was not run on the same machine. Table 4.3 and Figure 4.10 show the results.

Table 4.3 Average four point bend test results for 80x80 mm profile with ± standard deviation. See Table 4.1 for grade definitions.

Compound	Number of Samples	Flexural Strength (MPa)	Flexural Modulus (MPa)	Strain at break
I	35[1]	13.6±2.7	911±111	0.022±0.007
GL	10	22.6±2.0	1448±60	0.025±0.004
GM	10	24.6±2.3	1749±170	0.024±0.002
GH	30	41.2±4.5	2945±206	0.021±0.003

[1] Four samples excluded for strength because break was above 0.03 strain.

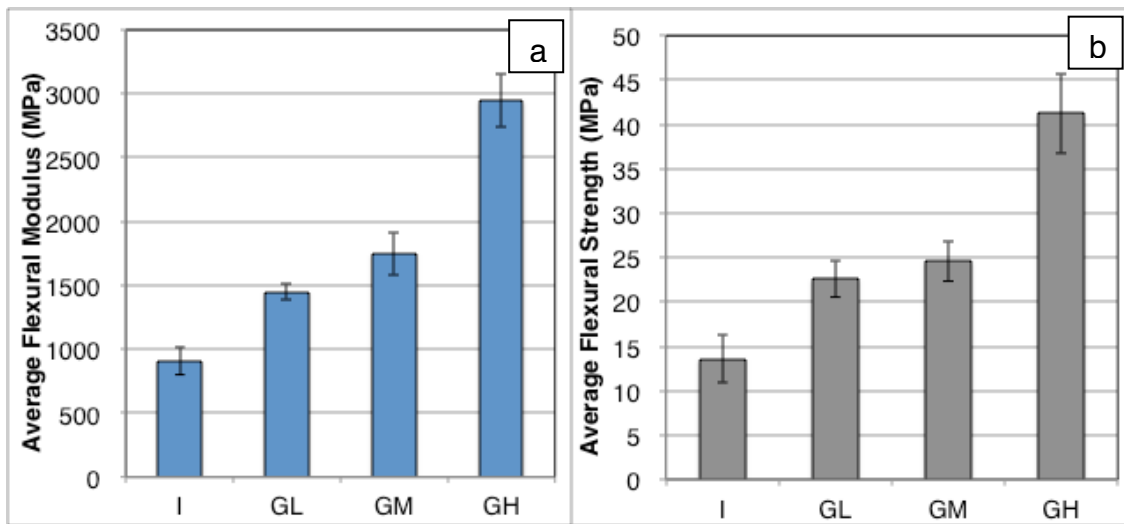Figure 4.10 Four point bend of 80x80 mm profile (a) average flexural modulus (b) average flexural strength with ± standard deviation. See Table 4.1 for grade definitions.

The strengths and modulus values were similar to those measured in three point flexure for the 250x130 mm sleepers, Section 4.4.1. In fact there was no statistical difference according to Welch's t test [137]. Previous studies have found that samples tested in three point flexure gave a higher strength than four point flexure, [131, 133]. This was because, in the three point bend test, the stress was concentrated in a much smaller area (see Figure 4.1), which implied a lower probability that there would be a significant flaw in the stressed area. Differences between the current tests may not be evident due to the small number of samples and the limited number of batches that were tested in the three point bend test. Studies of modulus variation between three and four point bending show no, lower or variable changes depending on the material [133, 145, 146]. The different test conditions used may have had an appreciable effect on the measured properties, because the effect of changing the strain rate, thickness, and span-depth ratio is complex [147]. For example, shear stress increases at lower span-depth ratio.

Likewise compared to the predicted values in Section 4.4.1, the 80x80 mm profile in four point bend deviated to the same degree as the 250x130 mm profile in three point bend.

The addition of glass fibre, and increasing the amount of glass produced a significant incremental improvement in performance. The value for GM is lower than would be expected compared to the rule of mixtures, the 250x130 mm in the three point bend test and injection moulded samples in three point flexure. Only ten samples of GM were tested from one batch. A larger sample size and number of batches would be required to produce a more accurate trend due to the variable nature of recycled polymers. This is explored further in the next section.

In conclusion, the trial found that the addition of glass fibre incrementally improved strength and stiffness. The mechanical properties of 80x80 mm profile measured in four point bend were not statistically different from those measured in three point bend on 250x130 mm profile. A larger sample size and larger number of batches would be required to get a more accurate result.

4.4.3 Standard Grade Four Point Bend

Standard grade was four point bend tested using 50x100 mm, 50x125 mm and 100x100 mm profile. The purpose was to compare profile sizes and to obtain batch-to-batch variation data. Profiles were taken from production over the course of 18 months, stored, then tested at the same time. 50x100 mm profile was tested in joist position at two strain rates. 125x50 mm profile was tested in joist and plank position. 100x100 mm profile was tested at the strain rate for joists. For a definition of joist and plank see Section 4.1.

Table 4.4 and Figure 4.11 show the results from this trial. The results were analysed for significance between data sets using Welch's t test for independent samples of unequal sample number and unequal variance in a normal distribution [137]. The differences between profiles were found to be significant to 99% confidence level. The large sample size ensured significance despite the wide standard deviation in some data sets, as discussed in ASTM D6662 [134]. The only exception was 100x100 mm profiles values, where only five samples were tested from one batch. These values have not been compared to the other profiles.

Table 4.4 Standard grade profile four point flex test results showing average values with ± standard deviation.

Profile cross-section and nomenclature		Strain Rate	Orientation & Number of samples		Flexural Strength (MPa)	Flexural Modulus (MPa)	Strain at break
125x50	125P	0.01	Plank	10	25.1±1.5	1023±93	0.037±0.005
50x125	125	0.003	Joist	30	18.2±1.9	1139±170	0.025±0.006
100x100	SQ	0.003	Joist	5	15.0±0.9	1182±28	0.019±0.002
50x100	100	0.003	Joist	36	16.2±1.3	1007±81	0.024±0.004
50x100	100f	0.005	Joist	18	17.7±2.3	1205±119	0.022±0.005

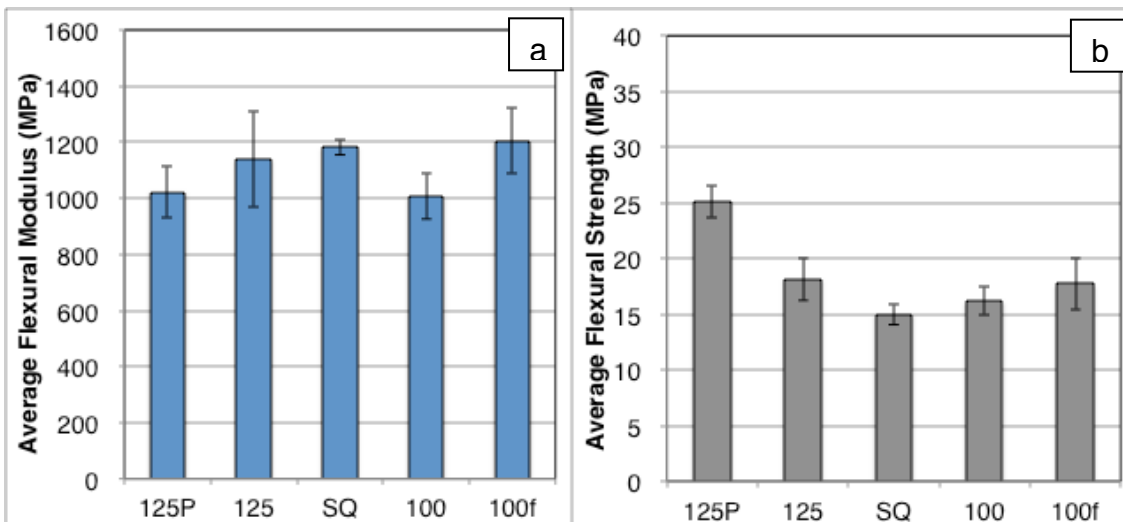Figure 4.11 Four point bend test of Standard grade profile (a) average flexural modulus (b) average flexural strength results with ±standard deviation. 125P = 125x50 mm plank, 125 = 50x125 mm joist, SQ = 100x100 mm, 100 = 50x100 mm joist at 0.003 strain rate, 100f = 50x100 mm joist at 0.005 strain rate.

Increasing the strain rate of 50x100 mm joist testing, raised the modulus by 20% and slightly increased the strength. This was expected since plastics are viscoelastic and change their response to varying strain rates [39]. At low strain rates, the polymer chains have sufficient time to flow giving higher elongations, lower modulus and lower strength. At high strain rates the material does not have time for viscous deformation. The effect has been observed for plastic

lumber in compression by Lynch and Lampo [148, 149] and in bending mode in other polymers [133].

125x50 mm profile tested in plank orientation compared to joist orientation, appeared to have significantly higher strength with a slightly lower modulus. Several different aspects need to be considered when comparing the results, because the span, strain rate and sample selection were different. Each of these factors will be considered separately.

Ideally, modulus and strength are fundamental material properties that do not change with orientation or shape, because the failure stress, σ_f, is normalised by the moment of inertia of the cross-sectional area, I:-

$$\sigma_f \quad = \quad \frac{M \, y_{max}}{I} \quad = \quad \frac{M}{Z} \qquad\qquad 4.15$$

where M = bending moment, y_{max} = maximum perpendicular distance from the neutral axis, Z = section modulus. This formula is often called the flexure formula [130].

The effect of profile orientation can be explored using structure factors [150]. The concept of structure factor is used to judge the stiffness or strength of beams of different shapes with the same cross-sectional area and length. Usually the comparison is with a standard round or square beam. The structure factor is independent of size, it is only the function of geometry. The structure factor is derived from shape factors. The flexure formula is used as the bending strength shape factor.

The bending strength structure factor, ϕ_{fpj}, for rectangular beam in plank position compared to joist position with the same span is:

$$\Phi_{fpj} \quad = \quad \frac{\sigma_{fp}}{\sigma_{fj}} \quad = \quad \frac{Z_p}{Z_j} \qquad\qquad 4.16$$

The suffixes j and p are for joist and plank respectively. The section modulus, Z, for a rectangular beam dimensions of width, b, and thickness, h, is:

$$Z = \frac{2I}{h} = \frac{2}{h} \cdot \frac{bh^3}{12} = \frac{bh^2}{6} \qquad\qquad 4.17$$

The structure factor, Φ_{fpj}, for plank position in comparison to joist of a rectangular beam with dimensions of x and y, where y > x, is:

$$\Phi_{fpj} = \frac{\sigma_{fp}}{\sigma_{fj}} = \frac{Z_p}{Z_j} = \frac{yx^2}{6} \cdot \frac{6}{xy^2} = \frac{x}{y} \qquad\qquad 4.18$$

For 125x50 mm profile tested at the same span, the bending strength of plank position would be expected to be 40% of joist position. However, in this case the loading span is proportional to the profile thickness. At 14 times the thickness, 50x125 mm profile in joist position had a span of 1750 mm, whereas in 125x50 mm plank position the span was 700 mm. For four point bend:

$$\sigma_f = \frac{P L}{b h^2} = \frac{14 P}{b h} \qquad\qquad 4.19$$

Using this equation, the structure factor becomes unity. By changing the span with profile thickness, the strength should be constant for joist or plank position.

The effect on modulus can be calculated using the same principle. Starting with the bending stiffness shape factor, S_b:

$$S_b \quad \propto \quad \frac{EI}{L^3} \qquad\qquad 4.20$$

Where E = modulus, I = moment of inertia, L = span. For a rectangular beam with dimensions of x and y, where y > x:

$$S_b \quad \propto \quad \frac{E}{L^3} \cdot \frac{bh^3}{12} \qquad\qquad 4.21$$

In joist position $\quad S_{bj} \quad \propto \quad xy^3 \qquad\qquad 4.22$

In plank position $\quad S_{bp} \quad \propto \quad yx^3 \qquad\qquad 4.23$

The bending stiffness structure factor, ϕ_{bpj}, for plank position compared to joist position:

$$\phi_{bpj} \quad = \quad \frac{yx^3}{xy^3} \quad = \quad \frac{x^2}{y^2} \qquad\qquad 4.24$$

For the 100x50 mm profile using the same span, the plank position will have a quarter of the stiffness. For 125x50 mm, the plank is 0.16 times the stiffness. When the change in span is taken into account, the bending stiffness factor for a rectangular beam becomes:

$$S_b \quad \propto \quad b \qquad\qquad 4.25$$

Hence, for this case the bending stiffness shape factor, ϕ_{bpj}, for plank position compared to joist position becomes:

$$\phi_{bpj} \quad = \quad \frac{y}{x} \qquad\qquad 4.26$$

So for the 125x50 mm profile, the plank position should have been 2.5 times stiffer and for 100x50 mm profile should be stiffer by the factor of 2.

In this case, changing the profile orientation alone should increase modulus and keep strength constant. However, the standard compensates for the inherent flexibility of plank samples by increasing strain rate from 0.003 mm/mm/min for joist to 0.01 mm/mm/min for plank, see Section 4.3.2 [95]. This in addition to the span change increases modulus and strength. However, only the strength increased significantly and that was beyond 3% strain. The plank samples failed at 0.037 strain. The joist samples failed at 0.025 strain. At this strain the plank samples reached 20.8 MPa stress value, slightly higher than 18.2 MPa for the joist samples.
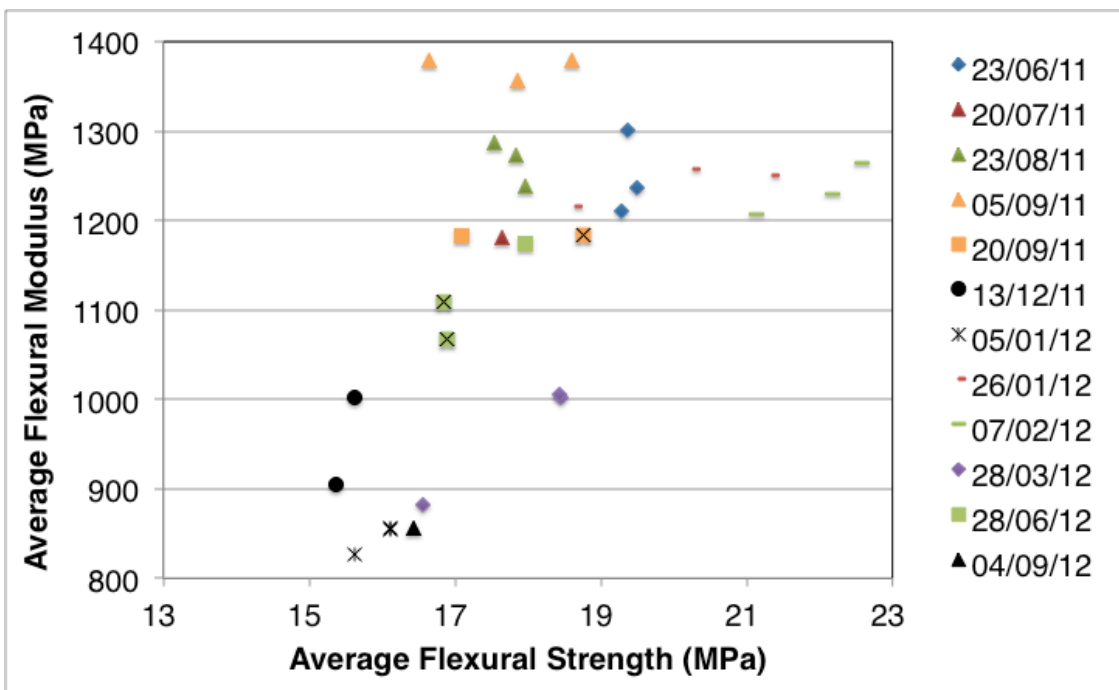

Figure 4.12 Variation between different production batches of 50x125 mm profile tested in joist position in four point bend test at 0.003 strain rate. Average flexural modulus plotted against average flexural strength. Samples with black markings had high contamination.
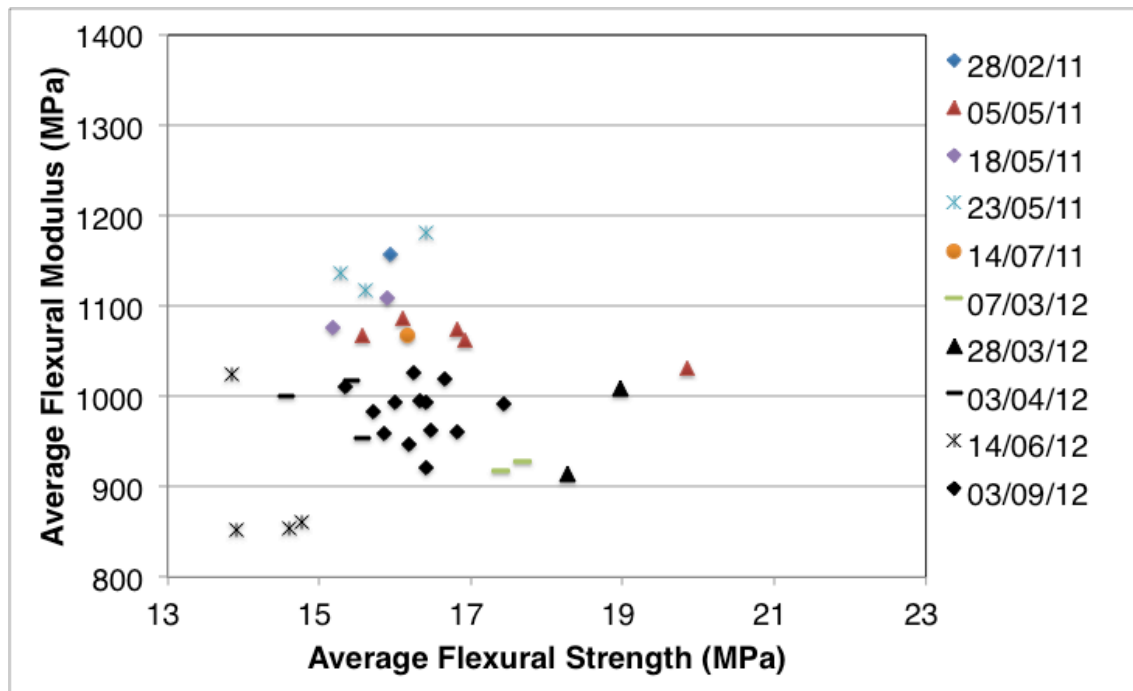
Figure 4.13 Variation between different production batches of 50x100 mm profile tested in joist position in four point bend at 0.003 strain rate. Average flexural modulus plotted against average flexural strength. Samples with black markings had high contamination.

Sample selection is an alternative explanation for the observed differences between joist and plank orientation. 30 joist position samples were tested from 12 different production runs occurring over a period of 15 months. Wherever possible three samples were taken from a production run. In comparison, 10 plank samples were tested from one production run. Unfortunately, the planks were cut too short to be tested in joist position as well. Figure 4.12 shows the spread in results according to batch for joist position. Batches tended to cluster, and there was a distinct difference between the batches. Every batch used the same formulation, however, the sources, quality and contamination levels changed depending on availability. Contamination was identified by observation of fracture surfaces.

The differences between joist and plank are very likely to be masked by batch-to-batch variability, due to the small sample size of the plank samples. The rise in strength may simply indicate a batch of low contamination, which could give a strength closer to the true material value.

A different set of factors needed to be considered when comparing different cross-section sizes. For 50x125 mm and 50x100 mm profiles, each data set contained over thirty samples taken from multiple production runs. The results showed 50x125 mm profile was 12% stronger and stiffer than 50x100 mm. Factors that can be considered are quality of samples, morphology and solid load bearing area.

The spread in the results for each profile size is shown in Figure 4.12 and Figure 4.13. Samples with high levels of small contaminant particles are marked in black in the figures, an example is shown in Figure 4.18. A black cross marks the samples where individual samples in a batch were contaminated. The presence of large amounts of small contaminants does not appear to consistently reduce the strength. Section 4.5.1 investigates the cause of failure further. Excluding the contaminated samples produces a marginal increase in the strength and modulus. For 100x50 mm low contamination profiles, the strength was 16.4±1.3 MPa with 1056±79 MPa modulus. For 50x125 mm low contamination profiles, the strength was 18.9±1.7 MPa with 1215±123 MPa modulus. This is a 15% difference in strength and modulus between the profiles types.

Differences in morphology between the cross-section sizes arise due to different flow in the mould and cooling rates. Larger and square profiles would be expected to cool slower, because cooling time is proportional to the square of thickness [26]. Cooling rate affects crystallinity as previously discussed in Section 4.4.1. The difference in cooling rate between these two profiles should have been minimal as they were both 50 mm thick. However, macroscopic differences in cross-section were seen on examination of the fracture surfaces. The blown areas were found to have different shapes that occurred at significantly different frequency. In 50x125 mm profile, 80% were rectangular and 20% were hourglass shaped, see Figure 4.19 and 4.21 for examples of hourglass shapes. In 50x100 mm profile, 45% rectangular and 55% were

hourglass shaped. It is unknown why hourglass shaped foamed areas were generated and why they were more common.

The solid load bearing area was calculated by analysing the fracture surfaces of the profiles. The solid outer wall thickness was measured on all four sides of every profile. It was measured where it was thinnest for profiles with the hourglass shaped foamed area. 50x125 mm profile had an average solid wall thickness of 13 mm, which was 2 mm thicker than that of 50x100 mm profile. This meant instead of having 2% less solid area, 50x125 mm profile had 5% more solid area as a proportion of the cross-sectional area compared to 50x100 mm. The standard flexural stress and strain equations assume a homogeneous material. The increase in wall thickness effectively means stronger and stiffer material was being used. Section 4.5.4 explores this further.

The presented results showed that there was a large batch-to-batch variation with plastic lumber. This meant that it was important to have large sample sizes selected from a wide range of batches when investigating the properties of recycled plastic lumber. It was also demonstrated that it was advisable only to compare data tested under the identical test parameters. Strain rate, span, profile orientation and profile cross-section all had a significant effect on the measured strength and modulus. Wall thickness variation between the profiles can make one profile size effectively stronger and stiffer than another even though the material used was the same.

4.4.4 Compression Testing

Compression testing was carried out on three grades: Impact grade (I), Standard grade (S), and glass reinforced with highest level of glass (GH). 100x100 mm and 80x80 mm profiles were tested in the longitudinal and transverse directions, see Figure 4.6 and 4.7. Five samples were tested in each orientation. For comparison to the relatively thin transverse samples, a 250x130 mm profile was indent tested on the wide face using a 80x40.5 mm steel block to indent the surface see Figure 4.6 and 4.7 A block had to be used, because

the machine could not supply sufficient force for such a large sample. Table 4.5, Figure 4.14 and 4.15 give the results.

Table 4.5 Average compressive strength and modulus measured longitudinal (L), transverse (T) and using a metal 80x40.5 mm block on the wide face of a 250x130 mm profile. Three grades were tested Standard grade (S), Impact grade (I), and glass reinforced with highest level of glass (GH). ± standard deviation is quoted.

Sample dimensions and Grade	Code	Compressive Strength (MPa)	Compressive Modulus (MPa)	Strain at yield
100x100x200 S	SL	-24.4±1.1	994±23	0.088±0.010
100x100x50 S	ST	-13.5±0.6	509±14	0.046±0.005
Block I	I	-43.5±2.3	1571±160	0.083±0.023
100x100x200 I	IL	-18.4±0.7	630±65	0.126±0.004
100x100x50 I	IT	-14.7±1.5	384±21	0.094±0.013
80x80x160 I	8IL	-20.4±1.1	758±69	0.167±0.055
80x80x40 I	8IT	-16.0±1.2	490±32	0.074±0.013
Block GH	GH	>77	3619±31	
80x80x160 GH	8GHL	-36.5*	1850±58	0.043*
80x80x40 GH	8GHT	-25.4±1.9	777±155	0.056±0.014

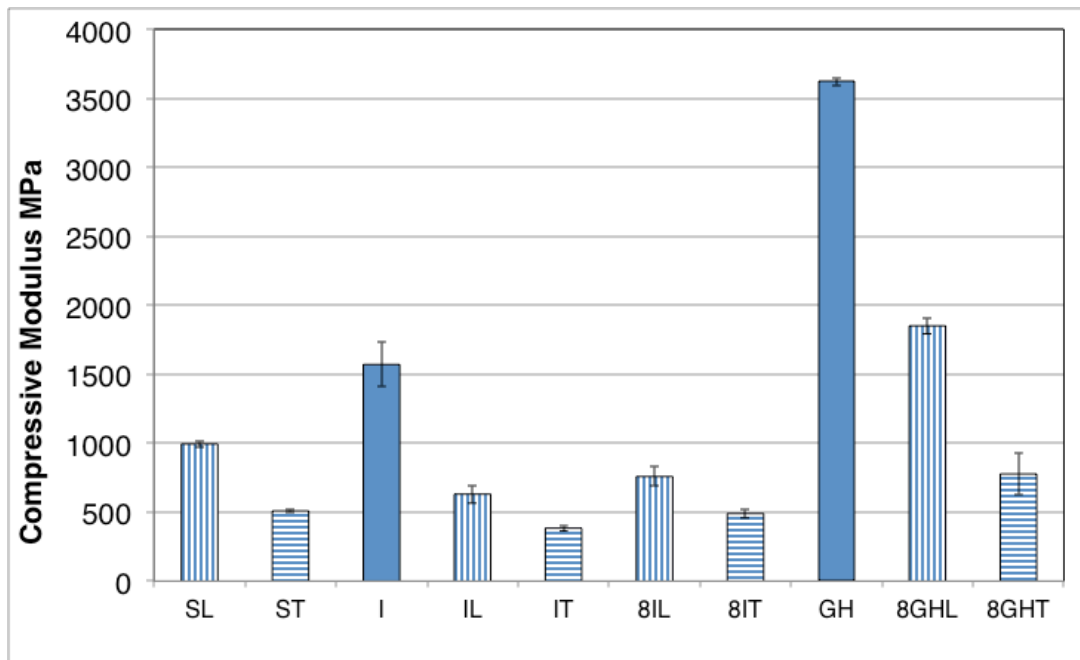* Results of one sample retested to a higher load.

Figure 4.14 Average compressive modulus measured longitudinal (L), transverse (T) and indentation of a metal 80x40.5 mm block on the wide face of a profile (solid blue). Grades - Standard (S), Impact (I), Glass reinforced (GH). $\pm$ standard deviation is plotted. No prefix 100x100 mm profile. 8 = 80x80 mm profile.
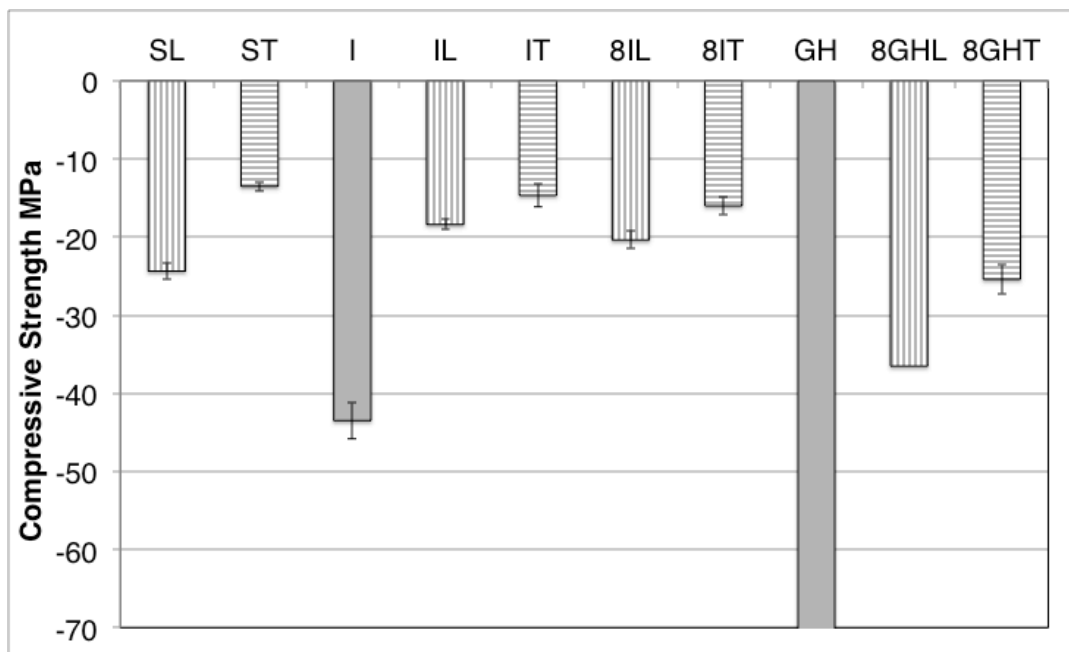

Figure 4.15 Average compressive strength of a range of profiles with $\pm$ standard deviation, see Figure 4.14 for nomenclature.
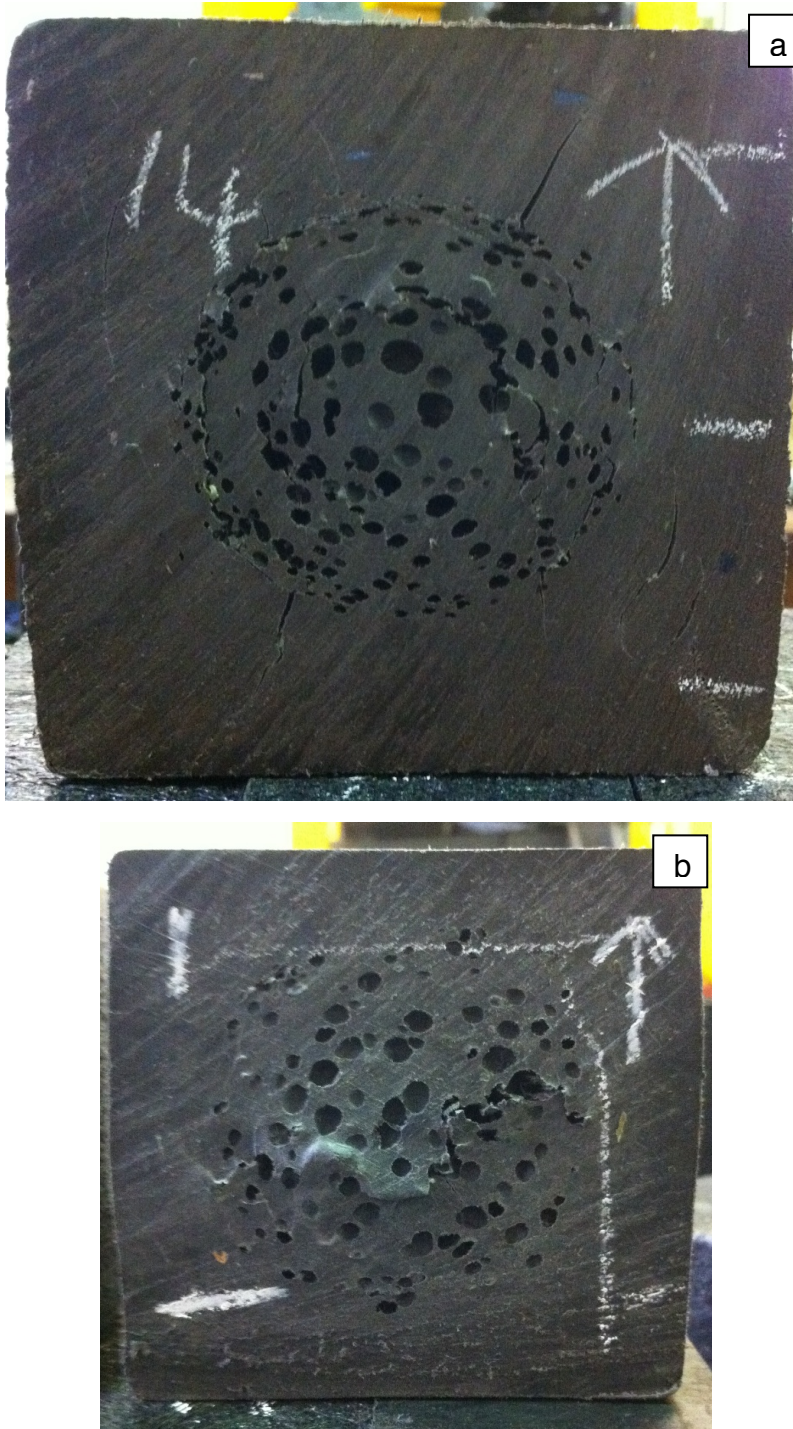
Figure 4.16 Transverse compression test samples showing different failure mechanisms. The mechanisms were not exclusive to one grade type. (a) 100x100 mm Standard grade cracked around the blown region (b) 80x80 mm glass filled grade with shear bands of crushed bubbles.

Longitudinal samples were 20-45% stronger than transverse samples and stiffer by 35-58%. In 7x9" railway sleepers a 72% difference in strength was reported for a polymer reinforced grade [61]. This would be expected because the longitudinal samples were effectively box beams compressed at the ends. The transverse samples were thin box sections compressed between two sides, which sheared as shown in Figure 4.16. Impact and glass fibre reinforced grades had shear bands of crushed bubbles. Standard grade cracked around the blown region. Standard samples had thick walls with a small, circular blown region, which may explain the different behaviour. In longitudinal samples, the failure mechanism was not apparent. The test was stopped when load plateaued and reduced.

Comparison of the grades showed the expected trend. In longitudinal orientation, Standard grade was 33% stronger and 58% stiffer than Impact grade, because it had higher amorphous polymer reinforcement. Glass fibre was 79% stronger and 144% stiffer than Impact grade. In transverse orientation, the difference between grades was less. Standard grade was 33% stiffer compared to Impact grade. The glass fibre reinforced grade was 59% stronger and stiffer than Impact grade. Alignment of morphology and fibres in the direction of flow could explain the larger difference between the grades in the longitudinal orientation. The effect of alignment in the polymer blended grades was shown in the small machined compression testing in Section 3.4. Additionally, the difference between longitudinal and transverse orientation was largest between glass filled samples and smallest between Impact grade samples i.e. a larger difference with the more effective the reinforcement type.

Increasing the profile size in Impact grade produced an unexpected result. The 80x80 mm samples were 20% stiffer than the 100x100 mm samples, despite profiles having the same proportion of solid area in the cross-section. The 100x100 mm samples would be expected to have slower cooling and so higher crystallinity. Orientation in the mould could be higher for a smaller profile. Most likely cause could be variation in raw materials. A far larger sample size would be needed to explore these explanations.

The highest results were for indenting a block into the wide face of a 250x130 mm profile. The metal block area was small compared to the surface area of the profile face. The thick, strong walls of the profile constrained and reinforced the area under compression.

This testing has shown that glass fibre is very efficient at improving compression strength and modulus. Fibre and morphology alignment in the mould significantly improves compression properties in the longitudinal direction and to a lesser extent in the transverse direction. Sample shape and profile size has a significant effect on the compressive properties measured and the failure mechanism observed.

4.4.5 Co-efficient of Thermal Expansion

Co-efficient of thermal expansion (CTE) was measured on 250x130 mm profiles in BP polymer blend grade, GH glass filled grade and a 35% polystyrene blend. Temperatures used were -28 to 54°C. Measurements were taken along the length of the profile.

Table 4.6 Co-efficient of thermal expansion of profile for different formulations and temperature ranges with ± standard deviation.

Grade	Temperature Range (^{o}C)	CTE x10^{-5} (mm/mm/^{o}C)
BP	-10 to 40	8.4 ± 2.9
BP	-19 to 54	12.1±1.5
35% PS grade	-23 to 57	10.1±0.3
GH	-10 to 40	4.8 ± 1.1
GH	-28 to 54	4.7±1.0

All the results passed the 1.35x10^{-4} mm/mm/^{o}C maximum requirement for railway sleepers, unlike standard values for PE and PP [25]. The CTE increased with temperature range particularly above room temperature, which is usual for polymers [25]. The CTE reduced slightly with increasing the PS content. Glass

fibre halved the CTE and kept it constant over a wider temperature range. The value for the glass fibre grade is consistent with published values [25].

This testing showed that glass fibre reinforcement is very efficient at reducing the co-efficient of thermal expansion over a wide temperature range.

4.5   Cause and Mode of Failure in Flexure

The fracture surfaces of the flexural testing samples were analysed to understand the causes and modes of failure. Samples were visually inspected for the cause of failure. Photographs were taken for later analysis. The fracture surfaces were investigated in greater detail using an SEM.

4.5.1   Cause and Mode of Failure

Photographs of the fracture surfaces were analysed in order to better understand the causes and modes of failure. A range of fracture surfaces is shown in Figure 4.17 – 4.22. The photographs also show fracture shapes, bubbles sizes, bubble distribution, white areas and crack initiators.

The cause of crack initiation was usually clear on inspection of the profile fracture surfaces, see Figure 4.17. In a survey of 188 flexure samples, 62% of cracks were caused by inclusions or contamination and 35% by an abnormally large hole or a cluster of holes very close together. In 6 samples the cause of failure was unclear.

The most common inclusion was flakes of PET bottle or film, Figure 4.17 and 4.22. PET did not melt at the process temperatures. Instead, the hot PET flakes stress relaxed and folded into a ball, hence they had a disproportionately large cross-sectional area in comparison to the PET wall thickness. The second most likely cause was contamination such as lump of fractional melt polyolefin or rubbery material (20%). These did not melt or flow during the process.

The foam pore size, amount and distribution varied greatly for the same profile size, the same grade and with the same type and amount of blowing agent, see Figure 4.17. Bubbles are nucleated on pigment particles, fillers, solid residues, dirt and other contaminants [151]. The number and types of nucleation sites would vary with the waste stream type and quality. A few very contaminated samples clearly showed damp material, such as a flake of wood, which caused abnormally large holes, as a result of steam formation, see Figure 4.18. Bubbles appeared to initiate cracks if they were positioned close to the edge, abnormally large, or a group of bubbles were clustered together. Internal irregular defects have been found to induce more stress than spherical-shaped pores, requiring a lower load to propagate fracture [131].

Both plank and joist samples exhibited three different fracture surface shapes – Y, L and I. Cracks initiated in the lower half of the sample, which was under tension.

Contaminated profiles tended to break with a perpendicular line, I, which often had an s shaped "wiggle" near the top surface, Figure 4.18. 66% 80x80 mm Impact grade profiles and 48% of 50x100 mm Standard grade profiles exhibited an I crack. However, only 13% of 50x125 mm and 10-20% of the glass filled grades fractured in an I crack. Increasing strain rate, increased the number of I cracks in 50x100 mm Standard grade, maybe because the rate of propagation was increased giving less time for deviation.
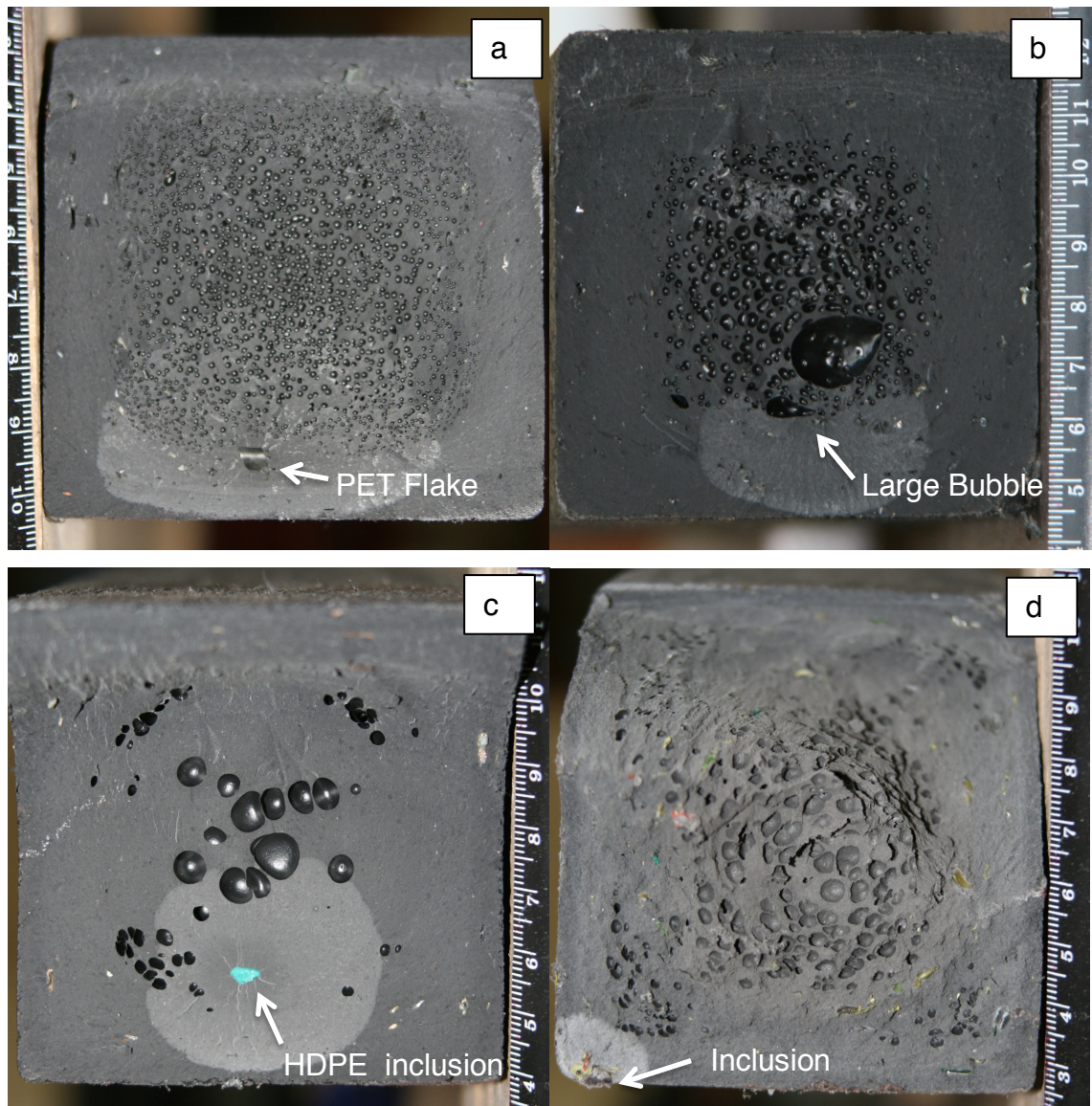
Figure 4.17 Fracture surfaces of 80x80 mm four point flexure samples loaded on the top surface (a) Impact grade - large area of fine bubbles with large ductile area initiated at PET flake (b) Impact grade - uneven bubbles and thick walls, with abnormal hole as crack initiator (c) Impact grade – large, sparse bubbles with HDPE inclusion as crack initiator. (d) GH grade – uneven pores with very small ductile area initiated at an inclusion on the edge, Y fracture appears to be along edge of bubbles.
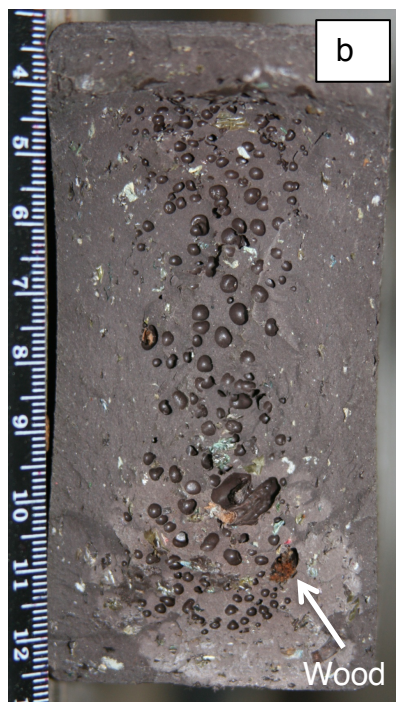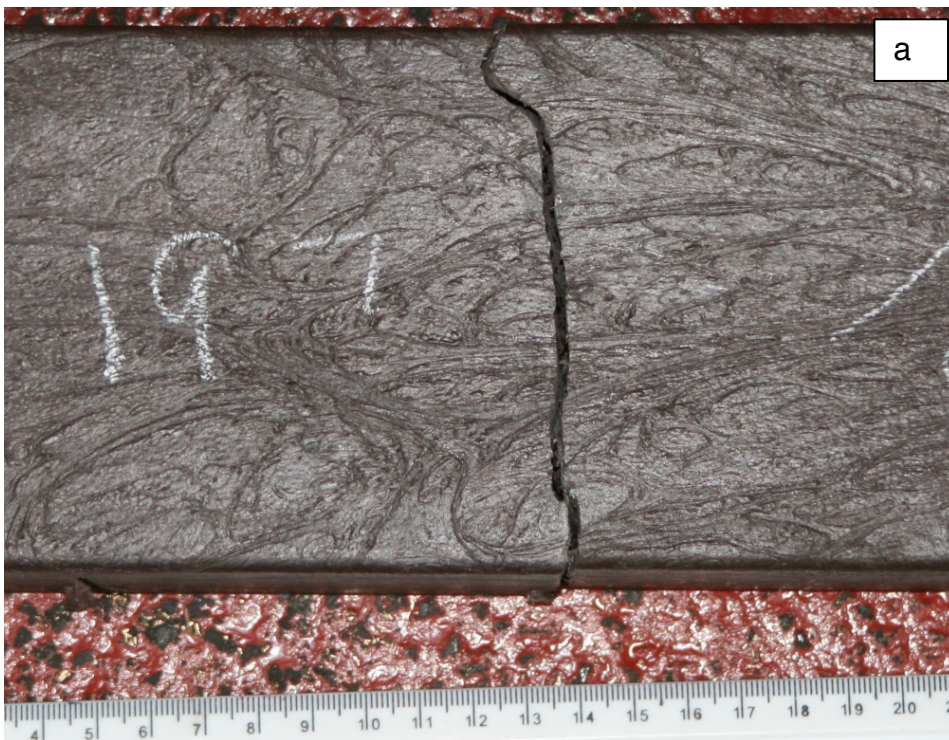
Figure 4.18 Four point flexure, Standard grade, 50x100 mm profile loaded from top surface (a) the I fracture in the profile from side-on and (b) a broken end with coarse bubbles and high PET contamination and an inclusion that gassed. This profile would have been rejected by Quality Control.

Figure 4.19 Four point flexure Standard grade 50x125 mm sample loaded on top surface (a) the curved L fracture in the profile from side-on and (b) the broken end with medium pores in an hourglass distribution and, a crack initiated by a cluster of bubbles.

Figure 4.20 Four point flexure Standard grade 50x125 mm sample loaded from top surface (a) the sharp L fracture in the profile from side-on and (b) a broken end with fine pore structure and a crack initiated by an inclusion. No visible cause for sharp change in crack direction.
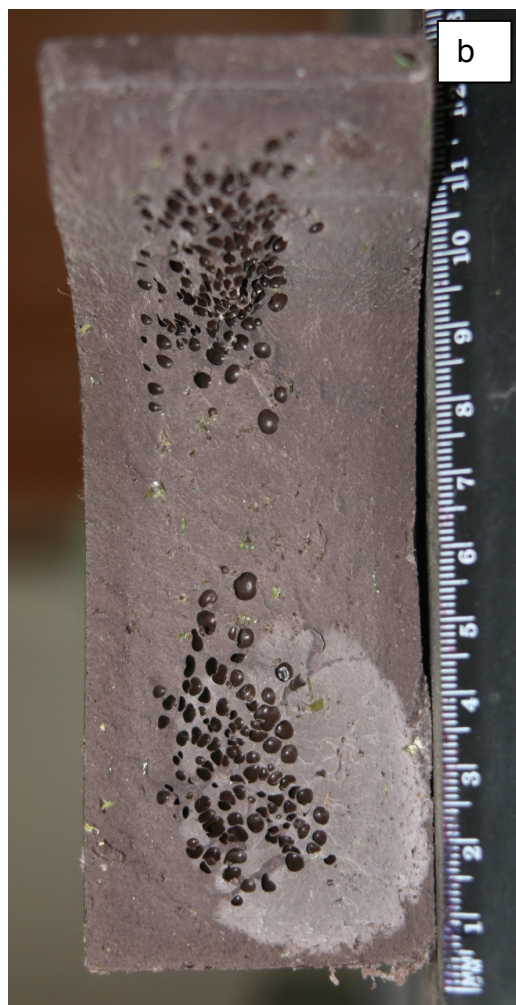
Figure 4.21 Four point flexure Standard grade 50x125 mm sample loaded from the top surface (a) the sharp Y fracture in the profile from side-on (b) the triangular top piece and (c) the broken end with medium pores in an hourglass distribution, and, a crack initiated by a lump of rubber. The crack then deviates at another lump. The L probably broke at sample failure.
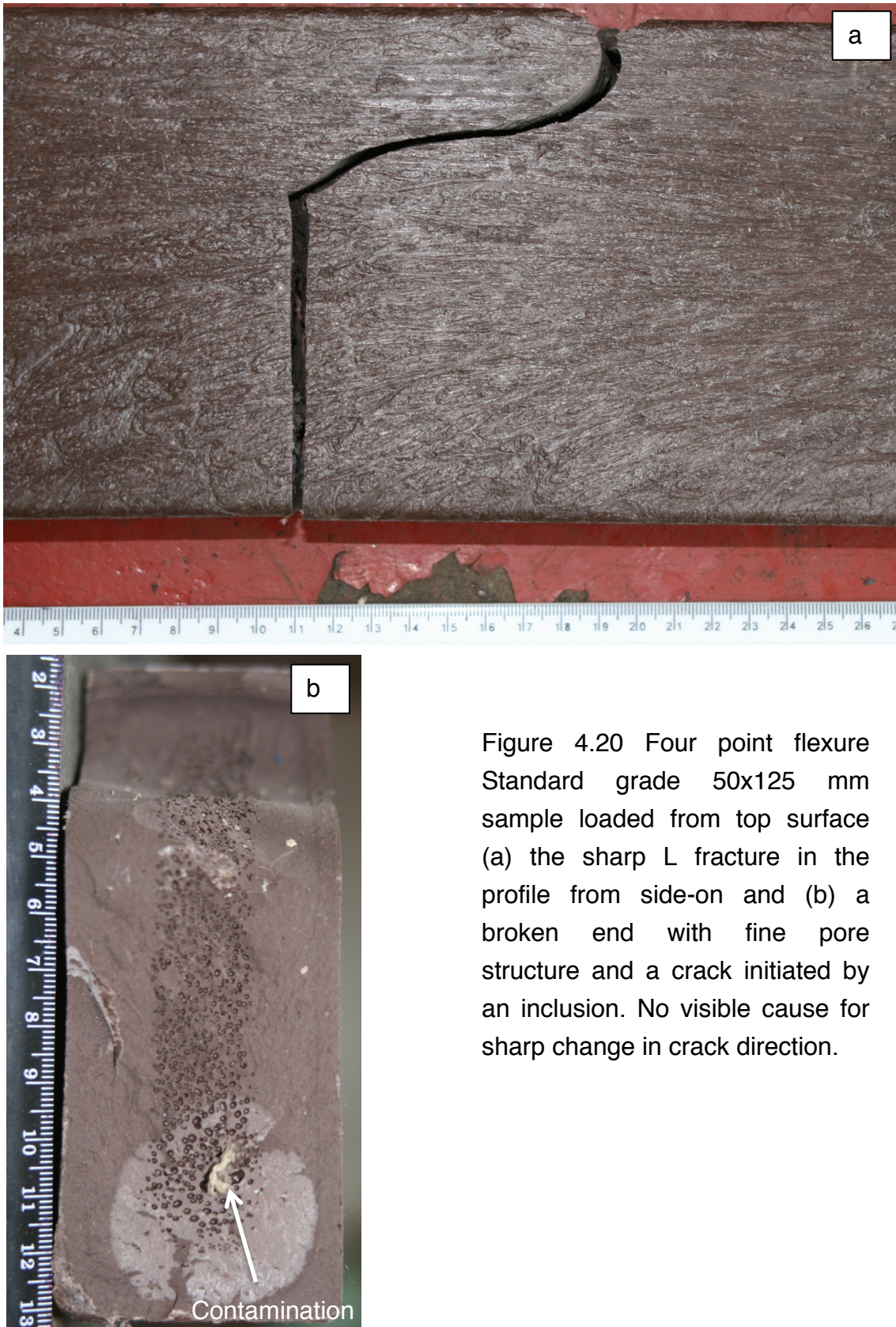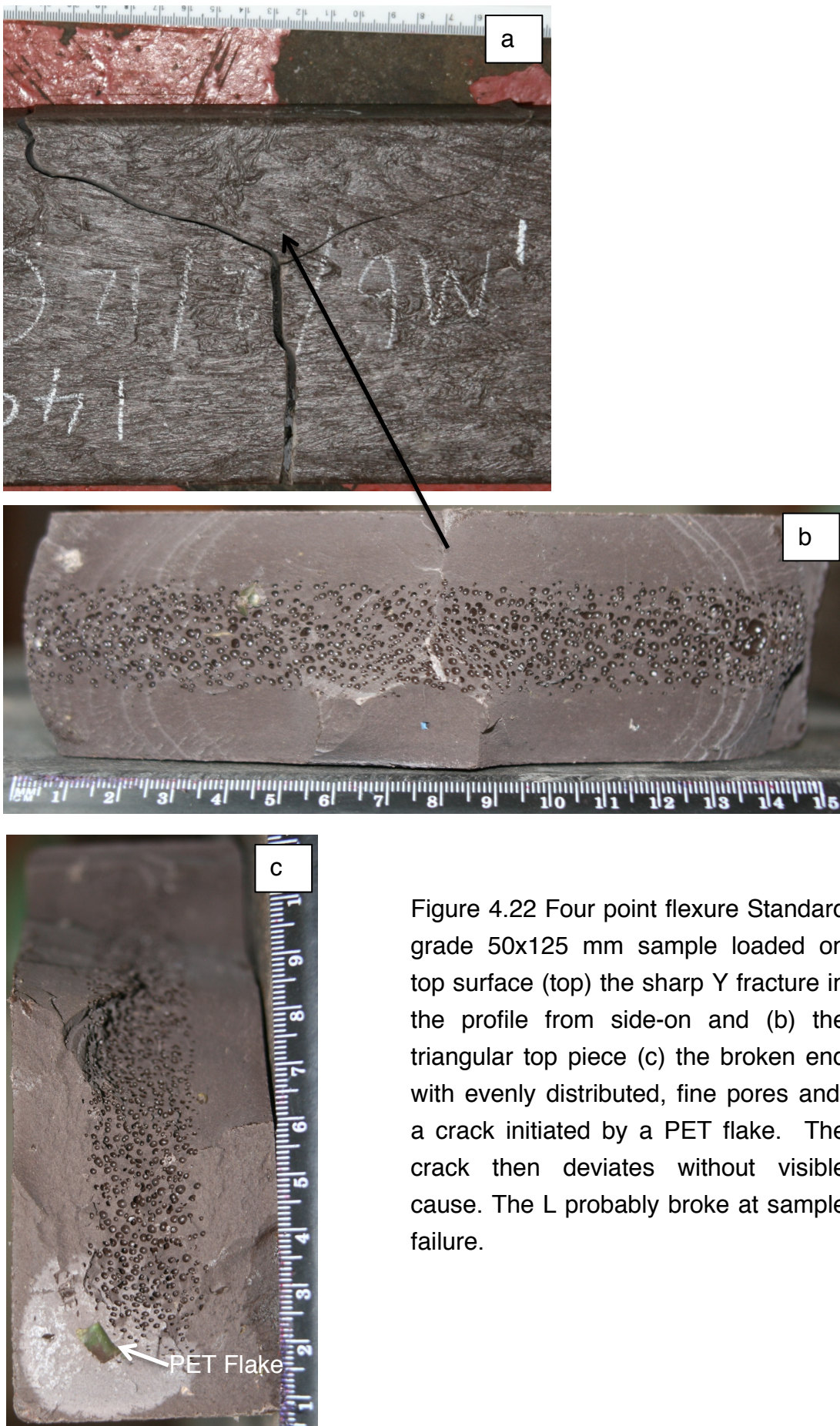
Figure 4.22 Four point flexure Standard grade 50x125 mm sample loaded on top surface (top) the sharp Y fracture in the profile from side-on and (b) the triangular top piece (c) the broken end with evenly distributed, fine pores and, a crack initiated by a PET flake. The crack then deviates without visible cause. The L probably broke at sample failure.

In L fractures, the crack usually started perpendicular to the bottom face, then veered off to one side. It was usually in the top half to a third in the foamed region. The crack deviated probably following planes of weakness following the direction of flow. The L varied from a few centimetres to over 13 cm long. In purer materials, the L fracture was longer with a smooth, curved change in direction, see Figure 4.19. The change of direction was sometimes a sharp angle, probably due to the crack hitting an inclusion, a large bubble or another defect, see Figure 4.20. The cause of deviation was rarely apparent. Generally about 75% of L and Y fractures changed direction sharply, the remainder gradually changed. 52% of 50x100 mm and 48% of 50x125 mm Standard grade samples fractured in an L crack. 34% of 80x80 mm Impact grade and 30-80% of 80x80 mm glass filled grades fracture in an L crack.

In Y surfaces, the crack bifurcated usually in the top half of the sample, which created a triangular piece that broke off from the top surface. The cause of the bifurcation was not apparent, except in 3 profiles, which had an inclusion at the triangular tip, see Figure 4.21 and 4.22. The force of failure may have caused the overhanging piece of the L to break of, creating the Y shaped fracture. Often the triangular piece was still attached to one side. 32% of 50x125 mm samples, 48% of 80x80 mm GH and 40% 80x80 mm GL fractured with a Y crack. 80x80 mm Impact grade and 50x100 mm Standard grade did not fracture with a Y. In 125x50 mm plank position, 70% of samples fractured with an L crack, and only 10% in a Y crack. These statistics suggest as the height of the sample increased, the crack was more likely to deviate and then bifurcate or the L nose to break. Adding glass fibre had the same effect.

From analysis of the fracture surfaces, it can be concluded profiles exhibit a range of bubble sizes, bubble distribution and foamed area shape. Cracks were initiated at inclusions, irregular bubbles and bubble clusters. The crack length and shape depended on the orientation, strain rate, quality, material grade and sample height. Cracks in glass filled grades and proportionally tall samples were more likely to deviate along the sample.

4.5.2 Electron Microscopy of Fracture Surface

Every fracture surface had a white area, see Figure 4.17. To investigate this, SEM microscopy was used on samples of Standard grade and GH grade from four point bend testing. The samples were carbon coated during the sample preparation procedure. The fracture surfaces were photographed using a Philips XL-20 SEM in secondary electron mode.

Figure 4.23 is the boundary of the white area on a Standard grade profile fracture surface. Figure 4.23(a) also shows an inclusion on the right side. The white area is at the top in each micrograph. This area shows multiple small fibrils of ductile fracture, which is shown at higher magnification in Figure 4.24(a). The bottom left area is flat, brittle fracture, see Figure 4.24(b) for greater detail.

Often a lump of contamination (Figure 4.23) or a larger bubble (Figure 4.26) was visible in the white zone, which would act as a stress raiser and lead to crack initiation. Then the material yielded and stress whitened, until it grew to a critical size. At this critical crack length, the crack propagated fast through the profile. The high speed release of energy was very apparent when witnessing a test. High strain rates can cause a material to transition for ductile failure to brittle fracture [21, 152, 153]. Areas characterizing different failure modes have been observed in isotactic polypropylene over a range of test speeds [154]. The size of the ductile zone is investigated further in the next section.
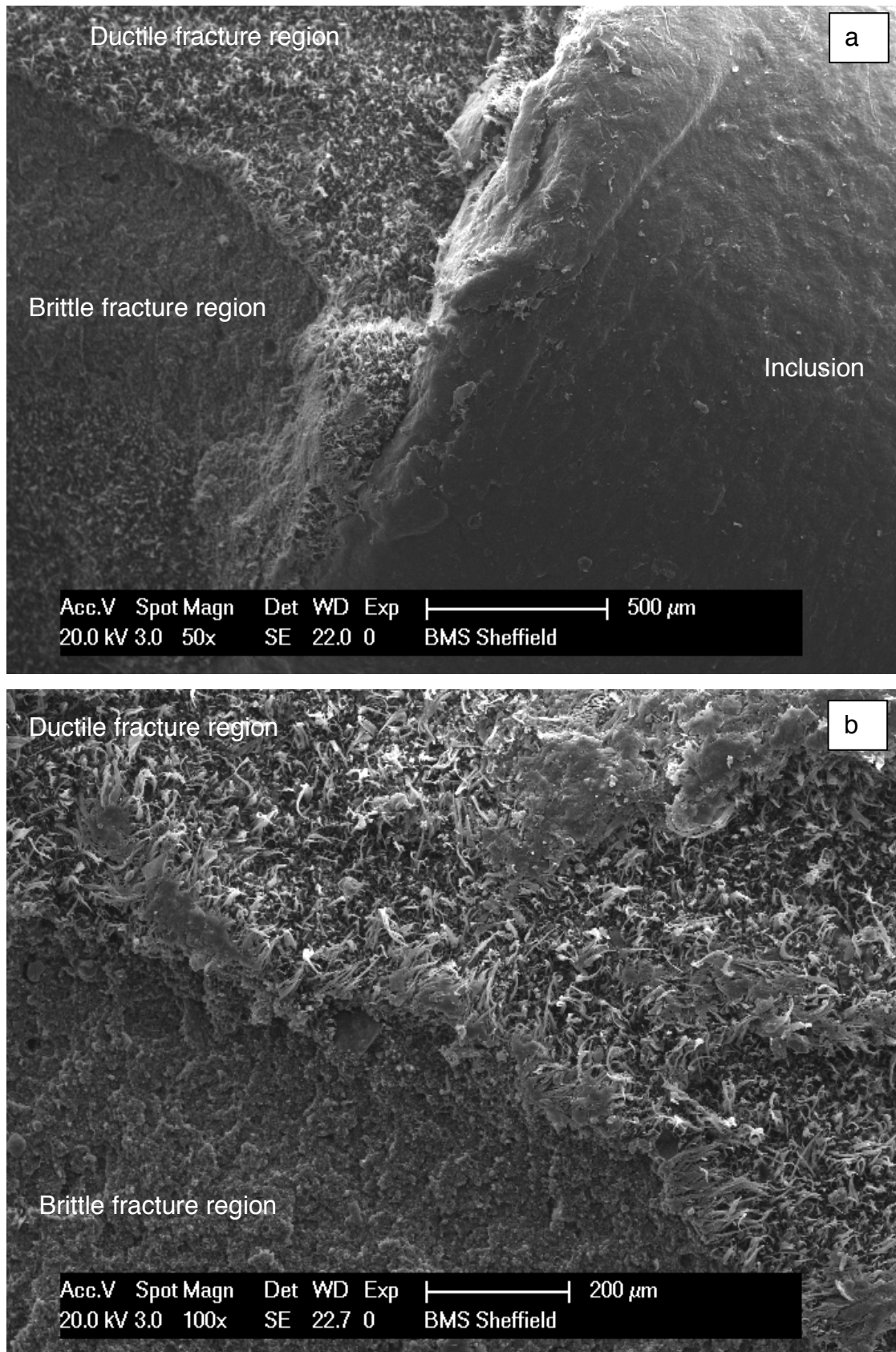
Figure 4.23 SEM micrographs of a Standard grade fracture surface. a) transition area with foreign inclusion x50 b) transition zone x100.
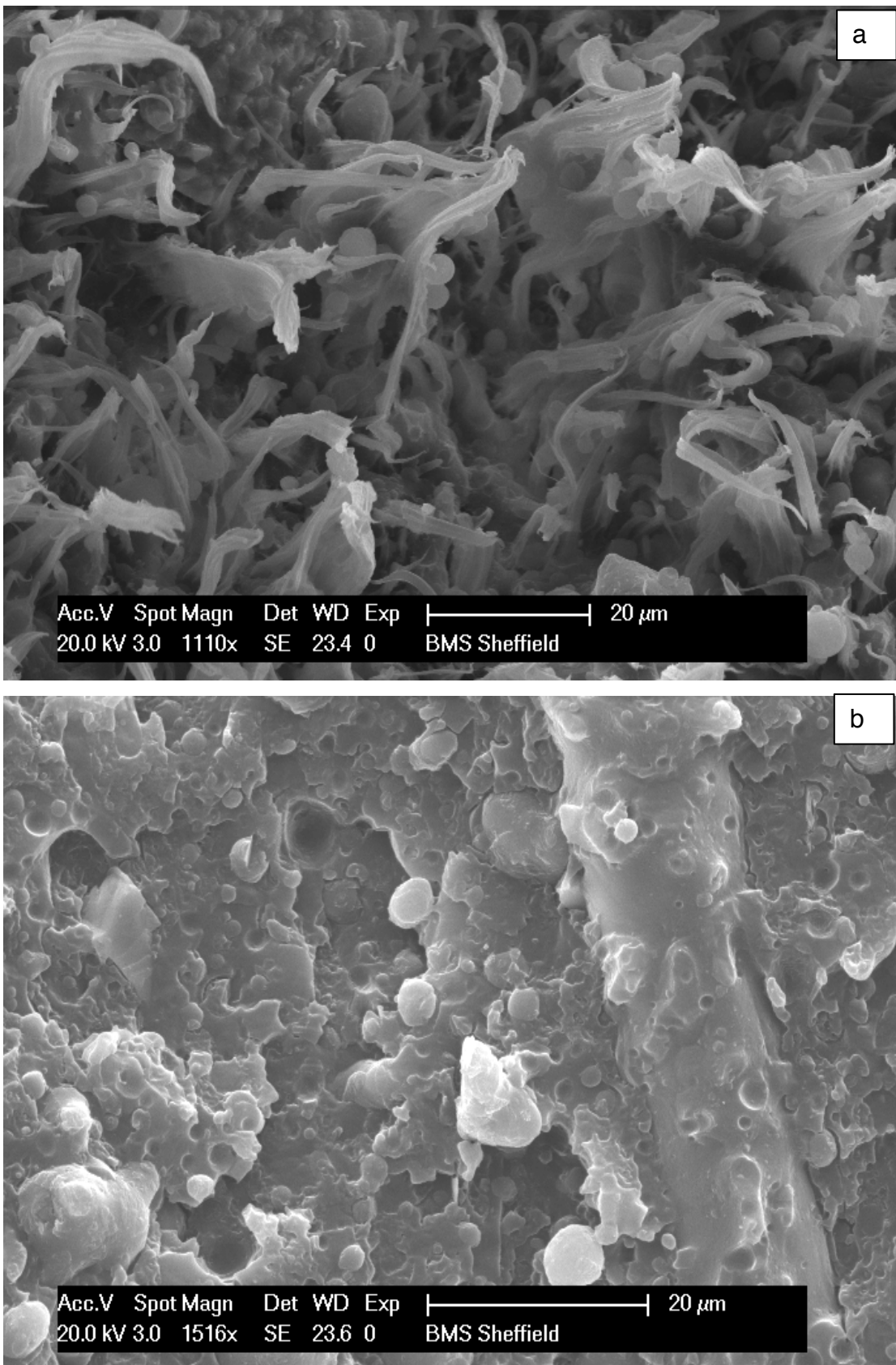
Figure 4.24 SEM micrographs of a Standard grade fracture surface. a) ductile fracture zone x1110 b) brittle fracture zone x1516.

Figure 4.25 shows the transition zone for the glass fibre reinforced material. The ductile fracture zone is at the top of each micrograph and the brittle fracture zone at the bottom.

Broken glass fibres can be seen sticking out of the matrix in Figure 4.25 - 4.27. The effect of glass fibres in the fracture process depends of the matrix and the strain rate [155]. In brittle matrices and dynamic tests (such as impact strength) fibres increase the work of fracture through debonding of the glass/matrix interface, fibre pull out, stress relaxation and friction between interfaces as with fibre pull out. Impact strength increases with glass fibre content up to a certain point. Then it remains static or decreases as fibre density hinders the mechanisms. In static testing the ductility of the matrix becomes important.

The work of fracture drops at first because the stiffer fibres restrict the high deformability of the ductile matrix at low loading rates. As can be seen in Figure 4.26, the fibrils are small so the effect is not large in this material. When loading rates increased, the matrix changes from ductile to brittle deformation and the mechanisms associated with brittle fracture are more important. This transition has been observed in glass fibre filled polyethylene by comparing low strain rate three point flex with high strain rate notched impact testing [155].

It can be concluded that at a critical size, the ductile crack transitioned to brittle failure. Glass fibre increased work of fracture through fibre pull out in the ductile and brittle crack propagation zones.
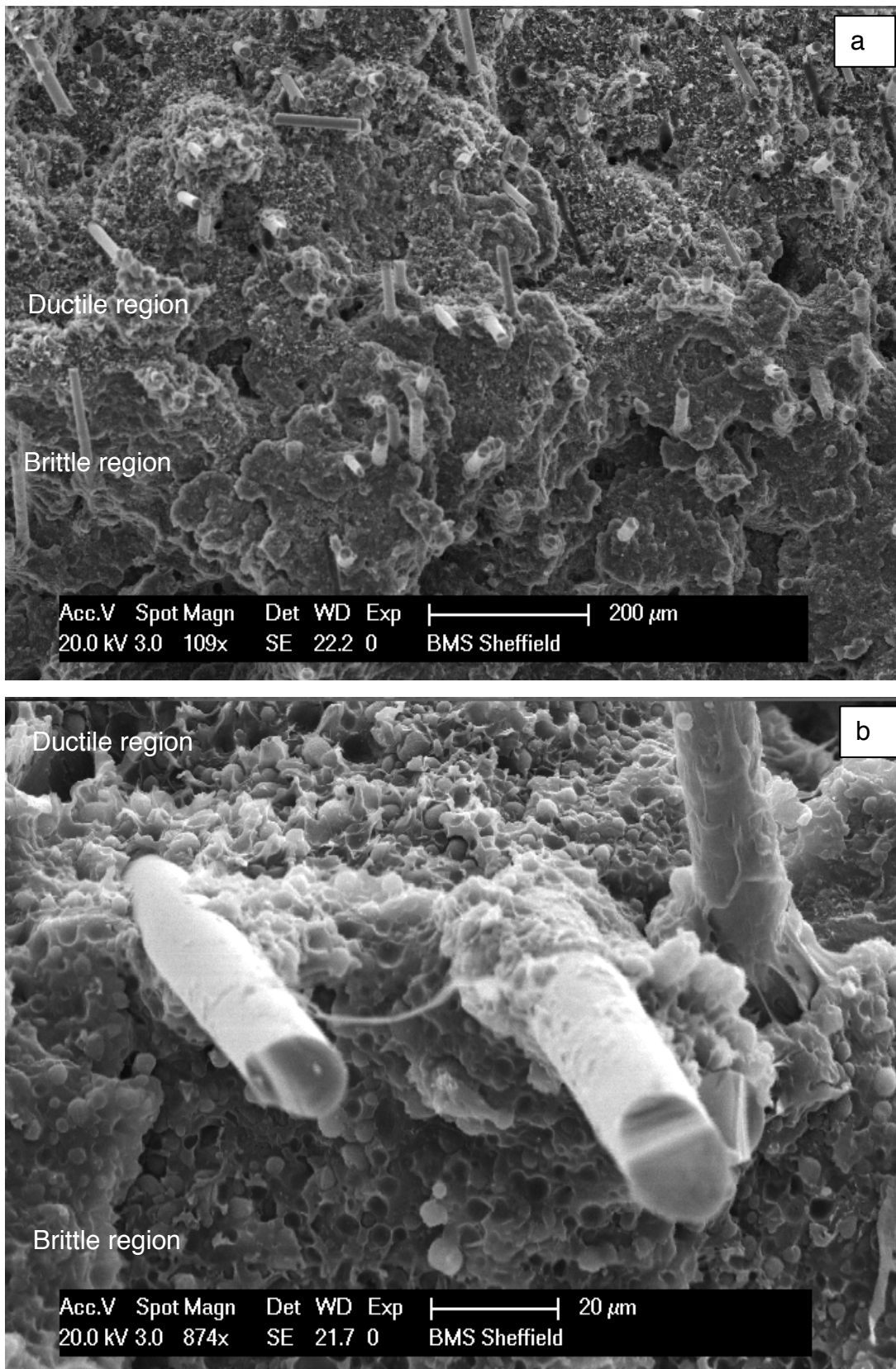
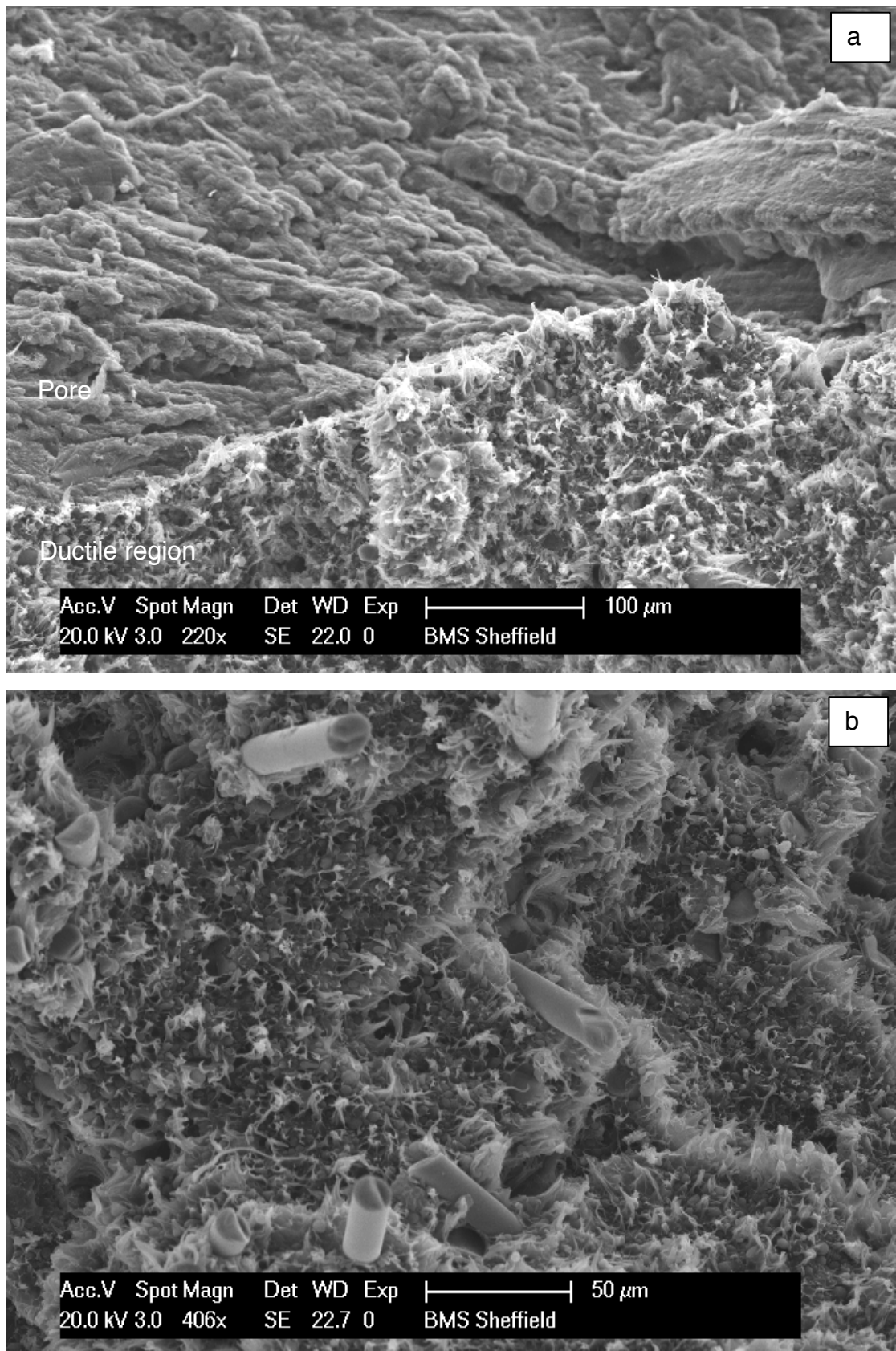Figure 4.25 Transition zone in the Glass fibre grade. a) x109 b) x874.

Figure 4.26 Micrographs of the glass fibre grade fracture surface in the ductile zone around a pore a) x220 b) x406.
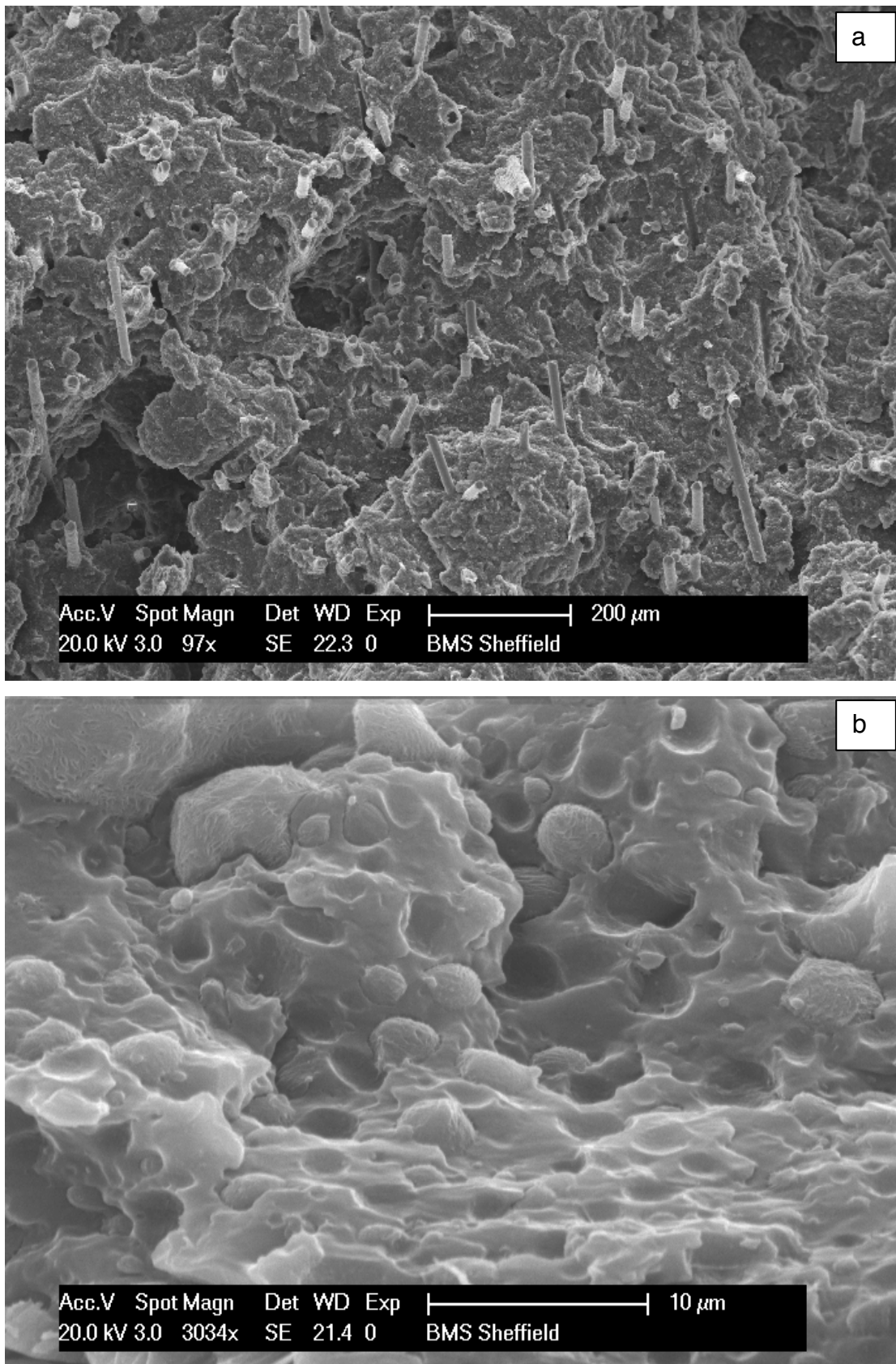
Figure 4.27 Micrographs of the glass fibre grade fracture surface in the brittle zone a) x97 (b) x3034 magnification.

4.5.3 Analysis of Ductile to Brittle Transition

The size of the ductile zone was measured in order to understand the ductile to brittle transition further. The size of the ductile zone was measured on 188 samples. The ductile area was calculated as being an ellipse. The average area of the ductile area was 5-20% of the total cross-sectional area, see Figure 4.28. The standard deviation is very large due to the variation shown in the previous photographs. Welch's t test was used to test for significance between results.
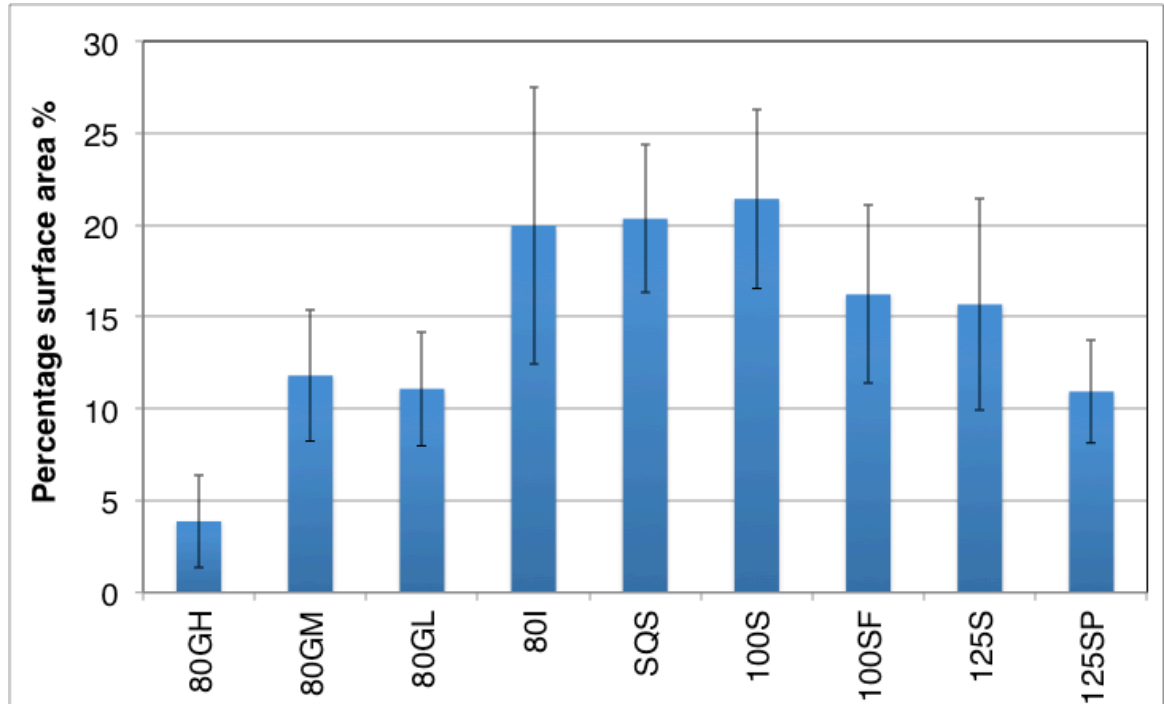
Figure 4.28 Percentage area of the ductile region of the total profile cross-sectional area displaying average and standard deviation. GH, GM and GL = glass reinforced grades. I = Impact grade. S = Standard grade. 80 = 80x80. 125 = 125x50 mm. SQ = 100x100 mm, 100 = 50x100 mm. P = plank orientation. F = 0.005 strain rate.

 In proportion to the cross-sectional area, the smallest area was for the most brittle material, GH, the high glass content grade. The trend in glass fibre content was confirmed in the 250x130 mm three point bend samples, which had average ductile area of 1, 9 and 22% for GH, GM and GL respectively. The Impact grade 250x130 mm had a low value of 5%. This was an average of four batches. The cause for the difference in ductile area between 80x80 mm and 250x130 mm Impact grade is unknown.

In proportion to the cross-sectional area, the largest ductile area was seen in square cross sections and in the shorter, joist samples. As would be expected, the high strain rate 50x100 mm test has a smaller ductile area than the lower strain rate 50x100 mm. The 125x50 mm plank sample had a smaller area than the 50x125 mm joist sample. This cannot be explained by the total area size because it does not sufficiently describe the defect size in relation to the profile dimension. Figure 4.29 expresses the ductile area dimensions as a percentage of the relevant profile dimension.
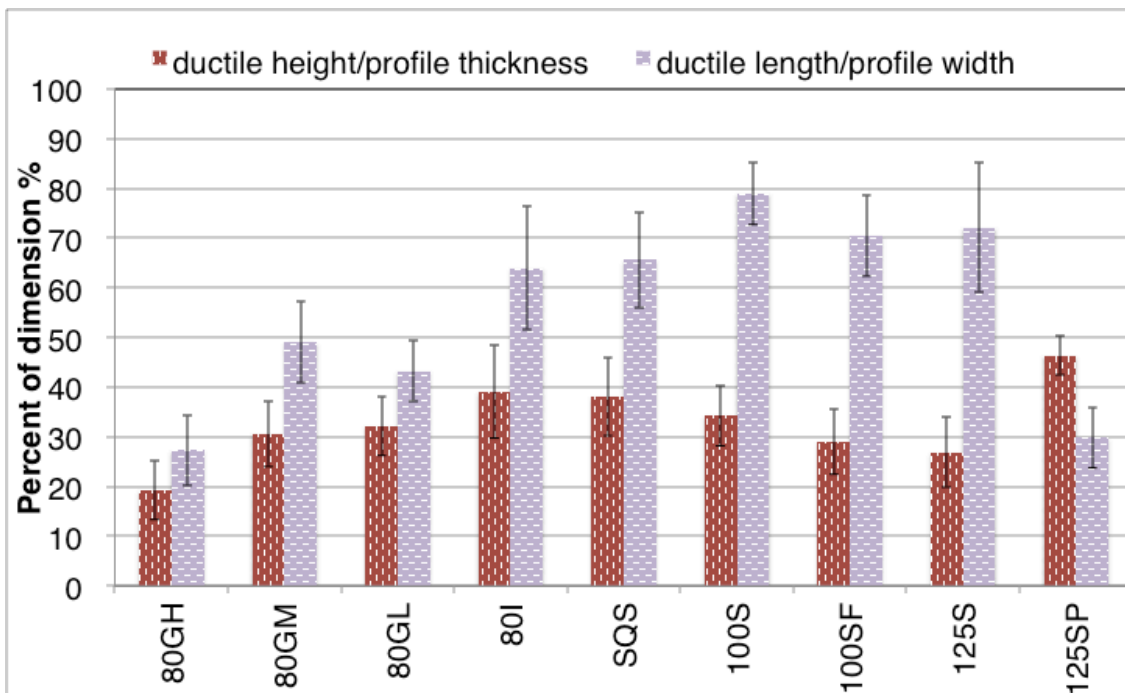
Figure 4.29 Defect height and width expressed as a percentage of the relevant profile dimension. Average and standard deviation plotted. GH, GM and GL = glass reinforced grades. I = Impact grade. S = Standard grade. 80 = 80x80 mm. 125 = 125x50 mm. SQ = 100x100 mm, 100 = 50x100 mm. P = plank orientation. F = 0.005 strain rate.

In this format the size of the ductile area appears much more significant. Compared to the height, the shortest joist profile 80x80 proportionally had the tallest ellipse (39%) and the tallest joist profile (50x125 mm) had proportionally the shortest ellipse (26%). 50x100 mm occupied 34% of the height, though it actually fractured at the same strain as 50x125 mm. Strain is proportional to the profile height, hence for the same crosshead displacement, the bottom surface of 125x50 mm profile would have been under higher strain.

The ductile area was usually largest in the plane perpendicular to the load, which is reflected in the proportion of sample width occupied by the ductile area. The maximum was 80% of the profile width for 50x100 mm, and over 60% for 80x80 mm, 100x100 mm, 50x100 mm fast and 50x125 mm. This suggests the crack propagated across the sample in the area of maximum stress, then transitioned to brittle failure at a critical size.

In comparison 125x50 mm plank orientation, it was only 30% of the profile width and 46% of the profile height. In this case, when the height of the ductile area reached a critical size, the sample could not support the load and transitioned to fast, brittle failure.

In conclusion, the ductile crack propagated across the width of the sample. The transition to brittle failure occurred at a critical width for joist samples and a critical height for plank samples. Increasing the strain rate reduced the ductile area size.

4.5.4 Proportion of Foamed Core to Solid Walls

The proportion of strong, load bearing solid wall in a profile was investigated. The wall thickness and profile dimensions were measured from fracture surface photographs. Then area of solid wall and foam was calculated assuming a rectangular foamed area. Figure 4.30 and Table 4.7 show the percentage of foamed area and solid wall in each cross-section. The solid area varied between 48 and 66%. The difference in wall section was higher than expected.

The standard deviation was large due to the small sample size, the large variation between samples and the measurement technique. There were parallax errors when taking measurements from the photographs, because the fracture surfaces were angled and not in the plane of the scale. This was overcome by scaling the measurements using the dimensions measured when the samples were tested. Directly measuring fracture surfaces would have been more accurate, however, the analysis was completed at a later date when

access to the samples was not possible. Welch's t test was used to check significance between values.
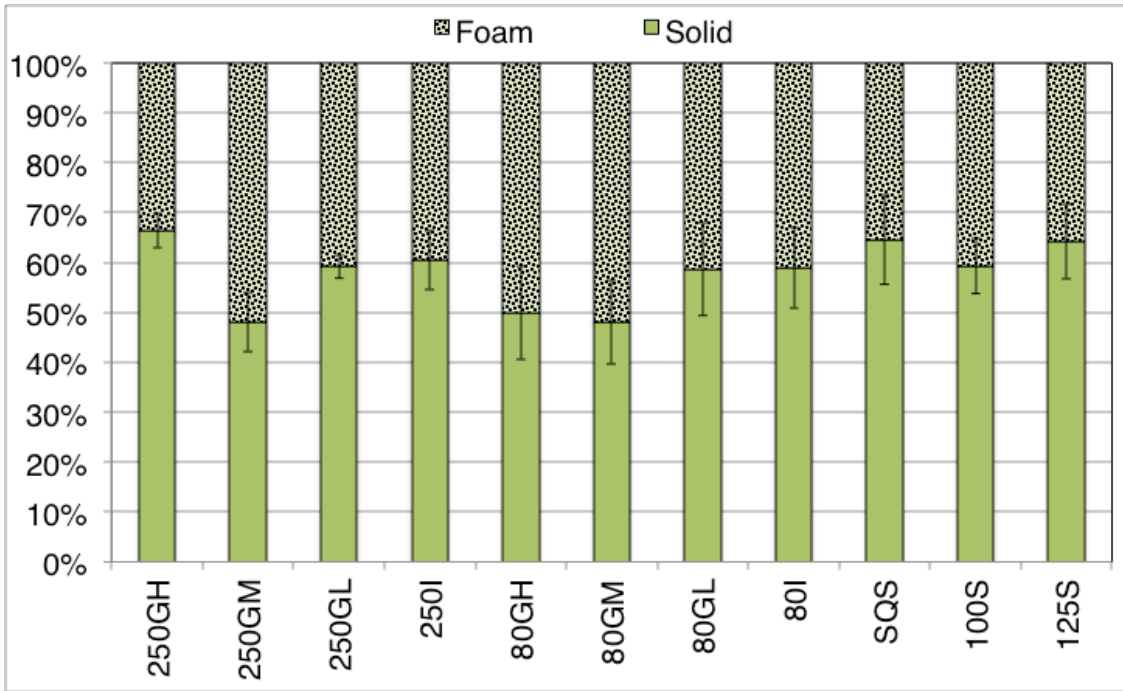
Figure 4.30 The proportion of foam to solid structure for different profile sizes and grades. Average and standard deviation plotted. GH, GM and GL = glass reinforced grades. I = Impact grade. S = Standard grade. 80 = 80x80 mm. 125 = 125x50 mm. SQ = 100x100 mm, 100 = 50x100 mm. P = plank orientation. F = 0.005 strain rate.

Table 4.7 Percentage area of solid outer wall to inner foam.

Profile size mm	Code	Number of Profiles	Wall thickness mm		% average area		
			Average	St. Dev.	Solid	Foam	St. Dev.
80x80GH	80GH	29	11.8	3.1	50	50	9.3
80x80GM	80GM	10	11.2	2.4	48	52	8.4
80x80GL	80GL	10	14.4	3.0	59	41	9.3
80x80I	80I	32	14.5	3.1	59	41	8.1
100x100S	SQS	5	20.1	4.5	65	35	9.0
100x50S	100S	51	11.4	2.4	59	41	5.6
125x50S	125S	41	13.3	2.6	64	36	7.5
250x130GH	250GH	2	35.1	3.5	66	33	3.4
250x130GM	250GM	3	24.4	4.2	48	52	5.9
250x130GL	250GL	3	30.8	2.8	59	41	2.3
250x130I	250I	3	32.8	4.6	60	40	5.9

50x125 mm profile had 5 % more proportion of solid area compared to 100x50 mm, because it had thicker walls. For a 11.4 mm wall section, theoretically 125x50 mm should have 2% less solid area than 100x50 mm. As the standard flexural stress and strain equations assume a homogeneous material, this effectively means the same material in a 50x125 mm profile would be stronger and stiffer. Testing in Section 4.4.3 measured Standard grade 50x125 mm was stronger than 50x100 mm profile.

In 80x80 mm profile GL and Impact grade had a higher proportion of outer wall than GM and GH. The 250x130 mm profiles did not confirm this trend though there was a very small sample size.

The relationship of wall thickness and sample dimensions is more important than the total solid area for flexural testing. The effect of the dimensions and wall thickness can be explored by comparing the section modulus, Z, of a solid rectangular beam and a box beam [135].

$$Z_{rectangle} \quad = \quad \frac{I_{rectangle}}{y} \quad = \quad \frac{bh^2}{6} \qquad\qquad 4.27$$

$$Z_{box} \quad = \quad \frac{I_{box}}{y} \quad = \quad \frac{(bh^3 - jk^3)}{6h} \qquad\qquad 4.28$$

Where Z = section modulus, I = moment of Inertia, y = h / 2, h = external height, b = external width, k = Internal height = h-2t, j = internal width = b-2t and t = wall thickness.

The stress at failure, σ_f, is inversely proportional to the section modulus, Z:

$$\sigma_f \quad = \quad \frac{M \, y_{max}}{I} \quad = \quad \frac{M}{Z} \qquad\qquad 4.29$$

Where M = moment.

Table 4.8 shows the effect of profile size and wall thickness on section modulus and the load required to reach the failure stress for a support span of 14 times beam height. Increasing wall thickness by 2 mm to 13 mm, improves strength 10%. Changing beam height has a far larger effect, because Z is proportional to the square of the beam height.

Table 4.8 Comparison of section modulus, Z, and the load required to produce the same stress in a solid beam and box beams with different wall thicknesses. These are theoretical values compared to a 50x100 mm box beam with 11 mm wall thickness for a support span of 14 times beam height [135].

Beam width mm	Beam height mm	Wall thickness mm	Percentage of Z %	Percentage of Load %
50	100	11	100	100
50	100	13	110	110
50	125	11	146	117
50	125	13	162	130
50	100	Solid	136	136

In conclusion, the variation in wall thickness with profile size has more effect on mechanical properties than the proportion of the solid area of the cross-section, due to the effect on section modulus. Standard stress and strain equations assume a homogeneous material. This effectively means the same material in a profile with thicker wall sections would be stronger and stiffer.

4.6 Conclusion

This Chapter investigated formulation, profile size and batch-to-batch variation. A number of conclusions can be drawn from this study.

Glass fibre was an efficient method of improving stiffness and strength in compression and flexure. Comparing all the different glass fibre reinforced flexure tests, moving from 5 wt% glass fibre to 10 wt% improved modulus by 20-25%. Increasing from 5 wt% to 15-20 wt% gave a 90% increase in modulus. An identical unreinforced base blend was not tested, though the properties were 60% higher in the 5 wt% grade compared to Impact grade, and 40% higher compared to a polyolefin waste stream.

The addition of 20 wt% glass fibre halved the expansion co-efficient to 4.8×10^{-5} mm/mm/^{o}C, and maintained this value over a wider temperature range. CTE of polymer reinforced grades increased when the temperature range was widened.

Comparing like for like test conditions was found to be important. Profile size and shape, span length, profile orientation and strain rate all effect the strength and modulus values obtained.

The batch-to-batch variation of production grade materials was significant. This wide variation means that a large sample size from a large number of production runs was required for accurate values and significant comparisons to be made. This variation was due to changes in raw materials and quality. Analysis of cross-sections showed a wide variety of solid wall thickness, bubble size, bubble density and distribution, plus type and amount of contamination and inclusions.

The variation in wall thickness with profile size has more effect on mechanical properties than the proportion of the solid area of the cross-section, due to the effect on section modulus. Standard stress and strain equations assume a homogeneous material. This effectively means the same material in a profile with thicker wall sections would be stronger and stiffer. This was demonstrated in flexure of 50x125 mm and 50x100 mm profile.

Strength and modulus were similar for four point bend of 80x80 mm profiles compared to three point bend of 250x130 mm profile. This was probably because, the effect of changing the strain rate, thickness, and span:depth ratio is complex. These parameters can have an appreciable effect on the measured properties. Compression strength and modulus was significantly higher along the profile length compared to the transverse direction, due reinforcement alignment and mode of failure.

The modulus of a polymer blend was higher when intrusion moulded into 250x130 mm profile compared to injection moulded test bars. The modulus of

250x130 mm intrusion moulded glass fibre reinforced profiles was not statistically different to small injection moulded test bars. A larger sample size was required to differentiate between the production methods. The modulus of intrusion moulded glass reinforced profiles was higher than predicted for fibre reinforced blends with randomly orientated fibres as calculated by Halpin Tsai equations. Calculation of the Halpin Tsai fibre orientation parameter was hindered by the complexity of the system. The parameter is also affected by changes to fibre length, fibre interactions and matrix crystallinity. Compared to injection moulding, intrusion moulding was expected to have lower fibre alignment however, far slower cooling rates would expect to increase crystallinity.

Strength of intrusion moulded profiles was significantly lower than that predicted by the rule of mixtures. The premature failure was caused by inclusions and contamination acting as crack initiation sites.

Inclusion and contamination was found to be the main cause of failure in flexure, though irregular bubbles and clusters of bubbles also initiated failure. These acted as stress raisers and initiated internal cracks. Cracks grew by ductile yielding to a critical size, visible by a white area on the fracture surface. The ductile crack propagated across the width of the sample. The sample failed at a critical width for joist samples and a critical height for plank samples. The high strain rate produced a transition to brittle failure. Increasing the strain rate reduced the critical size before transition. Contaminated formulations tended to break in a line perpendicular to the lower surface. The crack often sheared to one side in more purer compounds, glass fibre filled grades and taller profiles to give L shaped fractures. Y shaped fractures formed where the crack bifurcated at a defect or plane of weakness, or where the force of failure broke off the L section.

5   Discussion and System Development

In this chapter the formulation development and product testing will be reviewed within the context of the resulting railway sleeper material, product and system tests, that were carried out as part of the sleeper qualification for Network Rail.

5.1   Formulation Development Review

The aim of the project was to exploit the use of lower grade recycled plastic waste streams to produce a high performance, higher value product for structural applications. The ultimate aim was to make a product capable of carrying significant in-service dynamic loads over a wide spectrum of temperatures and harsh environments for railway sleepers.

The project had constraints imposed by the sponsor Company and by the development agreement from Network Rail. The sponsor Company stipulated that economically viable waste streams were blended, without any added compatibilisers or stabilisers, and processed using their existing intrusion moulding process. Network Rail stipulated the size of product, mechanical properties, and other aspects that will be discussed in the next section.

During the project, the recycling industry was in a period of change. The prices of recycled plastics rose significantly, because of the increased demand from the mainstream processors for good quality recycled plastic compounds, in order to replace increasingly expensive virgin polymers. The project benefited from new waste streams becoming available, though other waste streams disappeared or became too expensive. It was important for the success of the project to select waste streams that were available in sufficient quantity at a suitable price.   Formulations tolerant of higher contamination levels were particularly of interest.

A review of the recycling industry, published literature and existing practice was undertaken to identify suitable polymers and formulations. Mixed blends of

polyethylene and polypropylene were identified as the most abundant, cost effective waste streams. These polymers had numerous desirable properties required for structural applications – mechanical properties, toughness, chemical stability and ease of processing. Without the use of compatibilisers, polyethylene and polypropylene form immiscible blends, which have been reported to exhibit synergistic behaviour in certain circumstances. Reinforcement was still required to overcome insufficient stiffness and low maximum operating temperature under load.

The use of polymer, mineral fillers and glass fibre reinforcement was investigated in an iterative program of laboratory tests on standard, injection moulded samples. Testing included flex, tensile, impact resistance, co-efficient of thermal expansion and maximum operating temperature.

The five laboratory trials successfully produced formulation guidelines that aided compound selection and experiment design for production trials and full product testing. It was found that the compounding method, sample production technique and test method significantly affected the measured mechanical properties. Therefore, the injection moulded samples and laboratory tests could only be used as an indicator of the final component properties.

Amorphous polystyrene was found to reinforce the semicrystalline blend of polypropylene and polyethylene to an acceptable level. A second trial using a lower polystyrene level found that the mechanical and impact properties were significantly affected by the type of polypropylene and polyethylene.

A far higher level of enhancement was obtained with glass fibre and plate-like mica. A synergistic enhancement of tensile strength was obtained using glass fibre in combination with mica, because mica enhanced the matrix and increased the forces constricting the glass fibre. The addition of glass fibre to the polyolefin matrix significantly improved strength, stiffness, co-efficient of thermal expansion and maximum operating temperature.

The formulations selected for large product trials used polystyrene:polyolefin blending and glass fibre reinforcement. Profiles were produced that ranged in cross-section from 250x130 mm to 100x50 mm. Two standard production grades and four trial formulations underwent a range of testing: three point bend test, four point bend test, compression, and co-efficient of thermal expansion measurement. Due to production scheduling constraints, not all the compounds could be produced in the same profile size or in bulk quantities. Where possible, the standard production grades were tested in statistically significant numbers from randomly selected batches that were run over the course of 15 months. This effectively demonstrated high batch-to-batch variation due to changes in the waste stream type and quality even though the formulation was identical. The profile cross-sections were found to have a wide variety of wall thicknesses, shape of foamed area, and bubble size and distribution.

Contaminant particles and inclusions were found to be the main cause of premature failure that significantly reduced strength compared to that predicted by the rule of mixtures. Investigation of flexure fracture surfaces showed that ductile crack growth was initiated at inclusions and other weak points. The crack grew to a critical size, and then high strain rate, brittle fracture occurred. The size of the ductile crack growth depended on the formulation, profile size and orientation, strain rate and location of the flaw. The brittle crack path was perpendicular to the profile length in profiles with high contamination level and certain profile sizes. The crack path deviated along the profile in relatively tall profiles or where glass fibre was present.

Comparing like for like, test conditions was found to be important. Profile size and shape, span length, profile orientation and strain rate all affected the strength and modulus values obtained. The 50x125 mm profile was 12% stronger and stiffer than 50x100 mm profile, due to higher wall thickness of the 50x125 mm profile. Increasing the strain rate increased strength and stiffness as expected for a viscoelastic material.

Table 5.1 compares the properties of the polymer blend grade and the glass reinforced grade. Standard production grade and the polymer blend trial grade are quoted in the polymer blend column. The formulations of the two grades were very similar, they differed in waste stream type and quality.

Table 5.1 Profile testing comparison of polymer blend and glass reinforced formulations.

Property	Units	Polymer	Glass
Density of 250 x 130 mm profile	kg/m^3	908	924
3pt Flexural strength	MPa	19.6	41.1
3pt Flexural modulus	MPa	1187	2905
4pt Flexural strength[2]	MPa	16.2[1]	41.2
4pt Flexural modulus[2]	MPa	1007[1]	2945
Compression strength	MPa	20.4[1]	36.5
Compression modulus	MPa	758[1]	1850
Co-efficient of Thermal Expansion -10 to 40 ^{o}C	x10^{-5} mm/mm/^{o}C	8.4	4.8
Co-efficient of Thermal Expansion -19 to 54 ^{o}C	x10^{-5} mm/mm/^{o}C	12.1	4.7
Vicat Softening Point ISO 306 B50[3]	^{o}C	57	>86
Charpy Unnotched @ RT[3]	kJ/m^2	52	30
Charpy Unnotched @ -30 ^{o}C[3]	kJ/m^2	17	27
Charpy Notched @ RT[4]	kJ/m^2	5.8	3.4
Charpy Notched @ -30 ^{o}C[3]	kJ/m^2	2.6	3.4

(1) Standard grade production polymer blend formulation.

(2) Polymer reinforced was 100x50 mm, glass reinforced was 80x80 mm profile.

(3) Injection moulded formulations.

The difference in product density was not a large as expected. The rule of mixtures gave a density of 950 and 1050 kg/m^3 respectively for polymer and glass reinforced grades. The polymer reinforced grade was measured at 1008 kg/m^3 using the immersion method in ISO 1183-1 [156]. The product densities were less, because blowing agent was used to give flat sides by counter acting

shrinkage during cooling. This produced a foamed centre to the profile. Network Rail specified that the 2600x230x130 mm sleeper needed to weigh under 100 kg, so that it could be carried by four people.

Using glass fibre doubled the flexural strength and almost tripled the flexural stiffness in three and four point bend compared to the polymer blend systems. The modulus of intrusion moulded profiles and injection moulded test bars were higher than predicted for a 3D random fibre orientation using Halpin Tsai equations. Calculation of the fibre orientation parameter was hindered by the complexity of the system. The parameter is also affected by changes to fibre length, fibre interactions and matrix crystallinity. The strength was 50% lower, due to a premature failure caused by stress concentration due to contamination. In compression, strength and modulus were approximately doubled with inclusion of glass fibre reinforcement.

Both grades passed the co-efficient of thermal expansion requirement for railway sleepers, whereas polyethylene and polypropylene would have failed [25]. For the polymer blend grade, CTE increased with temperature range, particularly above the room temperature, which is usual for polymers [25]. Glass fibre halved CTE and kept it constant over a wider temperature range. The value for the glass fibre grade is consistent with published values [25].

The Vicat softening temperatures showed an important improvement when using glass fibre, however, it was significantly below published values for glass filled polypropylene and polyethylene [25, 124]. The increase was important because the product would be suitable for hotter climates and tendency to creep deformation is reduced. Creep deformation was a major concern for plastic beam under constant load particularly where there are areas unsupported underneath. The railway ballast bed moves over time and lengths of sleeper can become unsupported. Good creep resistance enables product to be used for applications such as bridges. Creep testing is discussed in Chapter 6.

Glass fibre reduced room temperature impact strength, however, impact strength at -30 ^{o}C was improved. The values were significantly different to 99% confidence level according to Welch's t test [137]. The values suggested the blends were notch sensitive, which was discussed in relation to other studies in Section 2.2.1. Compared to published data grades, the unnotched values were good but the notched values were low even at room temperature [40, 124, 126, 129]. The use of compatibilisers to improve impact and notch sensitivity is discussed in Chapter 6.

Glass fibre produced a significant improvement in properties, however, it did not match the mechanical properties of softwood. In comparison, EN338 structural softwood timber class C27 has a flexural strength of 27 GPa, a modulus parallel to the grain of 11.5 GPa and a modulus perpendicular to the grain of 0.38 GPa. The compressive strength parallel to the grain is 22 GPa compared to 2.6 GPa compressive strength perpendicular to the grain [157]. The co-efficient of thermal expansion of wood is $0.3-0.5 \times 10^{-5}$ mm/mm/^{o}C parallel to the grain, and $3.5-6 \times 10^{-5}$ mm/mm/^{o}C perpendicular to the grain [112]. Perpendicular to the grain properties are comparable to glass fibre grades, however, the properties of wood are significantly better parallel to the grain despite the density being half that of the glass fibre reinforced grade (0.450 kg/m^{3}) [157]. The structure of wood creates a very stiff, strong, robust, light material. However, plastic lumber can still be fit for purpose with the correct design and the additional benefits of no water absorption, no rotting, insects and animals do not eat it, no splintering, no chemical leaching, no preservatives and no maintenance requirement to maintain preservation level. These factors make plastic lumber very desirable for use in retaining walls, buried underground, immersed in water, wetland areas, sites of special scientific interest, around livestock, and where maintenance is difficult or costly e.g. railways and for public authorities.

For example, treated softwood timber is used in crib systems for retaining earth embankments, however, in certain conditions they rot in under 10 years despite a predicted design life of 50-100 years [17]. After an extensive test program, the British Board of Agrément approved the polymer reinforced blend in the first

polymer crib earth retaining wall system [20]. The approval permits the system to be used for motorway embankments amongst many other situations. It has been used extensively in housing estates.

Figure 5.1 Ecocrib earth retaining wall system using the polymer reinforced product [17].

5.2   Performance in Railway Sleeper Testing

The sponsor company signed a development agreement with Network Rail to develop the first, UK approved recycled plastic railway sleeper. Network Rail stipulated that the product must be a drop-in replacement for softwood sleepers with the exact same dimensions and using standard equipment to install identical "rail furniture" (baseplates, chairscrews, rail pads, etc.).   Network Rail specified certain railway specific tests. They also required a range of material tests that had to be developed during the project. Finally after a lifetime of 50 years in track the product had to be recyclable.

A specification was developed for Network Rail that covered eighteen material, product and system tests, and is currently being implemented as the technical information for a new ISO standard for plastic railway sleepers. Material tests investigated chemical composition, electrical properties and resistance to a variety of agents. Product tests ranged from dimensions, flexure testing to co-efficient of thermal expansion. The system tests investigated the interface of the

sleeper with the chair screw, ballast/track bed and the full assembly. Wherever possible applicable standard tests were used, if necessary they were adapted or new tests developed. This required five new, large, testing rigs to be built at the University of Sheffield. The pass mark was not known for some tests, therefore, wooden sleepers had to be tested to obtain a benchmark value. The specification for wooden sleepers only defined the wood types, dimensions, quality, acceptable defects and preservative treatment required [158].

Fluid absorption was a material test in which there was a significant difference in absorption. Absorption of a range of oils, greases and water was measured for both blends and wood. In an eight week immersion test, the fibre reinforced blend absorbed 25-50% less than the polymer reinforced blend, which had low fluid absorption itself. In the comparison test, wood absorbed over ten times the amount of fluid than that of the polymer blend. The absorbency of softwood wood is demonstrated by the preservative specification that states the wood must absorb at least 128 kg/m^3 of creosote and other preservatives [159]. That means a UK railway sleeper holds at least 10.8 kg of wood preservatives. The preservative improves the sleeper life from 5.5 years to over 30 years depending on the conditions [159]. Preservation tests measure the efficacy of the preservative after long term leaching soil immersion tests [160]. For the polymer blends, separate tests proved the materials did not leach chemicals into water, did not contain banned harmful substances nor did they produce toxic smoke.

Chair screw pull out force was another test that needed a wood reference test. A chair screw was screwed into the sleeper and the force required to pull it out was measured. The polymer blend had 30% improvement in pull out force compared to wood. The glass reinforced blend required over double the force. Chair screw retention is a problem in wooden sleepers. Over time the screw loosens as the wood moves and degrades. In thermal cycling tests, the chair screw pull out of the blends did not reduce significantly.

Long timescale properties were assessed using material tests of weathering and microbiological attack, plus system tests for ballast abrasion and fatigue testing. Microbiological attack is the effect of microbes growing on the surface, consuming substances in the material, and the effect of excreta and by-products on the surface. Tests usually involve long term burial or exposure in a laboratory. Weathering is the effect of solar UV radiation, temperature fluctuations, humidity and water. Outdoor and laboratory testing is further discussed in Section 6.5. Weathering and microbiological attack were assessed by testing recalled product that had been in suitable conditions for 8 years in the field. The mechanical properties of the surface was compared to the internal bulk properties and normalised by similar testing of current product. The results found any deterioration was limited to the top surface layer and had not affected the bulk properties. In a separate test, ten 125x50 mm standard grade samples were weathered for 18 months on a building roof in the north of England. These were four point flex tested in plank position using the method described in Section 4.3.2. Results were compared to those of retained, unexposed samples of the same batch. Though the colour had faded, there was no sign of surface cracking, crazing, chalking or other surface degradation. The tensile strength and modulus reduction was only 5%. In a trial of decking boards made from "curbside tailings" (household recycling consisting of mostly polyethylene bottles), after 11 years the colour had faded but there was only a minor change in strength and modulus had increased [134].
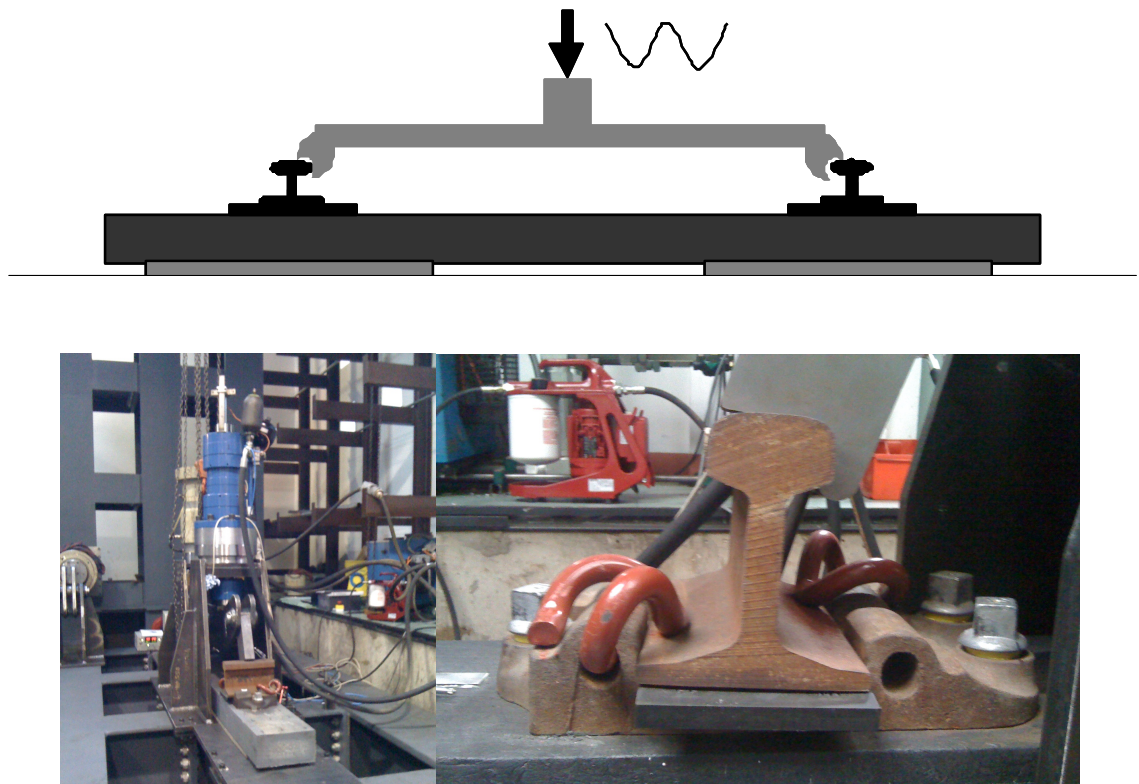
Figure 5.2 Railway sleeper fatigue rig: schematic (top), rig (bottom left), loading point through rail and baseplate assembly (bottom right).

The long term fatigue test was the most stringent test, see Figure 5.2. The sleeper was installed with baseplates attached by three chairscrews and, short lengths of rail fixed on the baseplates with pandrol clips. The sleeper was placed on rubber matting pads of specific compliance that mimicked the deflection of the ballast track bed when a train passed across. A cyclic load was applied at an angle to the rails to simulate the load applied by the wheels of a train. On the first test the load cycled between 10 and 240 kN for 3,000,000 cycles at a rate of 2 Hz. If the sleeper passed the test, the upper load was increased by 10 kN on the following test. Each test used a new sleeper.

The polymer blend sleepers passed 240 kN for 3 million cycles and 250 kN for 5 million cycles, however, they failed at 260 kN across the plane of the chair screw holes. Optimisation of the polymer waste streams improved performance, however, Network Rail introduced an even more demanding fatigue

performance requirement. The decision to introduce the glass reinforcement system was made at this stage.

The glass reinforced sleepers passed 260 and 270 kN each with 5 million cycles. For the final test, a sleeper passed a ramped test - 270 kN for 2 million cycles, 280 kN for 1 million cycles, 290 kN for 1 million cycles and 300 kN for 1 million cycles. In total it passed 5 million cycles.

3 million cycles represented ≈20 years service in low category line, whereas 5 million cycles represented ≈20 years service of main line, simulated track use [19]. 250kN was the minimum load requirement to replace softwood sleepers, and was equivalent to axle loads of the UK's heaviest rail vehicles [19]. 270kN or more was the requirement for hardwood sleepers. On the basis of this criteria, the polymer reinforced sleepers passed >20 years service equivalent to softwood sleepers on secondary track. The glass reinforced sleepers passed 20 years service of equivalent to hardwood sleepers on mainline track.

Glass reinforced sleepers were the first recycled plastic composite sleepers approved for track trial by Network Rail in 2012. The sponsor Company terminated the project before sleepers could go into track due to other unforeseen circumstances, when the investors made the decision to close down i-Plas. A small number of polymer reinforced railway sleepers were selectively installed in a Heritage railway very successfully, and are still in use at the time of writing.

Figure 5.3 Polymer reinforced recycled plastic sleepers installed in track.

6   Technology Improvement and Further Understanding

For further adoption of the Technology developed in this project, further testing and enhancements are required. The work falls into three categories:

– Research required in order to obtain greater understanding of the compound properties to enable adoption for structural applications.

– Further optimisation of the formulation for improvement in morphology, mechanical properties, and lifetime.

– Expanding the formulation to include greater number of polymers, with relatively low stochastic variations in order to enable mass production of structural products from varied polymer recycling streams.

The latter objectives have another underlying goal of enabling the use of lower cost waste streams. Formulations that reduce the price of plastic lumber are necessary, because plastic lumber costs twice as much as wood [161, 162]. Customers buy product based on price and performance rather than on environmental credentials, and the lower maintenance costs that effectively subsidize the initial costs of the more expensive products are usually overseen.

The ability to use rigid/flexible plastic packaging (pots, tubs and trays) would be very advantageous. Government legislation is increasing recycling targets, and to meet these targets this technically challenging waste stream has to be recycled [163]. The recycling industry is investing significantly in processing equipment to find an economic method of recycling this low grade recyclate. The packaging is often contaminated with food and coloured with carbon black, which prevents sorting by near infrared. Many different types of plastic are present and commonly have films attached. Thin plastic films are difficult to handle, because they are lightweight, cannot be cut and, are often multi-layer laminates of different polymers with tie layers to give superior barrier properties. A variety of the proposals may enable adoption of this waste stream such as improvement of manufacturing technique, addition of stabilisers and compatibilisers and investigation of acceptable contamination limits.

6.1 Study of Contamination

In the work presented in this thesis, contaminants were found to be a major cause of premature failure. The failure strengths were significantly below those predicted by the rule of mixtures. However, the presence of high levels of contamination did not systematically reduce the failure strength. Studying the effect of size, shape and distribution of contaminants could produce design and quality guidelines that increase the strength and consistency of results.

6.2 Improvement in Morphology and Manufacturing Technique

This project did not investigate alternative manufacturing techniques. The blends were processed using a single screw extrusion, which is widely available and thus inexpensive. This method has the advantage that it produces comparatively low shear, hence does not degrade the material as much as other techniques. The disadvantage is that it has poor distributive and dispersive mixing. In some mixes, poor dispersion of lower melt fractions was clearly visible. Twin screw compounding was trialed with a toll manufacturer, however, there were difficulties with the filters clogging due to contamination and low melt flow fractions.

Studies have shown that finer morphologies produce improved mechanical properties [52, 53]. The process conditions, viscosity of the component polymers and the interfacial tension between the polymers all have an effect on the morphology produced [38, 59].

A further more detailed study is recommended to optimise compounding parameters, especially when mixing more than three polymers in order to achieve the demanding engineering standards of structural components. Improved mixing may allow addition of cheaper, lower melt polymers that may be advantageous in terms of mechanical properties.

6.3 Use of Compatibilisers

The formulations in this project were immiscible blends. Conventional thinking is that compatibilisers are required to create miscible blends in order to achieve the best properties [21].

Immisicible blends tend to have coarse morphology and poor interfacial adhesion, which gives low impact strength, low strain at break and poor yield strength. Compatibilisers improve mechanical properties by reducing interfacial tension, which facilitates fine dispersion, and through increasing interfacial adhesion, which improves stress transfer [21]. The morphology is also stabilised during processing, which improves the reproducibility and batch-to-batch consistency.

There is a wide range of compatibilisers that are suitable for mixing with various polymers. Studies have used mixtures of SBR, SEBS, EPR and Surlyn for virgin and recycled blends with PP, PE, PS and HIPS [164–167]. The compatibilisers produced finer morphologies and stabilised the morphology in an unstable blend. Impact strength and ductility improved, though strength decreased in some systems. However, high recyclate degradation, due to multiple thermal processing cycles, reduced the level of potential improvement [166]. In studies of EPDM and EVA compatibilisers in PP and HDPE blends, it was found that different beneficial effects were produced by each compatibiliser in the same blend, though each was most effective in different blends [52, 53, 168].

The studies show that the effect of a compatibiliser can be complex. Although toughness and ductility can be improved, strength and stiffness is sometimes reduced, because crystallite size and total crystallinity is altered [21]. In some systems, interfacial failure actually provides a toughening mechanism by dissipating energy [153]. The criteria for success need to be clear when assessing the benefits of a compatibiliser [21]. A study would show if the benefits of consistency and potentially improved properties would outweigh the extra cost in this complex blend.

6.4   Degradation and the Effect of Stabilisers

This project assessed the maximum performance of blends without added stabilisers. Stabilisers prevent oxidation and degradation during processing, thermal ageing and UV degradation. The conventional theory is that stabilisers are required to gain maximum performance from virgin or recycled plastic [21, 38].

Oxidation is a complex process that varies for polymer type, polymer grade, type of oxidation and length of exposure [169–171]. The degradation of a polymer blend depends upon the individual polymers, the interaction and the morphology [38]. A product is classed as failed when either loss of appearance is too great or the reduction in mechanical properties is unsatisfactory.

Colour and colour consistency is very important to customers, even in a recycled product. Colour consistency was very difficult to obtain, because the underlying colour of the waste streams changed the final colour, which when blended together they were grey tinged red, yellow, white, etc. The most stable black and brown pigment masterbatches were used, but the colour still faded over time. Carbon black was used, which is a very efficient UV screen and is also one of the most stable black pigments. One study showed the photo-oxidative stability of a LDPE, HDPE, PP, HIPS recyclate blend was low, and was improved to a satisfactory level by the addition of carbon black or a commercial photo-stabiliser [166]. 3% carbon black is used as UV screen in agricultural films to protect them [38].

Mechanical property stability is important for 50-120 years product lifetime requirement. Historically, recyclates probably had residual levels of stabilisers but, as waste streams have changed the residual stabiliser levels may have altered. For example, production scrap used to be the main waste source, which should have high levels of stabilisers as it had been only processed once and not aged at all. By the end of the project packaging waste streams were commonly used. Packaging is a short life cycle product that does not need large amounts of stabilisers [170]. Products designed for long life or for

outdoors start with high levels of stabilisers that reduce over time. It has been shown that processed and recycled products degrade more when reprocessed because oxidation products auto-accelerate the degradation rate [169, 170, 172, 173]. Repeated reprocessing and ageing cycles caused a significant decrease in properties after each aging cycle that recovered significantly when the material was reprocessed [174]. Thermal processing aged the entire material to a certain extent each cycle. Weathering and thermal aging degraded only the surface layer of the polymer, which severely effected the test film properties [175, 176]. On reprocessing the material became homogenous and the properties were restored. Embrittlement studies have been usually based on thin wall products that are microns thick film, ~1 mm thick injection mouldings [170, 172, 173, 177]. These are relevant to reprocessing of those types of products into similar products. The use of proprietary stabilization packages have be shown to satisfactorily stabilise the material for use in the same article [172, 173, 178].

Plastic lumber is 25-140 mm thick. Section 5.2 discussed ~10 year studies that showed no surface cracking, crazing, embrittlement or substantial loss in mechanical properties. Full profile testing studies are recommended to compare product with and without stabilisers in harsher climates, longer tests and thermal aging trials to optimize performance to meet the long lifetime requirement.

6.5   Weathering

All weathering trials to date have been conducted outdoors in a Northern European Climate for under 10 years. More extensive trials are required to demonstrate suitability for extended lifetimes and sunnier climates. Weathering is a complex process. The relative durability of plastics can be very different depending on the weathering location, time of year, time of wetness, temperature, pollutants, biological attack and year-to-year climatological variations [179].

Many standards and studies favour testing in specialised laboratory chambers for reproducibility and the ability to accelerate testing. The disadvantage is that they cannot fully mimic nature, and the equipment is expensive to buy, operate or rent. There are a wide range of technologies that use different light sources - xenon arc [180], fluorescent UV [181] and carbon arc [182]. The light sources each mimic a portion of the solar spectrum, see Figure 6.1. Fluorescent ultraviolet emits in the 295-400nm range, which is the most damaging region of the spectrum for polymers, and is suited for investigating change in mechanical properties. Xenon arc is most suited to investigating colour change, because pigments and dyes can be severely effected by longer UV and visible [179].
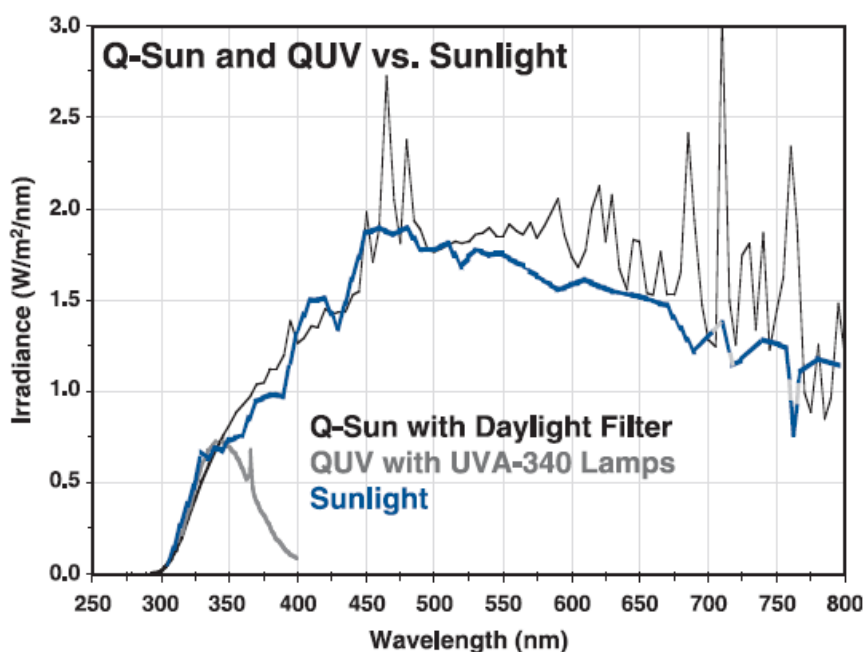
Figure 6.1 Comparison of spectra from Xenon Arc (Q-Sun), Fluorescent UV (QUV) and natural sunlight [179].

Different degradation mechanisms are triggered depending on the light source, temperature, moisture, periods of darkness, etc., see Figure 6.2. Some exposure schemes increase the temperature to accelerate testing. For example, a 10 ^{o}C increase in temperature can double the rate of photo-initated degradation [183]. However, increasing the temperature can trigger thermal degradation mechanisms not seen in outdoor conditions [184]. Moisture affects the rate and type of degradation by a variety of mechanisms [179, 185, 186]. Dissolved oxygen in the water promotes oxidation of the surface. Rain

can produce thermal shock on a hot surface, and expose new material by eroding the top surface. Dew can remain on a surface for many hours each day producing high moisture absorption, which may dissolve soluble additives. Relative humidity changes the speed at which a surface dries and can cause physical stress where the material is trying to equilibrate with changes in humidity. Periods of darkness are stipulated in some test regimes, though most regimes eliminate dark periods to accelerate testing. ISO 4892-1 states that critical dark reactions may be then eliminated [184]. Dark periods are important for thermally driven reactions to "catch up" or for diffusion limited reactions to transport chemical species to the surface to continue the photochemical reactions [187].
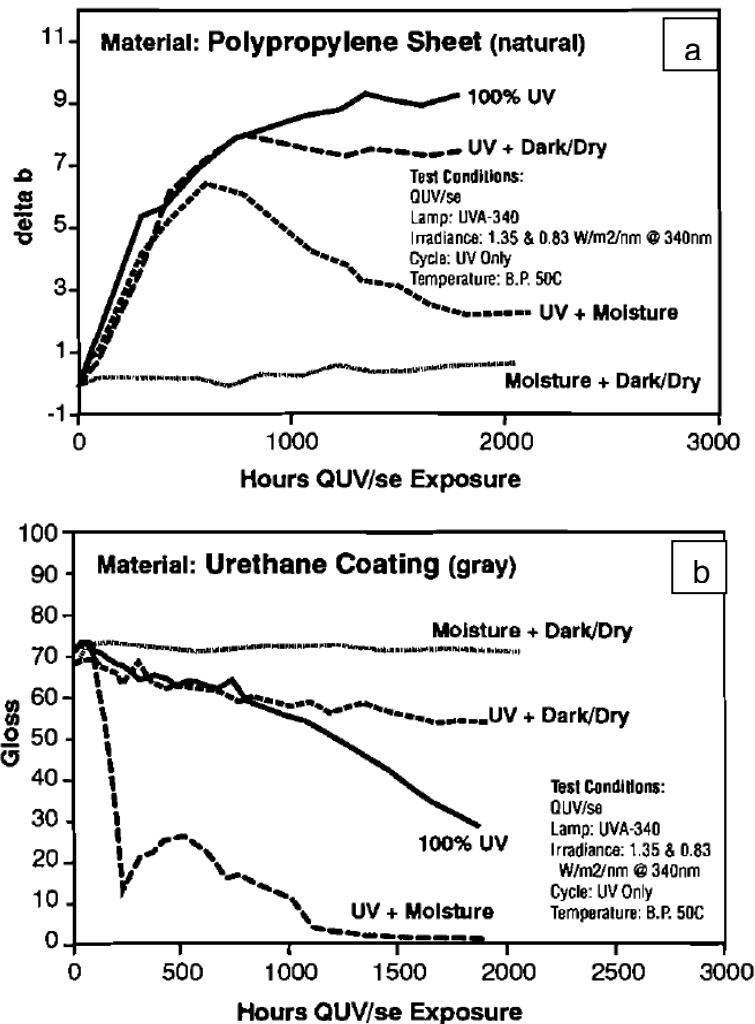

Figure 6.2 Degradation in different regimes of UV, moisture and dark of (a) PP by yellowing and (b) urethane by gloss reduction. QUVA-340 lamp, irradiance 1.35 and 0.83 W/m^2/nm @340 nm, temperature 50 ^{o}C [186].

The standards clearly state that the different tests are not comparable and can only be used to rank materials [184]. Network Rail requested a laboratory test, so that different types of sleeper could be compared. Testing was never carried out. Trials had also been planned to complete harsh outdoor testing at large specialist test sites in Florida and Arizona. It is recommended that longer and harsher natural weathering trials are conducted to confirm the required lifetimes claims. In addition, laboratory testing should be completed to obtain a satisfactory comparison.

6.6 Fatigue Properties at Low Temperature

The catastrophic nature of the failure mechanism was one major concern about the use of plastic lumber for structural applications. In flexural and fatigue testing failure was abrupt with no warning signs. Warning cracks and other signs of stress are usually visible in other structural materials such as wood and metal. The transition from ductile crack propagation to catastrophic brittle failure was observed during flex testing, notched impact testing and testing at cold temperatures.

Notched sample tests are a very severe type of fracture toughness test, because the notch concentrates the stress. To evaluate fracture toughness, it is better to use test conditions similar to those in use, because toughness is not a fundamental material property [153]. The fracture process is very complex and is strongly dependent on specimen geometry, test type, test speed and also processing technique, morphology, and residual stress. Therefore, results are difficult to correlate from different tests or to use to predict final performance. For example, Charpy and Izod tests use a highly oriented sample, which is broken in its strongest direction, however, falling weight tests usually use sheet material, which breaks in its weakest direction. Different tests describe different aspects of a material's performance, hence using a range of tests is recommended [153].

Toughness can be improved by optimising crystalline morphology, by incorporating a discrete rubbery phase or by adding reinforcement such as fibres [153]. For immiscible polymer blends, the use of compatibilisers has already been discussed in Section 6.3.

In morphology studies, increased crystallinity has been found to reduce impact strength above and below the T_g, and that impact resistance is inversely related to spherulite size [49, 153]. The sleeper profile had a very large cross-section, which cooled very slowly, producing high crystallinity and large spherulite size. A previous study attributed the brittleness of slow-cooled PP to segregation of impurities and void formation at spherulitic boundaries [188].

The formulations used in this study contained a significant proportion of polypropylene, whereas most plastic lumber products are almost completely polyethylene. Polyethylene has a very low glass transition temperature ~ -70 °C. However, the maximum operating temperature under load is within ambient temperature range [27]. Polypropylene has a higher maximum operating temperature, whereas, it has a Ductile to Brittle Transition (DBTT) between 0 and 20 °C. This is increased when notched to 100 °C unless suitable copolymers are used [153]. The addition of glass fibre is one potential area for investigation. Increasing fibre length and concentration of glass fibre mats in PP have been shown to increase impact and virtually eliminate the ductile to brittle transition in the range -50 to 40 °C [189].

Understanding the ductile to brittle transition and its suppression particularly at cold temperatures will be an important safety factor in the acceptance for certain applications. Though the polymer reinforced sleeper passed the fatigue test at 250 kN for softwood sleeper replacement. The failure mechanism at 260 kN was judged unsatisfactory. The safety margin was increased by using glass fibre reinforcement, however, this solution was deemed uneconomic for softwood replacement whilst using the current manufacturing technique. The decision was made without taking into consideration the benefits of longer durability and lower maintenance over the decades in service.

6.7 Creep Properties

Creep is the permanent deformation resulting from prolonged application of stress below the elastic limit [190]. For structural applications, creep is a major consideration when using viscoelastic polymers instead of traditional construction materials. Polymers have a far higher tendency to creep and their complex behaviour is very sensitive to the actual application. The excessive deformation caused by creep is often the limiting factor when deciding the maximum working stress [134]. Creep is dependent on polymer, morphology, time, temperature, environment, mode of loading and level of stress. The wide variation of recycled material makes creep more complex, for example, the properties of recycled pilings were found to vary by manufacturer, waste stream composition and production season [191, 192].
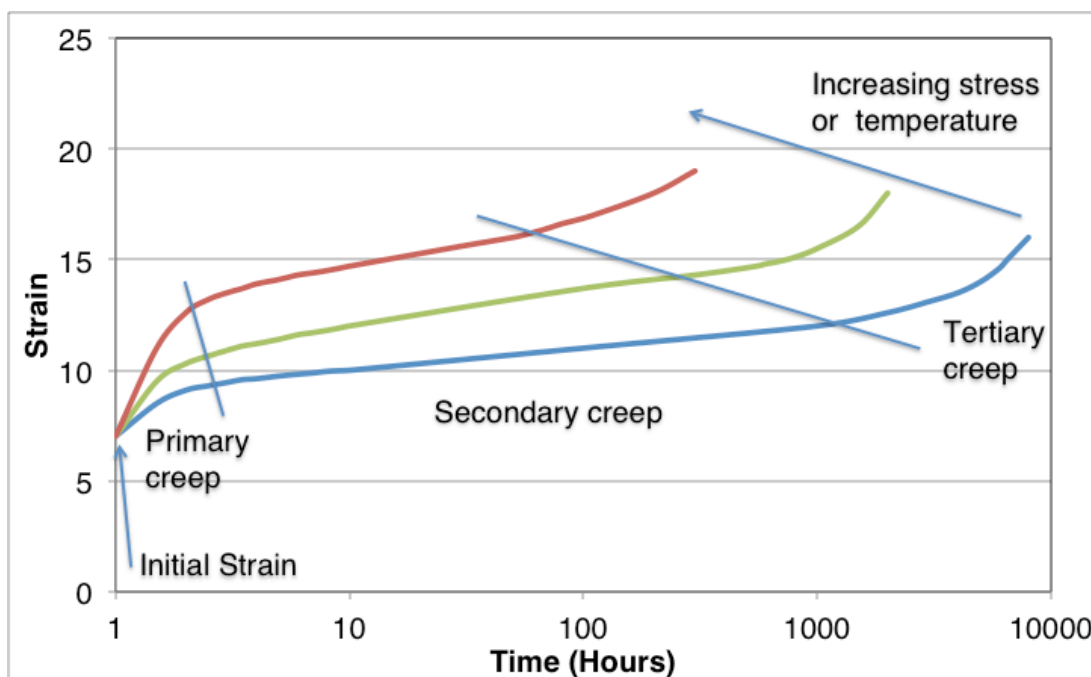
Figure 6.3 The stages of the creep life cycle and the effect of increasing stress or temperature on the creep curve [190].

During a creep test there are three key stages as shown in Figure 2.3 [190]. The gradient of the curve is the strain rate. The sample deforms elastically giving the initial strain immediately the load is applied. In the primary creep region the strain rate decreases. The strain rates settles to a constant amount in the secondary creep region. Finally the strain rate increases until fracture in

the tertiary creep stage. The transition of tertiary creep ends the serviceable life of a component.

Semi-crystalline polymers are more creep resistant, because increasing crystallinity hinders molecular movement. Other factors that hinder movement are high molecular weight, chemical sidegroups, molecular branching, increasing crystallinity, certain additives and reinforcement [190]. Even though polyolefins are semicrystalline, they have the disadvantage that softening and reduction of load bearing properties can significantly decrease within ambient temperatures. In one study, low creep polystyrene was blended with high creep HDPE. Their blends were found to have better creep resistance than individual components, though the effect was non linear [193].

Fibre reinforcement improves creep resistance. It hinders molecular movement and changes the deformation processes [190]. Under creep load, the fibre reinforced segments straighten, which requires simultaneous creep of the matrix. Then highly stressed regions of matrix creep, which transfers the stress from fibre to fibre. The interface between the matrix and the fibre gradually ruptures, causing slip between areas. Finally the fibres break.

Long term testing is expensive and takes years, hence is often not practical. Particularly as standards such as ASTM D5262 only allows extrapolation of data by one log cycle (e.g. from 10,000 to 100,000 hrs) [194]. Many researchers have used different approaches to predict long term tensile creep behaviour in different materials. There are far fewer studies in compression creep. Two common approaches are thermal methods and energy methods [195]. In thermal methods, time is effectively accelerated by increasing the temperature, e.g. Time Temperature Superposition (TTS) and its derivative Stepped Isothermal Method (SIM). Curves from different test temperatures are stitched together to predict the lifetime at the operating temperature. The technique can only accelerate time by a factor in the order of 33 for HDPE, because the mechanical properties of polymers change with temperature [196, 197]. Energy Methods use the principal of energy equivalence between tests at different

strain rates e.g. the strain energy density method. Long term, static creep behaviour is predicted by extrapolating the results from tests at different strain rates [148, 198].

Dead load compressive creep studies were carried out as part of this project. Polymer blend and glass reinforced samples were tested at different stress levels. Financial restrictions prevented complete refurbishment of the test rigs prior to testing. Stability issues with the logging equipment and fundamental design errors in the position sensing system created errors that were out of range in the resulting data.

Refurbishment of the creep rigs would enable a new set of testing to be completed. Long term, compressive creep data for recycled polymers and blends is scarce. Such data could be used to calibrate predictive models, that could predict properties in 50-100 years. Such data is important for the adoption of recycled polymer railway sleepers in bridge applications and switch and crossing bearers. Railway ballast bed can move over time sections of sleepers and bearers can become unsupported.

6.8 Replacement of Hardwood Sleepers

The composite sleeper was approved for track trial to replace softwood sleepers, however, sleepers were never put into track. The steep rise in recycled plastic prices made it uneconomic to replace cheap, softwood sleepers in the current rail market, which is driven by initial purchase cost not whole life cost.

The development of a product to replace softwood sleepers was always seen as a first proving stage in a conservative industry. The actual aim was replacement of hardwood sleepers, bridge timbers and, switch and crossing bearers. It is very expensive and difficult to source sustainably grown, good quality, hardwood timbers of lengths up to 8.4 m and cross-sections up to 300x150 mm. Replacement of hardwood timbers is economically much more advantageous [19]. The glass reinforced sleeper actually passed the fatigue life

requirement for hardwood sleepers. Discussions had started to define a specification for hardwood sleepers when the project ended.

Hardwood timbers are used for their longer service life, greater density, better dimensional stability and resistance to twist, warping and bowing. The higher density (up to 1300 kg/m^3) makes hardwood timbers suitable for use in Continuous Welded Rail (CWR), where sleeper weight is a key element in the control of rail buckling due to high compression forces in the rail during hot weather. Ballast shoulders resist horizontal movements and deflections, with sleeper weight being key in resisting vertical deflections. With the longer lengths of timbers used in Switch and Crossing layouts (up to 6 metres) twist, warp and bow are more likely to occur, and these cause problems in the maintenance of the rail levels across the layout. Composite sleepers should be far more dimensionally stable. The loads are no greater per track, however, multiple tracks are attached to one switch bearer, which can be simultaneously loaded. Hardwood timbers tend to be bespoke sizes depending upon the project. They can be cut to size, shaped and sections cut out if required during installation. It is possible to use standard woodworking techniques with composite sleepers, though it would need to proven that the structural integrity of a composite sleeper would not be affected by such actions. Bridge timbers would be a very good application to replace hardwood timbers. Bridge timbers lie parallel to the rails and are fully supported in metal channels, where water can be retained for long periods of time. Long term immersion in water reduces the lifetime of the timbers. Large numbers of timbers are required for a bridge, however, many bridges have unique size requirements. It is a major and expensive project to replace bridge timbers. Developing, qualifying and manufacturing composite sleepers to replace hardwood timbers would need to be for a specific project. Extensive work would be required to prove batch-to-batch consistency, the manufacturing technique and the robustness of the formulation. The rewards for the manufacturer, the rail company and the environment would be worth the investment.

7 Conclusions and Further Work

7.1 Conclusions

– An amorphous, phase separated semicrystalline polymer blend was developed using recycled plastic waste streams. The blend passed fatigue testing equivalent to >20 years service of softwood sleepers on secondary track.

– Blending recycled glass fibre with polyoefin waste streams significantly improved strength, stiffness, co-efficient of thermal expansion and maximum operating temperature. The optimised blend demonstrated improved fatigue performance equivalent to 20 years service of hardwood sleepers on mainline track.

– Railway sleepers 2600x250x130 mm in size, were produced by intrusion moulding. Blends passed a rigorous, Network Rail specification that covered 18 material, product and system tests, and is currently being implemented as the technical information for a new ISO standard for plastic railway sleepers.   The specification was developed as part of the project. Glass reinforced sleepers were the first recycled plastic composite sleepers approved for track trial by Network Rail.

– A synergistic enhancement of tensile strength was obtained using glass fibre in combination with mica, because mica enhanced the matrix, arrested the polymer chain mobility, and complemented the forces constricting the glass fibre.

– Measured flexural and compressive properties were significantly affected by the compounding method, sample production technique, sample size, and test methods.

– Testing of recycled plastic profiles requires large sample sizes from a high number of production runs for accurate values and valid quality control. For the same formulation, high batch-to-batch variation was measured due to changes in the waste stream type and quality. The profile cross-sections had a wide range of wall thicknesses, foamed area, and bubble size and distribution. Wall thickness significantly affected mechanical properties.

– In intrusion moulded profiles, the achieved strength value was significantly below predicted values because ductile crack growth was initiated at inclusions and other weak points. The crack grew to a critical size, and then high strain rate, brittle fracture occurred. The size of the ductile crack area depended on the formulation, profile size and orientation, strain rate and location of the flaw.

– British Board of Agrément approved the polymer reinforced blend in the first polymer crib earth retaining wall system.

7.2   Further Work

– Studying the effect of size, shape and distribution of contaminants could produce design and quality guidelines that increase the strength and consistency of results.

– Optimising compounding parameters, especially when mixing more than three polymers in order to achieve the demanding engineering standards of structural components. Improved mixing may allow addition of cheaper, lower melt polymers.

– Evaluating the use of compatibilisers would show if the benefits of consistency and potentially improved properties would outweigh the extra cost in this complex blend.

– Full product testing studies are recommended to compare product with and without stabilisers in harsher climates, longer tests and thermal aging trials to optimize performance to meet the long lifetime requirement.

– Longer and harsher natural weathering trials would confirm the required lifetimes claims. In addition, laboratory testing should be completed to obtain a satisfactory comparison to satisfy Network Rail's requirement of a comparative laboratory weathering test.

– Understanding the ductile to brittle transition and its suppression particularly at cold temperatures will be an important safety factor in the acceptance for certain applications. Fatigue testing at low temperature would confirm this.

- Long term, compressive creep data for recycled polymers and blends could be used to calibrate predictive models, that could predict properties in 50-100 years. Such data is important for the adoption of recycled polymer railway sleepers in bridge applications and switch and crossing bearers.

- Developing, qualifying and manufacturing composite sleepers to replace hardwood timbers e.g. bridge timbers. Extensive work would be required to prove batch-to-batch consistency, the manufacturing technique and the robustness of the formulation. The rewards for the manufacturer, the rail company and the environment would be worth the investment.

Appendix 1 – Calculation of Deflection for Four Point Flexure

During the four point bend test, the standards require the deflection to be measured at the midpoint of the beam. During testing the deflection at the loading points was measured. It is possible to calculate the deflection at the midpoint from the deflection at the loading points by using standard formulae [135]. The following symbols are used in the calculations.

E = modulus of elasticity of the material

I = moment of inertia of the cross-section of the beam

Z = section modulus of the cross-section of the beam

b = width of the beam

h = depth of the beam

L = span = distance between the beam supports

a = distance between support and loading point

W = load on beam
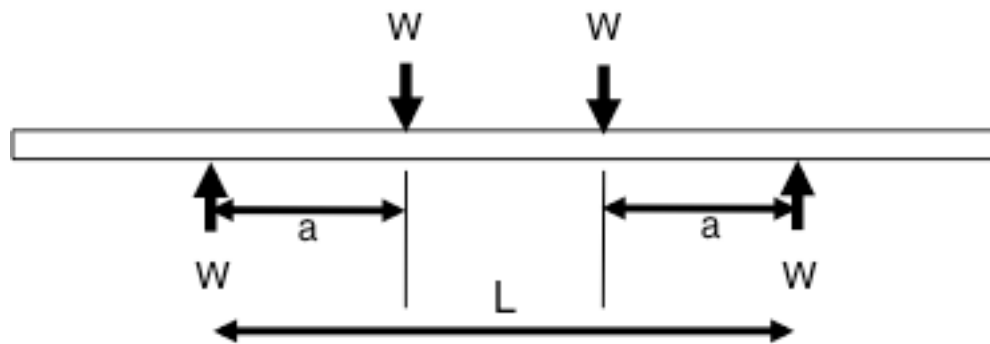
1. Beam supported at both ends, two symmetrical loads

Distance between support and loading point, $a = \dfrac{L}{3}$ (1)

The deflection equations are:

Deflection at each load $= \dfrac{Wa^2}{6EI}(3L - 4a)$ $\qquad$ (2)

Maximum deflection at centre $= \dfrac{Wa}{24EI}(3L^2 - 4a^2)$ $\qquad$ (3)

The deflection at each load can be calculated by substitution of equation 1 into equation 2.

Deflection at each load $= \dfrac{5\,WL^3}{6\,EI(3)^3} = \dfrac{20}{24}\dfrac{WL^3}{EI(3)^3}$ $\qquad$ (4)

Maximum deflection at the centre in terms of the deflection at each load can be calculated by substitution into equation 3 of equation 1 then equation 4.

Maximum deflection at centre $= \dfrac{23}{24}\dfrac{WL^3}{EI(3)^3}$

$\qquad\qquad\qquad\qquad\qquad = \dfrac{23}{20}$ Deflection at each load

$\qquad\qquad\qquad\qquad\qquad = 1.15$ Deflection at each load $\qquad$ (5)

References

[1]   British Standards Institute, *BS EN ISO 75-1:2004 Plastics — Determination of temperature of deflection under load — Part 1: General test method.* British Standards Institute, 2004.

[2]   ASTM International, "ASTM D648-07 Standard Test Method for Deflection of Plastics under Flexural Load in the Edgewise Position," in *ASTM Volume 08.01 Plastics (I)*, ASTM International, 2007.

[3]   Department of Business Innovation & Skills, "Environmental regulations," *www.gov.uk/environmental-regulations*, 2014. [Online]. Available: https://www.gov.uk/environmental-regulations.

[4]   European Parliament - Council of the European Union, *Directive 2012/19/EU of the European Parliament and of the Council of 4 July 2012 on waste electrical and electronic equipment (WEEE) Text with EEA relevance.* EU, 2012.

[5]   British Plastics Federation, "Plastics Recycling," *www.bpf.co.uk/sustainability/plastics_recycling.aspx*, 2014. [Online]. Available: http://www.bpf.co.uk/sustainability/plastics_recycling.aspx.

[6]   Platts, "Asian Polymers Overview," *www.platts.com*, 2014. [Online]. Available: http://www.platts.com/news-feature/2013/petrochemicals/asia-polymers/hdpeldpe.

[7]   D. Snallfot, I. Leisner, M. Skovgaard, and A. Warberg Larsen, "Action 4.1 Market for Plastics recycling," 2013.

[8]   RECOUP, "UK Household Plastics Collection Survey 2013," Peterborough, 2013.

[9]   British Standards Institute, *PAS 141:2011 Reuse of used and waste electrical and electronic equipment (UEEE and WEEE). Process management. Specification.* 2011.

[10] European Parliament - Council of the European Union, *European Parliament and Council Directive 94/62/EC of 20 December 1994 on packaging and packaging waste*. EU, 1994.

[11] European Parliament - Council of the European Union, *Directive 2000/53/EC of the European Parliament and of the Council of 18 September 2000 on end-of life vehicles - Commission Statements*. 2000.

[12] Valpak, "Packflow 2017 Final Report," 2012.

[13] Environmental Services Association, "Overseas options: the importance of exports to UK recycling," London, 2012.

[14] WRAP, "Collection and Sorting of Household Rigid Plastic Packaging," 2012.

[15] DEFRA, "Packaging waste - producer responsibility regimes," *GOV.UK website Department for Environment, Food & Rural Affairs*, 2014. [Online]. Available: https://www.gov.uk/government/policies/reducing-and-managing-waste/supporting-pages/packaging-waste-producer-responsibility-regimes.

[16] RAPRA and ARBURG, *ARBURG Practical guide to injection Moulding*. Rapra Technology.

[17] P. Cross, "Personal correspondence." 2011.

[18] G. van Erp and M. McKay, "Recent Australian Developments in Fibre Composite Railway Sleepers," *Electron. J. Struct. Eng.*, vol. 13, no. 1, pp. 62–66, 2013.

[19] P. Squire, "Personal communication with Railway Consultant." 2011.

[20] BBA, "Ecocrib Retaining Walls 12/H194," 2012.

[21] L. A. Utracki, *Polymer Blends handbook*. Dordrecht: Kluwer Academic Publishers, 2003.

[22] J. Brydson, *Plastics Materials*, 7th ed. Oxford: Butterworth-Heinemann, 2000.

[23] C. Bainbridge, "NOVEL HIGH ADDED VALUE MATERIALS FROM MIXED POST-CONSUMER POLYMER WASTE," Manchester Metropolitan University, 2013.

[24] Open University, "Introduction to Polymers," *Open University*, 2014. [Online]. Available: http://www.open.edu/openlearn/science-maths-technology/science/chemistry/introduction-polymers/content-section-5.6.1. [Accessed: 09-Apr-2014].

[25] C. Maier and T. Calafut, *Polypropylene - The Definitive User's Guide and Databook*. William Andrew Publishing/Plastics Design Library, 1998.

[26] G. Erhard, *Designing with Plastics*. Cincinnati: Hanser Gardner Publications, 2006.

[27] United Laboratories, "Polyethylene (PE) Typical Generic HDPE," *UL IDES Prospector website*, 2014. [Online]. Available: http://plastics.ides.com/generics/27/c/t/polyethylene-pe-properties-processing/sp/5.

[28] United Laboratories, "Polyethylene (PE) Typical Properties Generic LLDPE," *UL IDES Prospector website*, 2014. [Online]. Available: http://plastics.ides.com/generics/27/c/t/polyethylene-pe-properties-processing/sp/14.

[29] British Standards Institute, *BS EN ISO 1183-1:2012 Plastics. Methods for determining the density of non-cellular plastics. Immersion method, liquid pyknometer method and titration method*. British Standards Institute, 2013.

[30] British Standards Institute, *BS EN ISO 1133:2005 Plastics — Determination of the melt mass-flow rate (MFR) and the melt volume-flow rate (MVR) of thermoplastics*. British Standards Institute, 2005.

[31]   British Standards Institute, *BS EN ISO 294-4:2003 Plastics. Injection moulding of test specimens of thermoplastic materials. Determination of moulding shrinkage.* 2003.

[32]   British Standards Institute, *BS EN ISO 527-2: 1996 Plastics — Determination of tensile properties — Part 2: Test conditions for moulding and extrusion plastics.* British Standards Institute, 1996.

[33]   British Standards Institute, *BS EN ISO 180:2000+A2:2013 Plastics. Determination of Izod impact strength.* British Standards Institute, 2000.

[34]   British Standards Institute, *BS EN ISO 306:2004 Plastics — Thermoplastic materials — Determination of Vicat softening temperature (VST).* British Standards Institute, 2004.

[35]   British Standards Institute, *BS ISO 974:2000 Plastics. Determination of the brittleness temperature by impact.* British Standards Institute, 2000.

[36]   ASTM International, "ASTM D150-11 Standard Test Methods for AC Loss Characteristics and Permittivity (Dielectric Constant) of Solid Electrical Insulation," in *ASTM Volume 10.01 Electrical Insulation (I)*, ASTM International, 2011.

[37]   R. Marsh and A. Griffiths, "Thermal degradation of polyethylene film materials due to successive recycling," *Proc. …*, vol. 220, pp. 1099–1108, 2006.

[38]   F. La Mantia, *Handbook of Plastics Recycling,* 1st ed. Shrewsbury: Rapra Technology, 2002.

[39]   M. G. R. D.V. Rosato, *Plastics Design Handbook.* Kluwer Academic Publishers, 2001.

[40]   SABIC, "Sabic datasheets," *www.plastics.sabic.eu*, 2014. [Online]. Available: wwww.plastics.sabic.eu.

[41]   British Standards Institute, *BS EN ISO 179-1:2001 Plastics —
        Determination of Charpy impact properties — Part 1: Non-instrumented
        impact test*, no. 2001. British Standards Institute, 2001.

[42]   M. Chanda and S. K. Roy, *Plastics Technology Handbook*, 4th ed. Taylor
        & Francis, 2007.

[43]   United Laboratories, "Styrolution PS 124N/L," *UL IDES Prospector
        website*, 2014. [Online]. Available: hwww.styrolution.com.

[44]   United Laboratories, "Stytrolution PS 454N," *UL IDES Prospector website*,
        2014. [Online]. Available: www.styrolution.com.

[45]   Z. Bartczak, A. Galeski, and M. Pracella, "Spherulite nucleation in blends
        of isotactic polypropylne with high density polythylene," *Polymer (Guildf).*,
        vol. 27, pp. 537–543, 1986.

[46]   Z. Bartczak, A. Galeski, and N. P. Krasinokova, "Primary nucleation and
        spherulite growth rate in isotactic polypropylene-polystyrene blends,"
        Polymer (Guildf)., vol. 28, no. September, pp. 1627–1634, 1987.

[47]   T. Xu, H. Lei, and C. Xie, "The research on aggregation structure of PP
        materials under different condition and the influence on mechanical
        properties," *Mater. Des.*, vol. 23, pp. 709–715, 2002.

[48]   D. Mileva, Q. Zia, and R. Androsch, "Tensile properties of random
        copolymers of propylene with ethylene and 1-butene: effect of crystallinity
        and crystal habit," *Polym. Bull.*, vol. 65, pp. 623–634, 2010.

[49]   D. Wright, R. Dunk, D. Bouvart, and M. Autran, "The effect of crystallinity
        on the properties of injection moulded polypropylene and polyacetal,"
        Polymer (Guildf)., vol. 29, p. 793, 1988.

[50]   R. Greco, G. Mucciariello, E. Ragosta, and E. Martuscelli, "Properties of
        polyethylene-polypropylene blends Part 1 Thermal swelling and

mechanical characterization of extruded unoriented specimens," *J. Mater. Sci.*, vol. 15, pp. 845–853, 1980.

[51]   S. Jose, A. S. Aprem, B. Francis, M. C. Chandy, P. Werner, V. Alstaedt, and S. Thomas, "Phase morphology, crystallisation behaviour and mechanical properties of isotactic polypropylene/ high density polyethylene blends," *Eur. Polym. J.*, no. 40, pp. 2105–2115, 2004.

[52]   H. P. Blom, J. W. Teh, and A. Rudin, "PP/PE Blends. IV. Characterization and Compatibilization of Blends of Postconsumer Resin with Virgin PP and HDPE," *J. Appl. Polym. Sci.*, vol. 70, pp. 2081–2095, 1998.

[53]   H. P. Blom, J. W. Teh, and A. Rudin, "i-PP/HDPE Blends. 111. Characterization and Compatibilization at Lower i-PP Contents," *J. Appl. Polym. Sci.*, vol. 61, pp. 959–968, 1996.

[54]   British Standards Institute, *BS EN ISO 527-1:1996 Plastics — Determination of tensile properties — Part 1: General principles*. British Standards Institute, 1996.

[55]   R. E. Robertson and D. R. Paul, "Stress–strain behavior of polyolefin blends," *J. Appl. Polym. Sci.*, no. 17, pp. 2579–2595, 1973.

[56]   R. K. Gupta, E. Kennel, and K.-L. Kim, *Polymer Nanocomposites Handbook*. CRC Press, 2010.

[57]   Z. Bartczak and A. Galeski, "Changes in interface shape during crystallization in two-component polymer systems," *Polymer (Guildf).*, vol. 27, no. April, pp. 544–548, 1986.

[58]   M. Xanthos, S. K. Dey, S. Mitra, U. Yilmazer, and C. Feng, "Prototypes for Building Applications Based on Thermoplastic Composites Containing Mixed Waste Plastics," *Polym. Compos.*, vol. 23, no. April, pp. 153–163, 2002.

[59] N. Tzankova Dintcheva, F. P. La Mantia, F. Trotta, M. P. Luda, G. Camino, M. Paci, L. Di Maio, and D. Acierno, "Effects of filler type and processing apparatus on the properties of the recycled 'light fraction' from muncipal post-consumer plastics," *Polym. Adv. Technol.*, vol. 12, pp. 552–560, 2001.

[60] T. J. Nosker and R. W. Renfree, "The Evolution of Recycled Plastic Lumber into Structural Applications," in *AMCA Technical Conference 1999 - Session 7 Advancements in the Structural Design of Plastic Lumber Applications*, 1999.

[61] J. K. Lynch, T. J. Nosker, and R. W. Renfree, *Polystyrene/Polyethylene Composite Structural Materials Volume 1: Railroad Crossties and their Properties*. Fredericksburg: Sheridan Books for AMIPP, Rutger's University, 2002.

[62] W. Viratyaporn, R. L. Lehman, and J. Joshi, "Impact Resistance of Selected Immiscible Polymer Blends," in *Society of Plastic Engineers (SPE) Annual Technical Conference Proceedings*, 2007.

[63] J. Joshi, R. Lehman, and T. Nosker, "Selected Physical Characteristics of Polystyrene/High Density Polyethylene Composites Prepared from Virgin and Recycled Materials," *J. Appl. Polym. Sci.*, vol. 99, pp. 2044–2051, 2006.

[64] R. W. Renfree, T. J. Nosker, D. R. Morrow, K. Van Ness, and E., "Physical Characteristics of the Dual Phase Region in Mixtures of Recycled Polystyrene/Curbside Tailings Materials," *AMIPP Compos. Cent. Rutgers Univ.*, 1994.

[65] G. M. Jordhamo, J. A. Manson, and L. H. Sperling, "Phase Continuity and Inversion in Polymer Blends and Simultaneous Interpenetrating Networks," *Polym. Eng. Sci.*, vol. 28, no. 8, pp. 517–524, 1986.

[66] J. Joshi, R. L. Lehman, and T. J. Nosker, "Mechanical grafting and morphology characterization in immiscible polymer blends," *Proc. Mater. Res. Soc.*, no. December, 2004.

[67] T. Nosker, R. Renfree, and J. Kerstein, "Use of Recycled Plastics for Preparing High Preformance Composite Railroad Ties," EP 1 151 038 B11999.

[68] D. R. Morrow, T. J. Nosker, K. E. Van Ness, and R. W. Renfree, "US5298214 Method of Deriving Polystyrene and Polyolefin Plastics Composite from recycled plastics," 52982141990.

[69] A.-M. Hugo, L. Scelsi, A. Hodzic, F. R. Jones, and R. Dwyer-Joyce, "Development of recycled polymer composites for structural applications," *Plast. Rubber Compos.*, vol. 40, no. 6/7, p. 317, 2011.

[70] M. Tolinski, *Additives for Polyolefins Getting the Most out of Polypropylene, Polyethylene and TPO*. William Andrew Publishing/Plastics Design Library, 2009.

[71] Technology Plastics OMYA AG, "Review technical information plastics R4-04 omyalene 102 M in PO pipes," 2003.

[72] G. Pritchard, "Plastics Additives - A RAPRA Market Report," Shrewsbury, 2005.

[73] G. Pritchard, *Plastic Additives - An A-Z reference*. London: Chapman & Hall, 1998.

[74] J. Hartikainen, P. Hine, J. S. Szabo, M. Lindner, T. Harmia, R. A. Duckett, and K. Friedrich, "Polypropylene hybrid composites reinforced with long glass fibres and particulate filler," *Compos. Sci. Technolology*, vol. 65, pp. 257–267, 2005.

[75]   R. Zhao, J. Huang, B. Sun, and G. Dai, "Study of the Mechanical
         Properties of Mica-Filled Polypropylene-Based GMT Composite," *J. Appl.
         Polym. Sci.*, vol. 82, pp. 2719–2728, 2001.

[76]   L. Scelsi, A. Hodzic, C. Soutis, S. A. Hayes, S. Rajendran, M. A.
         AlMa'adeed, and R. Kahraman, "A review on composite materials based
         on recycled thermoplastics and glass fibres," *Plast. Rubber Compos.*, vol.
         40, no. 1, pp. 1–10, 2011.

[77]   L. A. Hollingbery, C. C. Briggs, R. C. Day, M. Gilbert, L. S. Tan, and L. S.
         Wan, "MICA IN GLASS FIBRE FILLED THERMOPLASTICS," in
         Eurofillers '97, 1997.

[78]   L. A. Canova, L. W. Ferguson, L. M. Parrinello, R. Subramanian, and H. F.
         Giles, "Effect of combinations of fibre glass and mica on the physical
         properties and dimensional stability of injection molded polypropylene
         composites," in *Antec '97*, 1997, pp. 2112–2116.

[79]   A. K. Nurdina, M. Mariatti, and P. Samayamutthirian, "Effect of Single-
         Mineral Filler and Hybrid-Mineral Filler Additives on the Properties of
         Polypropylene Composites," *J. Vinyl Addit. Technol.*, vol. 15, pp. 20–28,
         2009.

[80]   G. Wypych, *Handbook of Fillers*, 2nd ed. William Andrew
         Publishing/Plastics Design Library, 2000.

[81]   H. W. Sullivan and W. A. Mack, "US5886078 Polymeric Compositions and
         Methods for making Construction Materials from them," 58860781996.

[82]   K. Riggs Larsen, "Thermoplastic Timber Is Constructed of Recycled Milk
         Jugs and Automobile Bumpers," *Mater. Perform.*, vol. January, no. 22–27,
         2010.

[83]   T. J. Nosker and R. W. Renfree, "WO98/08896 Composite Building
         Materials from Recyclate Waste," WO98/088961996.

[84] R. W. Renfree, "WO2006/125111 A1 Use of recycled plastics for structural building forms," WO2006/125111 A12006.

[85] A. K. Banerjie, "WO92/20733 Construction material obtained from Recycled Polyolefins containing other polymers," WO92/207331991.

[86] J. D. Muzzy, "US2003/0087973 A1 Fiber-reinforced recycled thermoplastic composite and method," US2003/0087973 A12002.

[87] T. E. Phillips and P. Krishmaswamy, "US6497956 Structural Recycled Plastic Lumber," US64979562001.

[88] United Laboratories, "UL 94 Flame Rating," *UL IDES Prospector website*, 2014. [Online]. Available: http://www.ides.com/property_descriptions/UL94.asp.

[89] British Standards Institute, *BS EN ISO 178:2003 Plastics - Determination of flexural properties*. British Standards Institute, 2003.

[90] P. J. Bates and C. Y. Wang, "The Effect of Sample Preparation on the Mechanical Properties of Nylon 66," *Polym. Eng. Sci.*, vol. 43, no. 4, pp. 759–773, 2003.

[91] ASTM International, "ASTM D790–03 Standard Test Methods for Flexural Properties of Unreinforced and Reinforced Plastics and Electrical Insulating Materials," in *ASTM Volume 08.01 Plastics (I)*, ASTM International, 2003.

[92] British Standards Institute, *BS EN ISO 3167:2003 Plastics — Multipurpose test specimens*. British Standards Institute, 2003.

[93] British Standards Institute, *BS EN ISO 604:2003 Plastics — Determination of compressive properties*. British Standards Institute, 2003.

[94] ISO TC 61, "ISO TC 61/SC11N886 ISO_xxxxx Plastics - Plastic Sleepers," 2008.

[95]   ASTM, "D6109-03 Standard Test Methods for Flexural Properties of Unreinforced and Reinforced Plastic Lumber," in *ASTM Volume 08.03 Plastics (III)*, ASTM International, 2003.

[96]   ASTM International, "ASTM D6108–03 Standard Test Method for Compressive Properties of Plastic Lumber and Shapes," in *ASTM Volume 08.03 Plastics (III)*, ASTM International, 2003.

[97]   Z.-L. Ma, J.-G. Gao, H.-J. Niu, H.-T. Ding, and J. Zhang, "Polypropylene– Intumescent Flame-Retardant Composites Based on Meleated Polypropylene as a Coupling Agent," *J. Appl. Polym. Sci.*, vol. 85, pp. 257–262, 2002.

[98]   Z.-L. Ma, J.-G. Gao, and L.-G. Bai, "Studies of Polypropylene– Intumescent Flame-Retardant Composites Based on Etched Polypropylene as a Coupling Agent," *J. Appl. Polym. Sci.*, vol. 92, pp. 1388–1391, 2004.

[99]   Richard Baker Harrison Ltd, "Mica MKT," Ilford, 2005.

[100]   Norwegian Talc AS, "Micro Mica W160," Knarrevik, 2001.

[101]   S. Endoh, Y. Kuga, H. Ohya, C. Ikeda, and H. Iwata, "Shape Estimation of Anisometric Particles Using Size Measurement Techniques," *Part. Part. Syst. Characterisation*, vol. 15, no. June, pp. 145–149, 1998.

[102]   S. Bose and P. A. Mahanwar, "Influence of particle size and particle size distribution on MICA filled nylon 6 composite," *J. Mater. Sci.*, vol. 40, pp. 6423–6428, 2005.

[103]   M. Hiljanen-Vainio, M. Heino, and J. V. Seppala, "Reinforcement of biodegradable poly(ester-urethane) with fillers," *Polymer (Guildf).*, vol. 39, no. 4, pp. 865–872, 1998.

[104]   J. Karger-Kocsis, *Polypropylene: Structure, Blends and Composites: Composites*, 3rd ed. Kluwer Academic Publishers, 1995.

[105] L. Dilandro, A. T. Dibenedetto, and J. Groeger, "The effect of fiber-matrix stress transfer on the strength of fiber-reinforced composite materials," *Polym. Compos.*, vol. 9, no. 3, pp. 209–221, 1988.

[106] H. L. Lee, S. K. Jeoung, H. Y. Hwang, S. G. Lee, and K. Y. Lee, "Empirical study on effects of disk shape filler content and orientation on thermal expansion coefficient of PP composites," *Polym.*, vol. 36, no. 3, pp. 281–286, 2011.

[107] Polypacific PTY Ltd, "Corton PDR 1623 HS," 2015.

[108] Polypacific PTY Ltd, "Polycomp PDR CB 08," 2015.

[109] Ginar Technology Co., "Aplax P1412GN," 2015.

[110] J. A. Nairn and P. Zoller, "Matrix solidification and the resulting residual thermal stresses in composites," *J. Mater. Sci.*, vol. 20, pp. 355–367, 1985.

[111] L. Miles Jackson and T. J. Nosker, "Technology, Applicability, and Future of Thermoplastic Timber," in *Department of Defence Corrosion Conference*, 2009.

[112] D. Robert, *Structural adhesive joints in engineering*. London: Chapman and Hall, 1997.

[113] A. Hayward, *Steel Details' Manual*. Oxford: Wiley-Blackwell, 2002.

[114] NCHRP, "Guidelines for early-opening-to-traffic Portland cement concrete for pavement rehabilitation, NCHRP report no. 540," Washington DC, 2005.

[115] J. L. Thomason, "The influence of fibre length and concentration on the properties of glass fibre reinforced polypropylene. 6. The properties of injection moulded long fibre PP at high fibre content," *Compos. Part A*, vol. 36, pp. 995–1003, 2005.

[116] G. Gow, "Private communcation." J.G.P. Perrite, Warrington, 2009.

[117] R. K. Mittal, V. B. Gupta, and P. K. Sharma, "Theoretical and experimental study of fibre attrition during extrusion of glass fibre reinforced polypropylene," *Compos. Sci. Technolology*, vol. 31, pp. 295–313, 1988.

[118] A. Ayadi, D. Kraiem, C. Bradai, and S. Pimbert, "Recycling effect on mechanical behavior of HDPE/glass fibers at low concentrations," *J. Thermoplast. Compos. Mater.*, vol. 25, no. 5, pp. 523–536, 2011.

[119] J. P. F. Inberg, P. H. Hunse, and R. J. Gaymans, "Long Fibre Reinforcement of Polypropylene/Polystyrene Blends," *Polym. Eng. Sci.*, vol. 39, no. 2, pp. 340–346, 1999.

[120] S. D. George and S. H. Dillman, "Recycled Fiberglass composite as a reinforcing filler in post-consumer recycled HDPE plastic lumber," in *58th ANTEC conference*, 2000, pp. 2919–2921.

[121] X. Liu, A. Boldizar, M. Rigdahl, and H. Bertilsson, "Recycling of Blends of Acrylonitrile–Butadiene–Styrene (ABS) and Polyamide," *J. Appl. Polym. Sci.*, vol. 86, pp. 2535–2543, 2002.

[122] C. H. Tselios, D. Bikaris, P. Savidas, and C. Panayiotou, "Glass-fiber reinforcement of in situ compatibilized polypropylene/polyethylene blends," *J. Mater. Sci.*, vol. 34, pp. 385–394, 1999.

[123] D. Bikiaris, P. Matzinos, J. Prinos, V. Flaris, A. Larena, and C. Panayiotou, "Use of Silanes and Copolymers as Adhesion Promoters in Glass Fiber/Polyethylene Composites," *J. Appl. Polym. Sci.*, vol. 80, pp. 2877–2888, 2001.

[124] J.G.P. Perrite, "Percom Technical Data," *http://www.perrite.com/percomTBL.jpg*, 2014. [Online]. Available: http://www.perrite.com/percomTBL.jpg. [Accessed: 20-Aug-2014].

[125] RTP Company, "RTP 701 Z HDPE GF10%," *www.matweb.com*, 2014. .

[126] RTP Company, "RTP 703 Z HDPE GF20%," *www.matweb.com*, 2014. .

[127] RTP Company, "RTP 701 CC GF10%," *www.matweb.com*, 2014. .

[128] TP Composites, "HiFill HDPE 10%GF," *www.matweb.com*, 2014. .

[129] TP Composites, "HiFill HDPE GF20," *www.matweb.com*, 2014. .

[130] R. C. Hibbeler, *Mechanics of Materials*, 7th ed. Singapore: Prentice Hall, 2008.

[131] S. A. Rodrigues Junior, J. L. Ferracane, and A. Della Bona, "Flexural strength and Weibull analysis of a microhybrid and a nanofill composite evaluated by 3- and 4-point bending tests," *Dent. Mater.*, vol. 24, pp. 426–431, 2008.

[132] British Standards Institute, *BS EN ISO 14125:1998 Fibre-reinforced plastic composites - Determination of flexural properties*. British Standards Institute, 1998.

[133] P. Chitchumnong, S. C. Brooks, and G. D. Stafford, "Comparison of three- and four-point flexural strength testing of denture-base polymers," *Dent. Mater.*, vol. 5, no. January, pp. 2–5, 1989.

[134] ASTM, "D6662-01 Standard Specification for Polyolefin-Based Plastic Lumber Decking Boards," in *ASTM Volume 08.03 Plastics (III)*, ASTM International, 2001.

[135] E. Oberg, F. D. Jones, H. L. Horton, and H. Ryffel, *Machinery's Handbook*, 18th ed. New York: Industrial Press Inc., 2008.

[136] ASTM International, "ASTM D6341-98 Standard Test Method for Determination of the Linear Coefficient of Thermal Expansion of Plastic Lumber and Plastic Lumber Shapes Between -30 and 140oF (-34.4 and

60oC),” in *ASTM Volume 08.03 Plastics (III),* vol. 08, West Conshoshocken: ASTM International, 1998.

[137] S. Boslaugh, *Statistics in a Nutshell.* O'Reilly Media, Inc., 2012.

[138] J. C. Halpin and J. L. Kardos, “The Halpin-Tsai Equations: a review,” *Polym. Eng. Sci.*, vol. 16, no. 5, pp. 344–352, 1976.

[139] N. M. L. Mondadori, R. C. R. Nunes, L. B. Canto, and A. J. Zattera, “Composites of Recycled PET Reinforced with Short Glass Fiber,” *J. Thermoplast. Compos. Mater.*, vol. 25, no. 6, pp. 747–764, 2011.

[140] A. Hodzic, “Design of composites: hybrids, short-fibre and random fibre reinforced laminates,” in *Lecture notes from Department of Mechanical Engineering, University of Sheffield*, 2015.

[141] C. L. Tucker and E. Liang, “Stiffness predictions for unidirectional short-fiber composites: Review and evaluation,” *Compos. Sci. Technolology*, vol. 59, pp. 655–671, 1999.

[142] B. Franzen, C. Klason, J. Kubat, and T. Kitano, “Fibre degradation during processing of short fibre reinforced thermoplastics,” *Composites*, vol. 20, no. 1, pp. 65–76, 1989.

[143] A. Dickson, D. Even, J. Warnes, and A. Fernyhough, “The effect of reprocessing on the mechanical properties of polypropylene reinforced with wood pulp, flax or glass fibre,” *Compos. Part A*, vol. 61, pp. 258–267, 2014.

[144] A. Bourmand and C. Baley, “Investigations on the recycling of hemp and sisal fibre reinforced polypropylene composite,” *Polym. Degrad. Stab.*, vol. 72, pp. 1034–1045, 2007.

[145] S. Vejelis and S. Vaitkus, “Investigation of Bending Modulus of Elasticity of Expanded Polystyrene (EPS) Slabs,” *Mater. Sci.*, vol. 12, no. 1, pp. 22–24, 2006.

[146] M. A. Hayat and S. M. A. Suliman, "Mechanical and structural properties of glass reinforced phenolic laminates," *Polym. Test.*, vol. 17, pp. 79–97, 1998.

[147] F. Mujika, "On the difference between flexural moduli obtained by three-point and four-point bending tests," *Polym. Test.*, vol. 25, pp. 214–220, 2006.

[148] J. K. Lynch, "The dependence of the mechanical properties of an immiscible poylmer blend," Rutgers University, 2002.

[149] R. G. Lampo and T. J. Nosker, "USACERL Technical Report 97/95 Development and testing of plastic lumber materials for construction applications," 1997.

[150] M. F. Ashby, *Materials Selection in Mechanical Design*, 4th ed. Butterworth-Heinemann, 2010.

[151] J. Thorne, "The foaming mechanism in rotational moulding," in *SPE/ANTEC 2000 Proceedings, Volume 1; Volume 3*, 2000.

[152] Q. Yuan, W. Jiang, L. An, R. K. Y. Li, and Z. Jiang, "Mechanical and Thermal Properties of High-Density Polyethylene Toughened with Glass Beads," *J. Appl. Polym. Sci.*, vol. 89, pp. 2102–2107, 2003.

[153] W. Perkins, "Polymer toughness and Impact resistance," *Polym. Eng. Sci.*, vol. 39, no. 12, pp. 2445–2460, 1999.

[154] R. Gensler, C. J. G. Plummer, C. Grein, and H.-H. Kausch, "Influence of the loading rate on the fracture resistance of isotactic polypropylene and impact modified isotactic polypropylene," *Polymer (Guildf).*, vol. 41, pp. 3809–3819, 2000.

[155] B. Lauke and B. Schultrich, "Calculation of fracture of work of short-glass-fibre reinforced polyethylene for static and dynamic loading rates," *Compos. Sci. Technolology*, vol. 26, pp. 1–16, 1986.

[156] British Standards Institute, *BS EN ISO 1183-1: Plastics — Methods for determining the density of non-cellular plastics Part 1: Immersion method, liquid pyknometer*. British Standards Institute, 2004.

[157] British Standards Institute, *BS EN 338: Structural timber — Strength classes*. British Standards Institute, 2009.

[158] British Standards Institute, *BS EN 13145: Railway applications — Track — Wood sleepers and bearers*. British Standards Institute, 2001.

[159] D. A. Webb, "The Tie Guide," 2005.

[160] British Standards Institute, *BS EN 350-1: Durability of wood andwood-based products — Natural durability of solid wood — Part 1: Guide to the principles of testing and classification of the natural durability of wood*. British Standards Institute, 1994.

[161] British Recycled Plastic, "British Recycled Plastic Price List," *www.britishrecycledplastic.co.uk*, 2014. [Online]. Available: www.britishrecycledplastic.co.uk.

[162] Robbins, "Robbins Timber Price List," *www.robbins.co.uk*, 2014. .

[163] RECOUP, "Plastics Recycling 2014," 2014.

[164] H. I. Halimatudahliana and M. Nasir, "Morphological studies of uncompatibilized and compatibilized polystyrene/polypropylene blend," *Polym. Test.*, vol. 21, pp. 263–267, 2002.

[165] H. I. Halimatudahliana and M. Nasir, "The effect of various compatibilizers on mechanical properties of polystyrene/polypropylene blend," *Polym. Test.*, vol. 21, pp. 163–170, 2002.

[166] S. Luzuriaga, J. Kovarova, and I. Fortelny, "Stability of model recycled mixed plastic waste compatibilised with a cooperative compatibilisation system," *Polym. Degrad. Stab.*, vol. 96, pp. 751–755, 2011.

[167] N. Equiza, W. Yave, R. Quijada, and M. Yazdani-Pedram, "Use of SEBS/EPR and SBR/EPR as Binary Compatibilizers for PE/PP/PS/HIPS Blends: A Work Oriented to the Recycling of Thermoplastic Wastes," *Macromol. Mater. Eng.*, vol. 292, pp. 1001–1011, 2007.

[168] H. P. Blom, J. W. Teh, and A. Rudin, "iPP/HDPE Blends. II. Modification with EPDM and EVA," *J. Appl. Polym. Sci.*, vol. 60, pp. 1406–1417, 1996.

[169] A. S. Maxwell, "Weathering of Recycled Photo-Degraded Polyethylene," *Polym. Eng. Sci.*, vol. 48, pp. 381–385, 2008.

[170] S. Luzuriaga, J. Kovarova, and I. Fortelny, "Degradation of pre-aged polymers exposed to simulated recycling: Properties and thermal stability," *Polym. Degrad. Stab.*, vol. 91, pp. 1260–1232, 2006.

[171] V. T. Breslin, U. Senturk, and C. C. Berndt, "Long-term engineering properties of recycled plastic lumber used in pier construction," *Resour. Conserv. Recycl.*, vol. 23, pp. 243–258, 1998.

[172] C. N. Kartalis, C. D. Papaspyrides, R. Pfaender, K. Hoffmann, and H. Herbst, "Closed Loop Recycling of Bottle Crates Using the Restabilization Technique," *Macromol. Mater. Eng.*, no. 288, pp. 124–136, 2003.

[173] C. N. Kartalis, C. D. Papaspyrides, and R. Pfaender, "Closed-Loop Recycling of Postused PP-Filled Garden Chairs Using the Restabilization Technique. III. Influence of Artificial Weathering," *J. Appl. Polym. Sci.*, vol. 89, pp. 1311–1318, 2003.

[174] A. Jansson, K. Moller, and T. Gevert, "Degradation of post-consumer polypropylene materials exposed to simulated recycling—mechanical properties," *Polym. Degrad. Stab.*, vol. 82, pp. 37–46, 2003.

[175] J. V. Gulmine, P. R. Janissek, H. M. Heise, and L. Akcelrud, "Degradation profile of polyethylene after artificial accelerated weathering," *Polym. Degrad. Stab.*, vol. 79, pp. 385–397, 2003.

[176] C. Tavares, J. V. Gulmine, C. M. Lepienski, and L. Akcelrud, "The effect of accelerated aging on the surface mechanical properties of polyethylene," *Polym. Degrad. Stab.*, vol. 81, pp. 367–373, 2003.

[177] N. Tzankova Dintcheva and F. P. La Mantia, "Photo-re-stabilisation of recycled post-consumer films from greenhouses," *Polym. Degrad. Stab.*, vol. 85, pp. 1041–1044, 2004.

[178] M. P. Luda, G. Ragosta, P. Musto, D. Acierno, L. Di Maio, G. Camino, and V. Nepote, "Regenerative Recycling of Automotive Polymer Components: Poly(propylene) Based Car Bumpers," *Macromol. Mater. Eng.*, no. 288, pp. 613–620, 2003.

[179] Q-Lab, "Technical Bulletin LU-8009 QUV & Q-Sun A comparison of two effective approaches to accelerated weathering & light stability testing," 2006.

[180] British Standards Institute, *BS EN ISO 4892-2: Plastics — Methods of exposure to laboratory light sources — Part 2: Xenon-arc lamps*. British Standards Institute, 2006.

[181] British Standards Institute, *BS EN ISO 4892-3: Plastics — Methods of exposure to laboratory light sources —Part 3: Fluorescent UV lamps*. British Standards Institute, 2006.

[182] British Standards Institute, *BS 2782-5: Method 540G: 1995 ISO 4892-4: 1994 Methods of testing Plastics — Part 5: Optical and colour properties, weathering - Method 540G: Methods of exposure to laboratory light sources — Open-flame carbon-arc lamps*. British Standards Institute, 1994.

[183] B. C. Hayes, "Fundamentals of atmosphere elements," in *ST133 Symposium on conditioning and weathering*, 1956, p. 132.

[184] British Standards Institute, *BS EN ISO 4892-1:Plastics — Methods of exposure to laboratory light sources — Part 1: General guidance*. British Standards Institute, 2001.

[185] G. R. Koerner, G. Y. Hsuan, and R. M. Koerner, "Photo-initiated degradation of geotextiles," *J. Geotech. Geoenvironmental Eng.*, vol. December, pp. 1159–1166, 1998.

[186] Q-Lab, "Technical Bulletin LU-8031 High Irradiance UV/Condensation Testers Allow Faster Accelerated Weathering Test Results," 1994.

[187] J.-L. Philippart, C. Sinturel, and J.-L. Gardette, "Imfluence of light intensity on the photooxidation of polypropylene," *Polym. Degrad. Stab.*, vol. 58, pp. 261–268, 1997.

[188] J. L. Way, J. R. Atkinson, and J. Nutting, "The effect of spherulite size on the fracture morphology of polypropylene," *J. Thermoplast. Compos. Mater.*, vol. 9, pp. 293–299, 1974.

[189] J. L. Thomason and M. A. Vlug, "Influence of fibre length and concentration on the properties of glass fibre-reinforced polypropylene: 4. Impact properties," *Compos. Part A*, vol. 28A, pp. 277–288, 1997.

[190] L. McKeen, *The Effect of Creep and Other Time Related Factors on Plastics and Elastomers*. William Andrew Publishing/Plastics Design Library, 2009.

[191] C.-W. Chen, H. Salim, J. J. Bowders, J. E. Loehr, and J. Owen, "Creep Behavior of Recycled Plastic Lumber in Slope Stabilization Applications," *J. Mater. Civ. Eng.*, vol. February, p. 130, 2007.

[192] M. Sanchez-Soto, A. Rossa, A. J. Sanchez, and J. Gamez-Perez, "Blends of HDPE wastes: Study of the properties," *Waste Manag.*, vol. 28, pp. 2565–2573, 2008.

[193] B. Xu, J. Simonsen, and W. E. Rochefort, "Mechanical Properties and Creep Resistance in Polystyrene/Polyethylene Blends," *J. Appl. Polym. Sci.*, vol. 76, pp. 1100–1108, 2000.

[194] ASTM, "ASTM D5262-07 - Standard test method for evaluating the unconfined tension creep and creep rupture behavior of geosynthetics," in *ASTM Volume 04.13 Geosynthetics*, ASTM International, 2007.

[195] A. Bozorg-Haddad, M. Iskander, and Y. Chen, "Compressive strength and creep of recycled HDPE used to manufacture polymeric piling," *Constr. Build. Mater.*, vol. 26, pp. 505–515, 2012.

[196] A. Bozorg-Haddad and M. Iskander, "Predicting Compressive Creep Behavior of Virgin HDPE Using Thermal Acceleration," *J. Mater. Civ. Eng.*, vol. 23, no. 8, pp. 1145–1162, 2011.

[197] A. Bozorg-Haddad and M. Iskander, "Comparison of Accelerated Compressive Creep Behavior of Virgin HDPE Using Thermal and Energy Approaches," *J. Mater. Eng. Perform.*, vol. 20, no. 7, pp. 1219–1229, 2011.

[198] A. Bozorg-Haddad, M. Iskander, and H.-L. Wang, "Compressive Creep of Virgin HDPE Using Equivalent Strain Energy Density Method," *J. Mater. Civ. Eng.*, vol. 22, no. 12, pp. 1270–1281, 2010.